NTNU – Trondheim
Norwegian University of
Science and Technology

Multiphase Flow Through Chokes

Evaluation of five models for prediction of
mass flow rates

Ragnhild Krogsrud Haug

Earth Sciences and Petroleum Engineering
Submission date: June 2012
Supervisor: Harald Arne Asheim, IPT
Co-supervisor: Martin Skottene, FMC Kongsberg Subsea
Kristian Holmås, FMC Kongsberg Subsea

Norwegian University of Science and Technology
Department of Petroleum Engineering and Applied Geophysics

Preface

This thesis was written as a master's thesis in the course TPG 4905 Petroleum Engineering - Petroleum Production at the Norwegian University of Science and Technology (NTNU), during the spring term 2012, at the Department of Petroleum Engineering and Applied Geophysics.

I want to thank my supervisor, Professor Harald A. Asheim at NTNU, for showing me his model for the prediction of mass flow rate across a choke, which is used in this work. He has been a great help, and I appreciate that he has always had his door open for me.

Also, I would like to thank Martin Skottene and Kristian Holmås at FMC Kongsberg Subsea for helping me define a topic for my thesis and giving me a lot of assistance and guidance along the way. They have truly been a great help.

Abstract

This thesis has evaluated five choke models described in the literature by comparing their predictions to measured flow rates for two different data sets. The models are the Bernoulli Equation with two-phase multiplier, Asheim's model, the Sachdeva et al. model, Al-Safran and Kelkar's model and the Hydro Model.

For single-phase flow, the prediction of mass flow rate across a choke for a given pressure drop is a rather straight-forward process. But for two-phase flow, it is more difficult. Many authors have developed models for two-phase mass flow rate predictions, but they are not as accurate as for single-phase flow.

Most emphasis has been given to the Hydro Model. Earlier work shown that there is room for improvement. Therefore, it was divided into parts and each part was evaluated separately. Some improvements were found, but all in all the resulting revised Hydro Model presented here is very similar to the original model. The largest difference is the removal of pressure recovery, which greatly simplifies the model and reduces run time drastically.

It was the Hydro Model that was best for one of the data sets, but worst for the other. The Bernoulli Equation with Simpson et al.'s two-phase multiplier was seen to be one of the best models for both data sets, in spite of its relative simplicity and the fact that it does not separate between critical and sub-critical flow.

It was found that the most important feature seems to be the inclusion of slip between the gaseous and liquid phases. Pressure recovery after the choke seems to be negligible in most cases. For calculation of density for a two-phase liquid, the mometum density appears to be the most suited for use in choke models.

Sammendrag

Denne oppgaven har vurdert fem modeller for strømning gjennom en strupeventil som er beskrevet i litteraturen ved å sammenligne modellenes forutsigelse med målt strømningshastighet for to ulike datasett. Modellene er Bernoullis ligning med to-fase multiplikator, Asheim modell, Sachdeva et al.s modell, Al-Safran og Kelkars modell og Hydromodellen.

For enfasestrømning er prediksjon av masserate over en strupeventil for et gitt trykkfall en ganske enkel prosess. Men for tofasestrømning, er det en god del vanskeligere. Mange forfattere har utviklet modeller for å forutsi strømningshastiget, men de er ikke like nøyaktig som for enfasestrømning.

Hydromodellen har fått mest oppmerksomhet her. Tidligere arbeider med denne har vist at det er rom for forbedring. Derfor ble modellen delt inn i forskjellige deler og hver del ble evaluert separat. Noen forbedringer ble funnet, men alt i alt er den reviderte Hydromodellen som presenteres her svært lik den opprinnelige modellen. Den største forskjellen er fjerning av trykketgjennvinning, noe som forenkler modellen og reduserer kjøretiden drastisk.

Det var Hydromodellen som var best for et av datasettene, men verst for det andre. Bernoullis ligning med Simpson et al. s tofasemultiplikator ble sett på som en av de beste modellene for begge datasett, til tross for sin relative enkelhet og det faktum at den ikke skiller mellom kritisk og subkritisk fstrømning.

Det ble observert at den viktigste enkeltdelen i en modell ser ut til å være inkludering av slip mellom gassfase og væskefase. Trykkgjennvinning etter strupeventilen synes å være ubetydelig i de fleste tilfeller. For beregning av tetthet av en tofasevæske, synes momenttetthet å være den mest egnet for bruk i denne type modeller.

Contents

List of Figures

List of Tables

1 Introduction

A choke is a restriction to fluid flow, which causes a pressure drop. It is widely used in the petroleum industry to control and optimize production rates. Another task is to provide back-pressure for the reservoir in order to avoid formation damage, large pressure fluctuations and back-flow. Pressure drop across the choke depends on flow rate. Therefore, flow rate may be measured indirectly by measuring the pressure drop across a choke. For single-phase flow, this is a standard method and can be done accurately, but for multiphase flow it is more difficult.

There are many models in the literature that describe multiphase flow through a choke. One of the challenges they meet, is that the flow entering the choke is difficult to model because it is not homogeneous but can have different flow patterns (stratified flow, annular flow, bubble flow, etc), and the geometry of the choke itself is very complex. Also, predicting the sub-critical-critical flow transition is important for the result. Therefore, a small change in the conditions upstream of the choke can give larger deviations in predicted mass flow than expected.

The objective of this thesis is to evaluate several models that use measured pressure drop across a choke to predict the mass flow for a multiphase fluid, given inlet parameters such as mass fractions and upstream pressure. The main focus will be on the Hydro Model, which will be thoroughly investigated. Considering work that has been done with it previously suggests that there are areas that can be improved. Therefore, a revised version of the Hydro Model will also be presented.

Two sets of data will be used in the evaluation; one from a test facility in Porsgrunn consisting of 508 measured flow rates, and one from a field from the Ekofisk area, consisting of 87 data points.

2 General Theory

2.1 Flow and Pressure Drop

A choke is a local reduction of flow area in a pipe, which causes the fluid flow to accelerate, thus inducing a pressure drop [13] according to the Bernoulli's law. In this situation, gravity effects can be neglected. Looking at steady state flow, and combining Newton's second law with the conservation of mass, Equation 1 is obtained, which is the Bernoulli Equation for a compressible fluid, and is valid along a streamline. [12]

$$dP + \rho u du = 0 \tag{1}$$

The mass must be conserved, $\frac{d}{dz}\dot{m} = 0$, and this implies the following relation between flow area, A and volumetric flow rate, Q:

$$A_i u_i \rho_i = Q_i \rho_i \tag{2}$$

where u is the velocity, A is the flow are,ρ is the density and i denotes any flowing fluid, for instance oil, water or gas. [12] For multiphase flow to be considered as one fluid, the value for density ρ and velocity u are interpreted as average values. Water and oil are similar in density, especially when compared to gas, and are therefore often treated as one liquid phase. The total mass flow rate is then by most models expressed as follows:

$$\dot{m} = \dot{m}_G + \dot{m}_L \tag{3}$$

where $\dot{m}_i = x_i \dot{m}$, and the mass fractions, x, of gas and liquid sum to unity.

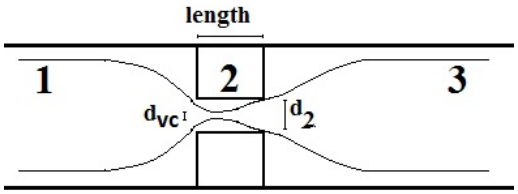

Figure 1: Sketch of a choke

A simplistic sketch of a choke is shown in Figure 1. The numbers (1) to (3) represent important positions in any choke model. Position (1) is the upstream condition, where the inlet parameters, such as mass fractions and upstream pressure are measured. The choke conditions are represented by position (2), the choke exit. Because the pressure at this position is difficult to measure, the downstream pressure is normally measured at position (3) instead. This downstream position is then chosen to be exactly at the point where the fluid flow reaches the pipe wall again and makes use of the entire area in the pipe. Thus, there is no direct contact between the flowing fluid and wall until after position (3), and wall friction between position (2) and (3) can be neglected. The distances between the positions do not matter. [16]

2.2 Density Averages

There are several ways of of calculating the density of a multiphase fluid. The most common ones are based on flow average (ρ_H), volume average (ρ_{TP}) and momentum (ρ_e). According to Chisholm [6], ρ_{TP} is most suitable to use in calculations where the pressure

change is related to elevation change, while ρ_e is better when the pressure drop is caused by acceleration of the fluid.

2.2.1 Two-Phase Density

To find an expression for the volume averaged two-phase density, we start with the expression [6]:

$$\rho_{TP} = \alpha\rho_G + (1-\alpha)\,\rho_L \tag{4}$$

where α is the in-situ volume fraction of gas. To make this expression easier to use with the choke models, it is better to have the density expressed in terms of mass fractions, rather than volume fractions. In order to do that, Equation (2) can be written in terms of α:

$$\begin{aligned} \dot{m}_G &= x_G\dot{m} = \alpha A u_G \rho_G \qquad (a) \\ \dot{m}_L &= x_L\dot{m} = (1-\alpha)\,A u_L \rho_L \qquad (b) \end{aligned} \tag{5}$$

where the phase velocity is $u_i = Q_i/A_i$. Combining these expressions and solving for α, thus eliminating $\dot{m}$ and A, the following expression is obtained:

$$\alpha = \frac{x_G\rho_L}{x_G\rho_L + kx_L\rho_G} \tag{6}$$

where k is the velocity ratio, or phase slippage: u_G/u_L, which will be further explained in Section 2.3. By inserting Equation (6) into Equation (4), we get an expression for a density including slippage between the gas and liquid phases:

$$\frac{1}{\rho_{TP}} = \frac{\frac{x_G}{\rho_G} + k\frac{x_L}{\rho_L}}{x_G + kx_L} \tag{7}$$

For the case of gas-only flow, the slip ratio, k disappears from the equation because $x_L = 0$. In order to avoid the slip for single-phase liquid flow as well, we depend on an expression for k which is equal to unity for $x_L = 1$.

2.2.2 Homogeneous Density

The homogeneous density, ρ_m is calculated as a flow averaged density where the gas and liquid phases are assumed to move with the same velocity, which is the same as setting $k = 1$ in Equation 7 above. This results in:

$$\frac{1}{\rho_m} = \frac{x_G}{\rho_G} + \frac{x_L}{\rho_L} \tag{8}$$

2.2.3 Momentum Density

By a different approach, looking at the momentum flux, the rate of transfer of momentum, $\dot{m}u$, for a unit area, there is another expression for the density [6]. Assuming separated flow, and beginning with

$$momentum\,flux = \frac{\dot{m}u}{A} = \left(\frac{\dot{m}}{A}\right)^2 \frac{1}{\rho} \tag{9}$$

where u is written as $\dot{m}/(A\rho)$ from Equation (2). Expanding this expression to two-phase (gas and liquid) flow gives:

$$momentum\,flux = \frac{\dot{m}}{A}\left(x_G u_G + x_L u_L\right) \tag{10}$$

where $\dot{m} = \dot{m}_G + \dot{m}_L$. Substituting Equation (5) for velocities, then using Equation (6) to eliminate α from the expression and rewriting, the following result is found:

$$momentum\,flux = \left(\frac{\dot{m}}{A}\right)^2 \left(\frac{x_G}{\rho_G} + k\frac{x_L}{\rho_L}\right)\left(x_G + \frac{x_L}{k}\right) \tag{11}$$

Comparing Equation (9) and (11), it can be seen that the first term is the same. Therefore, also the second parts should be comparable, and we can define the momentum density as:

$$\frac{1}{\rho_e} = \left(\frac{x_G}{\rho_G} + k\frac{x_L}{\rho_L}\right)\left(x_G + \frac{x_L}{k}\right) \tag{12}$$

The subscript e is added to separate this definition of the density derived from momentum flux, from the one given in Equation (7). Similarly, there is a u_e so that $\dot{m} = Au_e\rho_e$. It should also be noted that if $k = 1$, the momentum density reduces to the homogeneous density, just like the two-phase density does. As is the case for the two-phase density, slip automatically drops out the equation when x_G but to avoid slip for $x_L = 1$ as well, the slip model should produce $k = 1$ for single-phase liquid flow.

Figure 2 show the graph of how the two-phase density in Equation (7), momentum density in Equation (12) and homogeneous density in Equation (8) vary with change in pressure and gas mass fraction. The two-phase density is always the highest, with the homogeneous density always being the lowest.

2.3 The Slip Ratio, k

Slippage is a phenomenon that occurs in any non-homogeneous multiphase flow where the phases flow with different velocities. The velocity ratio, or slip ratio, is defined as [6]:

$$k = \frac{u_G}{u_L} \tag{13}$$

where u_G and u_L are the average velocities of the gas and liquid phases, respectively. Oil and water are again assumed to constitute one phase because of their similar properties, and thus flow with the same velocity. Normally, gas flows faster than liquid, leading to slip ratio larger than unity. In homogeneous flow, the assumption is that gas and liquid flow with the same velocity, and $k = 1$, that is, no slippage occurs.

Finding a value for this ratio directly is difficult, therefore several models have been developed. Chisholm [5, 6] formulated an expression based on frictional pressure drop and flow theory for separated flow that is applicable in many settings, among others for contraction of flow area like in a choke. The expression is given in Equation (14) below.

$$k_{Ch} = \begin{cases} \left(\frac{\rho_L}{\rho_H}\right)^{1/2} = \sqrt{1 + x_G\left(\frac{\rho_L}{\rho_G} - 1\right)} & \chi > 1 \quad (a) \\ \left(\frac{\rho_L}{\rho_G}\right)^{1/4} & \chi \leq 1 \quad (b) \end{cases} \tag{14}$$

where χ is the Lockhart-Martinelli parameter. With Blasius' exponents, it is:

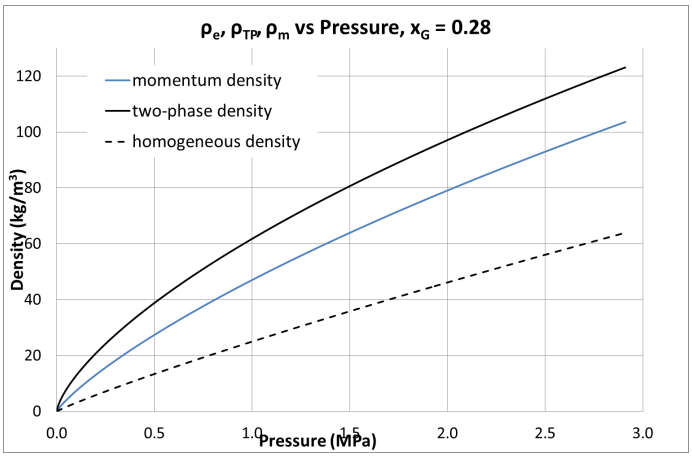

(a) Density equations vs P

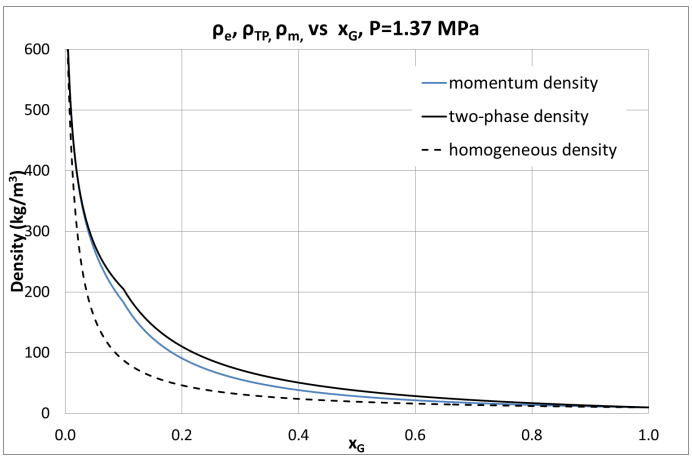

(b) Density equations vs x_G

Figure 2: Different density equations with Chisholm's slip model

$$\chi = \frac{x_L}{x_G}\sqrt{\frac{\rho_G}{\rho_L}} \tag{15}$$

This means that for flows with little liquid content, the slip ratio is independent of x_G. As an example, a fluid with $\rho_G = 100\,kg/m^3$ and $\rho_L = 800\,kg/m^3$, the slip ratio depends on x_G as long as $x_G < 0.26$. For $\chi = 1$, Equation (14a) and (14b) give the same value of k. [6] In the case of liquid-only flow, $k_{Ch} = 1$, that is, there is a no-slip prediction, which is in good agreement with the definitions of density in Section 2.2.

Simpson et al. are among others that have developed an expression for the slip ratio similar to Equation (14b). This model, however, does not include the gas mass fraction, but only the phase densities: [7, 3]

$$k_{Si} = \left(\frac{\rho_L}{\rho_G}\right)^a \tag{16}$$

where $a = 1/6$ or can be adjusted to the situation. Here, the slip is a function of gas density, which is to say, pressure, but does not depend on how much gas there is compared to the amount of liquid. The disadvantage here is that the slip ratio will not approach unity for single-phase liquid flow.

2.4 Critical Flow

Related mainly to the pressure difference across the choke, one can divide the flow into two regimes; sub-critical and critical (choked) flow. Due to their different behavior, it is important to distinguish between them when predicting the flow rate.

The criterion for critical flow is for the velocity of the flowing fluid to reach its sonic velocity. Pressure waves, caused by the change in pressure, propagate through the flow with the speed of sound. But if the fluid flows faster than the waves can travel, the waves are unable to move upstream, or have any effect on the flow. Once this border is reached, the flow is independent of downstream pressure, and we have critical flow. Any further reduction in the downstream pressure will not increase the flow rate. [13]

For an absolutely incompressible fluid, the speed of sound is infinite, and critical flow cannot occur in practice. Many liquids are almost incompressible, or are treated as that in modeling, and therefore critical flow in liquid-only flow is rare. However, if the downstream pressure is reduced below the flashing point, the liquid will start to vaporize and critical flow is possible. [12] If the fluid is compressible, it will expand as the downstream pressure is lowered. This also means that the density is lowered, which will again cause a further pressure reduction. If allowed to, this may start a self-reinforcing process until critical flow is reached. [4]

Very roughly, the transition from sub-critical to critical flow happens when the pressure ratio of downstream to upstream pressure, $y = P_2/P_1$, is around 0.6, as long as the flow does not approach liquid-only flow. Unless x_G is very low, the critical pressure ratio varies very little with it, when all other properties are equal. [4, 9]

In multiphase flow, the liquid contributes with high density and the gas with high compressibility, which will result in elastic pressure waves that propagates slowly. Therefore, sound of speed in multiphase flow is often found to be lower than for single phase flow for any of the fluids. [4] The sonic velocity depends mostly on the pressure upstream of the choke and fluid's density, which again is a function of the mass fractions, (gas and liquid). For a higher upstream pressure and higher liquid mass fractions, the overall density of the fluid is higher and the sonic velocity is higher, thus giving a larger mass flow rate and pressure difference to reach critical conditions. On the other hand, increasing the temperature will decrease the density of the gas and then reduce the sonic velocity of the fluid. [13]

2.5 The Discharge Coefficient

When flowing through a sudden contraction where the entrance is not a smooth curve, which is the case for most choke geometries, the fluid is unable to turn around the sharp corner and make use of the entire choke area, as has been sketched in Figure 1. Therefore, the flow area is smaller than the choke area. This location with the minimum flow area is called vena contracta, and is also the point with the highest fluid velocity. [12] To account for this in calculations, a contraction coefficient C_C is often introduced.

$$C_C = \frac{A_{vc}}{A_2} \tag{17}$$

where vc is vena contracta. The value of C_C depends on several things, among others the roundness of the choke entrance, the contraction compared to the upstream pipe diameter and the fluid's Reynold's number. A typical value for a 90 degree, sharp corner is 0.61 [12]. The rounder and larger the opening into the choke is, the closer to unity C_C is. Of

course, it can never be larger than one as the flow area can never be larger the geometric area in the choke.

Using Chisholm's [6] definition, there are two main categories of chokes: long and short. In a long choke, the length of the contraction is more than half its diameter. Otherwise, it is called short. The vena contracta will always occur within a long choke and the flow area may have time to expand to the choke walls before exiting. But in the case of a short choke, vena contracta may be located after the choke itself [16].

As will be seen in Section 3, it is quite common to expand the meaning of the contraction coefficient to a discharge coefficient to account for both the minimal flow area in vena contracta and losses due to energy dissipation around the entrance region, thus turning it into a loss coefficient as well. As for the contraction coefficient, the discharge coefficient is expected to be smallest for a small choke opening area and then increase in value as the opening increases in size. Because a discharge coefficient depends on all the same things as a contraction coefficient, it should be adjusted to the situation, and every choke geometry and opening may have a different C_D. This is also something thing that will be shown in the following sections.

3 Existing Choke Models

In this section, five models to predict the mass flow rate across a choke are presented. These models are the Bernoulli Equation with two-phase multiplier, Asheim's model, the Sachdeva et al. model, Al-Safran and Kelkar's model and the Hydro Model. All but the Bernoulli Equation with two-phase multiplier differentiate between sub-critical and critical flow, and the two latter, Al-Safran and Kelkar's model and the Hydro Model include slip.

All models assume the mass fractions to be constant over the choke. Therefore, the subscript of position has been omitted to simplify notation, and mass fractions are expressed as x_i and refer to the upstream value of the variable.

3.1 The Bernoulli Equation With Two-Phase Multiplier

Starting with Equation (1), the expression can be easily integrated by assuming constant density. Then substituting $u = \dot{m}/\rho A$, the following expression is found:

$$\dot{m} = A_2 \sqrt{\frac{2\rho\left(P_1 - P_2\right)}{1 - \left(\frac{A_2}{A_1}\right)^2}} \tag{18}$$

This is the Bernoulli Equation for incompressible flow, which is well known and much used because of its simplicity. As it was developed for single-phase flow, adjustments have to be made to make it applicable for multiphase flow as well. For multiphase flow the pressure drop is larger than single-phase flow. There are several models for two-phase multiplier for pressure drop in the literature, in the form of $\Delta P_{TP} = \Phi_{TP} \Delta P_{1P}$. Including this multiplier, the Bernoulli Equation is shown in Equation (19): [12, 9]

$$\dot{m} = C_D A_2 \sqrt{\frac{\frac{2\rho(P_1 - P_2)}{\Phi_{TP}}}{1 - \left(\frac{C_D A_2}{A_1}\right)^2}} \tag{19}$$

where Φ_{TP} is the two-phase multiplier, ρ a suitable density and C_D is a discharge coefficient.

Many of the authors who have developed slip models have also developed expressions for a two-phase multiplier. Two of these are Chisholm [6] and Simpson et al. [7]. The multipliers are given in Equation (20) and Equation (22), respectively.

$$\Phi_{2P,Ch} = 1 + \left(\frac{\rho_L}{\rho_G} - 1\right)\left(B x_G x_L + x_G^2\right) \tag{20}$$

where

$$B = \frac{\left(\frac{1}{k_{Ch}}\right)\left(\frac{\rho_L}{\rho_G}\right) + k_{Ch} - 2}{\frac{\rho_L}{\rho_G} - 1} \tag{21}$$

and k_{Ch} as given in Equation (14) on page 5. Simpson et al.'s two-phase multiplier is:

$$\Phi_{2P,Si} = \left(1 + x_G\left(k_{Si} - 1\right)\right)\left(1 + x_G\left(k_{Si}^5 - 1\right)\right) \tag{22}$$

In developing their multiplier, Simpson et al. used data from pipe diameters up to $12\,cm$ and with a considerable amount of gas present. [7]

As a two-phase multiplier relates the single-phase pressure drop of a liquid to a multiphase pressure drop, the density that should be used in Equation (19) is the liquid density. [6] In the Bernoulli Equation without such a multiplier, it will most likely be advantageous to use a two-phase density such as Equation (8) or (7) or (12) with a slip model.

That the flow is assumed to be incompressible is expected to be a severe limitation when applied to gas. The Bernoulli Equation may give too high mass flow rates when there is gas present; the density that is assumed constant will actually decrease. [9] One way to accommodate this could be to use an average of the upstream and downstream density or only downstream properties, but this will still remain a constant throughout the calculation and can instead be accommodated for in a discharge coefficient. ρ_{G1} is therefore used at all times, also in the two-phase multipliers. Because the Φ_{TP}s only relate single-phase pressure drop to two-phase pressure drop, but do not involve any change in density, the same issues are expected when including them in the Bernoulli Equation.

Another thing to be aware of is that the Bernoulli Equation does not separate between sub-critical and critical flow; a larger pressure change will lead to larger predicted flow rate until the downstream pressure is reduced to zero, beyond which there is no physical meaning. [12, 9] The pressure at the choke throat, P_2, is assumed to be equal to the downstream pressure P_3.

Summarized, the assumptions are:

- Stationary and frictionless flow in one dimension
- Incompressible fluids, i.e. constant density
- Sub-critical flow
- No pressure recovery after the choke
- (two-phase multipliers:) Constant gas quality

It is worth noting that using the momentum density of Equation (12) with Simpson et al.'s slip model from Equation (16) ($a = 1/6$) is the same as using the liquid density and Simpson et al.'s two-phase multiplier directly. In addition, by inserting k_{Si} into $\Phi_{2P,Ch}$ (instead of using Chisholm's own slip model) the same result is obtained. That is, rearranging any of the right hand sides of Equations (23a)-(23c) will yield (23d).

$$
\begin{aligned}
\rho_e(k_{Si}) &= \frac{1}{\left(\frac{x_G}{\rho_{G1}} + k_{Si}\frac{1-x_G}{\rho_L}\right)\left(x_G + (1-x_G)\frac{1}{k_{Si}}\right)} && (a)\\
\frac{\rho_L}{\Phi_{2P,Si}} &= \frac{\rho_L}{\left[1 + x_G\left(k_{Si}-1\right)\right]\left[1 + x_G\left(k_{Si}^5-1\right)\right]} && (b)\\
\frac{\rho_L}{\Phi_{2P,Ch}(k_{Si})} &= \frac{\rho_L}{1 + \left(\frac{\rho_L}{\rho_{G1}}-1\right)\left(\frac{(1/k_{Si})(\rho_L/\rho_{G1})+k_{Si}-2}{(\rho_L/\rho_{G1})-1}\left(1-x_G\right)x_G + x_G^2\right)} && (c)\\
&= \frac{\rho_L}{1 + x_G^2\left(k_{Si}^6 - k_{Si}^5 - k_{Si} + 1\right) + x_G\left(k_{Si}^5 + k_{Si} - 2\right)} && (d)\\
\rho_e(k_{Si}) &= \frac{\rho_L}{\Phi_{2P,Si}} = \frac{\rho_L}{\Phi_{2P,Ch}(k_{Si})} && (e)
\end{aligned}
\qquad (23)
$$

For any value of a Equation (23a) and (23c) will be the same, but they will only be equal to (23b) for $a = 1/6$, which is the original value of a suggested by Simpson et al. [7]

3.2 Asheim's Model

Starting with Bernoulli's expression for pressure drop due to acceleration $dP + \rho u du = 0$, and assuming homogeneous density of the multiphase flow, Asheim developed a formula for the mass flow through a choke. [4, 9]

Using the gas law as a model for gas expansion:

$$\rho_G = \frac{PM}{ZRT} \tag{24}$$

and then integrating the following:

$$udu = -\left(\frac{x_G}{\rho_G} + \frac{x_L}{\rho_L}\right) dP \tag{25}$$

gives:

$$u_2 = \sqrt{2\left(x_G \frac{ZRT}{M} ln\frac{P_1}{P_2} + \frac{x_L}{\rho_L}(P_1 - P_2)\right)} \tag{26}$$

The velocity before the choke is assumed to be much smaller than the velocity at the choke and is therefore neglected. During the integration, the temperature T, along with Z and the molar mass M are held to be constant. Especially for low pressures, this is a reasonable assumption, as the value of Z is close to unity. That the molar mass is assumed to be constant follows from the assumption that there is no mass transfer until after the choke exit.

Multiplying by the flow area and density at the choke to get the mass flow rate, gives Equation (27). There is not considered to be any pressure recovery from the choke exit to measured downstream pressure, thus $P_2 = P_3$. [4]

$$\dot{m} = \frac{C_D A_2 \rho_L P_2}{x_G \rho_L ZRT/M + x_L P_2} \sqrt{2\left(x_G \frac{ZRT}{M} ln\frac{P_1}{P_2} + \frac{x_L}{\rho_L}(P_1 - P_2)\right)} \tag{27}$$

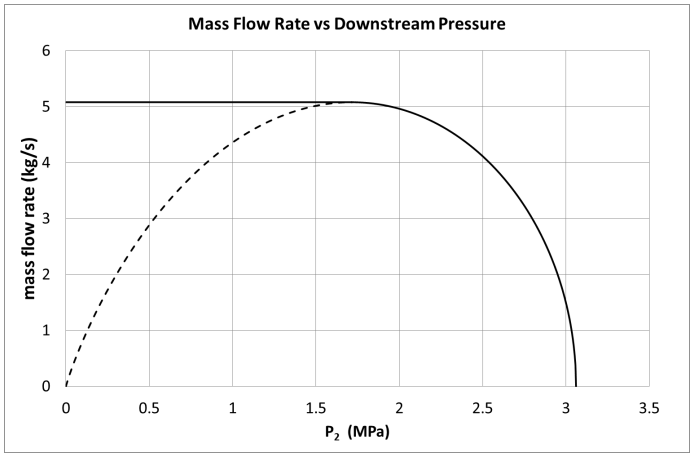

Figure 3: Mass flow rate vs P_2

$\dot{m}$ in Equation (27) follows the general path shown in Figure (3), where it reaches a maximum point and then decreases again as the downstream pressure is further reduced. This reduction, the dotted line, does not occur in reality, but the flow rate remains at the

maximum value, represented by the straight line. This maximum point can be found by differentiating Equation (27), and solving for P_2 when the derivative is zero. Due to the complicated expression, this has been done numerically here.

The mass flow rate reaches a maximum value at critical pressure. Therefore, if the actual downstream pressure is lower than the critical pressure, it is the value of the critical pressure that should be used for P_2 in Equation (27). In this case, there is critical flow. On the other hand, if the actual downstream pressure is higher than the critical pressure, the actual pressure should be used in calculations. Asheim found that the critical pressure ratio varies only little with P_1 and x_L except for very high x_L, so that it is almost constant at $P_{2c}/P_1 = y_c \approx 0.6$. [4, 9]

The assumptions for this model are summarized below:

- Stationary, homogeneous flow in one dimension
- Incompressible liquid phase
- The velocity of the gas and liquid phase are equal at the choke throat, (no slip)
- The free gas quality is constant, (frozen flow) across the choke
- Constant temperature over the choke
- No pressure recovery after the choke

Because no slippage is assumed, it is believed that the actual pressure drop will be somewhat higher and by that the flow rate somewhat lower than predicted. [4].

It should also be noted that, if assuming adiabatic gas expansion instead of using the gas law, when integrating Equation (25), Asheim's model turns into the same model as that of Sachdeva et al., which is described below.

3.3 The Sachdeva et al. Model

In 1986, Sachdeva, Schmidt, Brill and Blais developed a model for two-phase flow through chokes. If there is dissolved gas in the liquid, the dissolved gas is considered to be a part of the liquid phase and should therefore be included in the liquid phase properties. It is derived from conservation of mass, momentum and energy equations. [13, 9]

Beginning with the Momentum Equation, and assuming that the dominant pressure term is caused by acceleration, Sachdeva et al. developed an expression for the highest pressure ratio that will give critical flow, y_c. The liquid and gas are assumed to flow with the same velocity, so that $u_G = u_L = \dot{m}/(A\rho_m)$. The homogeneous density in Equation (8) can be differentiated by making an assumption that the gas expands polytropicly according to Equation (28) and considering the liquid as incompressible. Because velocities through chokes normally are high, it is assumed to be no time for mass transfer between the liquid and gaseous phase at the choke throat. This means that also the mass fractions are constant and equal to x_{G1} and x_{L1}.

$$\frac{1}{\rho_G} = \frac{1}{\rho_{G1}} \left(\frac{P_1}{P}\right)^{1/n} \tag{28}$$

where

$$n = \frac{x_G \kappa C_{V,G} + x_L C_L}{x_G C_{V,G} + x_L C_L} \tag{29}$$

For comparison, if the gas expansion was assumed to be isothermal, then $n = 1$, or adiabatic; $n = \kappa = C_{P,G}/C_{V,G}$.

Sachdeva et al. start with the same equation as Asheim, Equation (25), but when integrating, they assume adiabatic gas expansion. Hence, κ also appears in their final expression [3]. In addition, $u_2 \gg u_1$ because $d_2 \ll d_1$, therefore u_1 can be neglected in expressions like $u_2^2 - u_1^2$, which simplifies the integration of (25). The result is:

$$\frac{x_L}{\rho_L}(1-y) + \frac{\kappa}{\kappa - 1} x_G \left(\frac{1}{\rho_{G1}} - y \frac{1}{\rho_{G2}} \right) = \frac{\dot{m}^2}{2\rho_{m2}} \tag{30}$$

Special for for critical flow is it that:

$$\frac{d\dot{m}_c}{dP_{2c}} = 0 \tag{31}$$

because the mass flow rate will be independent of downstream pressure. P_{2c} is the highest downstream pressure that will give critical flow. The momentum equation then reduces to

$$-A_2^2 = \dot{m}_c^2 \frac{d}{dP_{2c}} \left(\frac{1}{\rho_m} \right) \tag{32}$$

Using Equation (28) to differentiate $1/\rho_m$ and rearranging, the result is

$$\dot{m}_c^2 = \frac{n A_2^2 P_{2c} \rho_{G2}}{x_G} \tag{33}$$

Inserting this expression into Equation (30) and solving for y_c gives:

$$y_c = \left(\frac{\frac{\kappa}{\kappa+1} + \frac{x_L(1-y_c)\rho_{G1}}{x_G \rho_L}}{\frac{\kappa}{\kappa-1} + \frac{n}{2} + \frac{n x_L \rho_{G2}}{x_G \rho_L} + \frac{n}{2}\left[\frac{x_L \rho_{G2}}{x_G \rho_L}\right]^2} \right)^{\frac{\kappa}{\kappa-1}} \tag{34}$$

where $y_c = P_{2c}/P_1$, which is the critical pressure ratio. An iterative procedure is necessary to solve this equation.

If the actual pressure ratio is less than y_c, there is critical flow and the critical pressure ratio is used in further calculations because the mass flow rate cannot increase any more above that given by y_c. And if the pressure difference is less, i.e. the ratio is higher than y_c, the actual pressure ratio is used. [13] Like in Asheim's model, there is assumed to be negligible pressure recovery so that $P_2 = P_3$.

The mass flow rate is given by solving Equation (30) for $\dot{m}$:

$$\dot{m} = A_2 C_D \sqrt{2 P_1 \rho_{m2}^2 \left[\frac{x_L(1-y)}{\rho_L} + \frac{\kappa x_G}{\kappa - 1} \left(\frac{1}{\rho_{G1}} - \frac{y}{\rho_{G2}} \right) \right]} \tag{35}$$

where

$$\frac{1}{\rho_{G2}} = \frac{1}{\rho_{G1}} y^{-\frac{1}{\kappa}} \tag{36}$$

and ρ_{m2} can be calculated from Equation (8). C_D is used as a tuning factor to account for errors caused by the assumptions of the model, for instance the neglection of friction. According to Sachdeva et al., best results were obtained when this is set to 0.85, and this is the authors' recommendation when the flow before the choke is not disturbed by any elbow or similar. If such an elbow exists, $C_D = 0.75$ would be a better value. A value of $C_D > 1$ would violate the laws of thermodynamics. [13] From this definition, it would seem that Sachdeva et al. have a different view on the discharge coefficient than what was described in Section 2.5, as they see it as a tuning constant only, without relating it to vena contracta.

The assumptions for the Sachdeva et al. model are:

- Separated flow in one dimension
- Incompressible liquid phase
- Acceleration is the main pressure term
- The velocity of the gas and liquid phase are equal at the choke throat, (no slip)
- The free gas quality is constant, (frozen flow) across the choke
- Gas expansion is adiabatic
- No pressure recovery after the choke

The equation is originally developed for field units, but as long as the units used are consistent, it can be used for SI units as well, without the need for any conversion factor. [4, 9]

3.4 Al-Safran and Kelkar's Model

Al-Safran and Kelkar developed in 2009 a model that builds on both Sachdeva et al.'s model and the Hydro model which will be described in the next section. The mathematical derivation of the model is also very similar, and so are the assumptions, but with a few important exceptions: Al-Safran and Kelkar include a pressure recovery term and phase slippage. [3, 9]

Because the downstream pressure is measured downstream of the choke, there is often though to be some pressure recovery after the choke, as the flow widens out again. [3, 14] Therefore, Al-Safran and Kelkar has included a term for pressure recovery. This means that $P_2 < P_3$ and that the pressure drop across the choke is larger than if setting $P_2 = P_3$. The pressure recovery equation is as follows:

$$P_2 = P_1 - \frac{P_1 - P_3}{1 - \left(\frac{A_2}{A_3}\right)^{0.925}} \tag{37}$$

where P_3 is the measured pressure downstream of the choke.

In order to include phase slippage, Al-Safran and Kelkar utilize the momentum density of Equation (12). From Equation (25) but with ρ_e instead of ρ_m, and assuming polytropic gas expansion, the following expression is obtained [3]:

$$k\frac{x_L}{\rho_L}(P_1 - P_2) + x_G\frac{n}{n-1}\left(\frac{P_1}{\rho_{G1}} - \frac{P_2}{\rho_{G2}}\right) = \frac{\dot{m}^2}{2}\left(\frac{1}{\rho_{e2}^2 A_2^2} - \frac{1}{\rho_{e1}^2 A_1^2}\right) \tag{38}$$

where n is as in Equation (29), k is the slip between the liquid and gas, and with ρ_{G2} from Equation (28) on page 12. During the integration, slippage has been assumed constant with regards to pressure. This is not strictly true, as the expression for slip includes gas density, which again is a function of pressure.

By ignoring u_1, like Sachdeva et al. did, the expression can be simplified. Further, solving Equation (38) for $\dot{m}$, substituting $y = P_2/P_1$ and introducing a discharge coefficient give:

$$\dot{m} = C_D A_2 \sqrt{\frac{P_1 \left[k\frac{x_L}{\rho_L}(1-y) + \frac{x_G}{\rho_{G1}}\frac{n}{n-1}\left(1 - y^{\frac{n-1}{n}}\right)\right]}{\left(\frac{x_G}{\rho_{G1}} y^{-1/n} + k\frac{x_L}{\rho_L}\right)\left(x_G + \frac{x_L}{k}\right)}} \tag{39}$$

The expression above is given slightly differently from what Al-Safran and Kelkar write [3]. Here, it is also relatively easy to recognize the momentum density in the denominator. The factor C_D is more or less the same as Sachdeva et al.'s C_D, and its appropriate value was found by the authors to be 0.75 for best results. [3]

Differentiating Equation (39) and rearranging yields [3]:

$$y_c^{1-\frac{1}{n}} = \frac{k\frac{x_L}{\rho_L}(1-y_c) + \frac{x_G}{\rho_{G1}}\frac{n}{n-1}}{\frac{x_G}{\rho_{G1}}\left[\frac{n}{n-1} + \frac{n}{2}\left(1 + k\frac{x_L}{\rho_L}\frac{\rho_{G1}}{x_G} y_c^{\frac{1}{n}}\right)^2\right]} \tag{40}$$

An iterative process is needed to solve this equation for y_c. As x_G appears outside the brackets in the denominator, it is not possible to solve this equation properly if $x_G = 0$. Luckily, that would not be necessary, because critical flow for the incompressible liquid is impossible in practice. Otherwise, if the actual pressure ratio $y = P_2/P_1$ is higher than the critical pressure ratio, the actual pressure ratio should be used in Equation (39), but if it is lower, the critical pressure ratio should be used because there is critical flow.

For phase slippage, Al-Safran and Kelkar introduce two different models. They observed that for sub-critical flow, k_{Si}, Equation (16) gave best results, while in the cases of critical flow, a version of Chisholm's slip model modified by Schüller et al. [14] was found to be more appropriate. The latter slip model, Equation (49) on page 18 will be discussed in Section 3.5.

However, there is an inconsistency here because k is also part of the expression for y_c. And we do not know whether we have sub-critical or critical flow until we have compared y_c to the observed value for y. The question is then; which expression for k to use when calculating y_c? [9]

When Al-Safran and Kelkar tested their model and compared it to that of Sachdeva et al., they found that Sachdeva et al.'s model gave too low results for the mass flow rate in sub-critical flow and too high results for critical flow. This model was better for the data sets tested by Al-Safran and Kelkar, which may not be surprising because their model allows for slip between the phases. [3, 9]

The following assumptions are made in this choke model:

- One dimensional flow
- Incompressible liquid phase
- Acceleration is the main pressure term
- The free gas quality is constant, (frozen flow)

- Gas expansion is polytropic

3.5 The Original Hydro Model

The Hydro Model, developed by Selmer-Olsen [16], and Schüller et al. [14, 15] consists of two sub-models, one called the long model for chokes that have a long contraction area relative to the opening, and one called the short model for chokes with shorter geometry. Chisholm's definition of long and short choke geometry in Section 2.5 on page 7 could be used. [16]

It is thought that a distinction between these two categories of chokes is necessary because of the differences in how the fluid flows through them. In a long contraction, the fluid will have time to widen its flow area after vena contracta out to the pipe walls, reaching A_2, from which point onwards there will be losses due to friction along the wall. There is considerable energy dissipation between the vena contracta and choke exit, and after the areal expansion right downstream of the choke. In this model, the main task of the discharge coefficient is to adjust for the flow area at vena contracta, but it also takes into account losses due to energy dissipation and friction between the wall and fluid. At the choke exit, the flow is assumed to have expanded to A_2, and it is therefore this area that is used when evaluating the transition from sub-critical to critical flow. In a short choke, on the other hand, the area of flow is the vena contracta flow area, A_{vc}. [16]

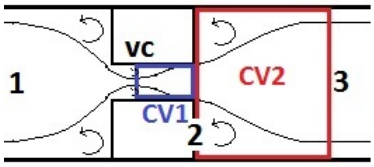

Figure 4: Sketch of choke for the Hydro Model, long version

Instead of starting with the momentum equation, the Hydro Model, long version, is developed by using two control volumes: one from the vena contracta inside the choke to the exit of the choke, see Figure 4 and one from the exit, position (2), to position (3). The short model has only one control volume from the choke exit to position (3). This is because vena contracta and choke exit is assumed to be in the same location. [16] By integrating Equation (1) from position (1) to vena contracta, we obtain the mechanical energy balance:

$$\frac{\dot{m}_{1-vc}^2}{2}\left(\frac{1}{A_{vc}^2\rho_{e,vc}^2}-\frac{1}{A_1^2\rho_{e1}^2}\right)+\int_{P_1}^{P_{vc}}\frac{1}{\rho_e}dP=0 \tag{41}$$

for an ideal situation with no irreversible losses. This differs from the previous models in that the velocity before the choke is not, and will not be neglected and the evaluation of how the density varies with pressure in the integral. The momentum density of Equation (12) has been utilized because we are looking at momentum flow through a control surface. [14]

Arriving at the first control volume for the long model, the momentum balance is used from vena contracta to position (2). Although differentiating between these two as positions, the fluid properties such as gas density, are assumed to be the same.

$$P_2 - P_{vc} = \dot{m}_{vc-2}^2 \left(\frac{1}{C_D A_2 \rho_{e2}} - \frac{1}{A_2 \rho_{e2}} \right) \tag{42}$$

This distinction between vena contracta and position (2) was thought useful because the flow is assumed to be loss free up until vena contracta, but there are losses from vena contracta to position (2) that cannot be ignored. As mass has to be conserved, $\dot{m}_{1-vc} = \dot{m}_{vc-2}$.

Upstream of the choke, the gas and liquid phases are assumed to flow with the same velocity, but in the choke, slippage is included in the model. Combining the pressure difference from the above equations and solving for for the mass flow rate, an additional term appears in the denominator:

$$\dot{m}_{1-2}^2 = \frac{2 \int_{P_1}^{P_2} \frac{1}{\rho_e} dP}{\frac{1}{A^2 \rho_{e1}^2} - \frac{1}{C_D^2 A_2^2 \rho_{e2}^2} + 2 \frac{1}{A_2^2 \rho_{e2}^2} \left(\frac{1}{C_D} - 1 \right)} \quad (long) \tag{43}$$

In the short model, it is not necessary to divide the pressure integral into two parts, and the mass flow rate is given adequately by:

$$\dot{m}_{1-2}^2 = \frac{2 \int_{P_1}^{P_2} \frac{1}{\rho_e} dP}{\frac{1}{A_1^2 \rho_{e1}^2} - \frac{1}{C_D^2 A_2^2 \rho_{e2}^2}} \quad (short) \tag{44}$$

However, the Hydro Model does not consider P_2 to be known. Therefore, a second set of equations is needed in order to find both the mass flow rate and the pressure at the choke. This is done by writing the momentum equation from position (2) to (3) as well, making up the second control volume. [16] The results are Equations (45) and (46) below. For a long choke, the flow has time and distance to widen again after vena contracta, therefore A_2 is used, while for a short contraction, $C_D A_2$ is used.

$$\dot{m}_{2-3}^2 = \frac{A_3 \left(P_3 - P_2 \right)}{\frac{1}{A_2 \rho_{e2}} - \frac{1}{A_3 \rho_{e3}}} \quad (long) \tag{45}$$

$$\dot{m}_{2-3}^2 = \frac{A_3 \left(P_3 - P_2 \right)}{\frac{1}{C_D A_2 \rho_{e2}} - \frac{1}{A_3 \rho_{e3}}} \quad (short) \tag{46}$$

These equations are only valid for sub-critical flow because they have made use of the assumption that the pressure on the first wall in the second control volume is equal to P_2, which is not the case for critical flow. [14] For critical flow, the mass flux can be maximized in Equation (1) so that:

$$\dot{m}_c^2 = -\frac{C_D^2 A_2^2}{\frac{\delta}{\delta P} \left(\frac{1}{\rho_e} \right)} \quad (short) \tag{47}$$

The equivalent for a long choke is:

$$\dot{m}_c^2 = -\frac{A_2^2}{\frac{\delta}{\delta P} \left(\frac{1}{\rho_e} \right)} \left(\frac{1}{\left(\frac{1}{C_D} - 1 \right)^2 + 1} \right) \quad (long) \tag{48}$$

The discharge coefficient in the short model is meant to correct for geometric effects, while for the long model, it should also correct for losses. [14]

In order to find the mass flow rate, two iteration procedures are necessary, making this model the most complicated model among those described in this thesis. The mass flow rate is constant through the choke, therefore $\dot{m}_{1-2}$ must be equal to $\dot{m}_{2-3}$ for sub-critical flow or $\dot{m}_c$ in the case of critical flow. By solving both these situations, a value for P_2 is found for critical flow and another for sub-critical flow, and mass flow rates for the two cases can be calculated using the expression for $\dot{m}_{1-2}$ or $\dot{m}_c$. As $\dot{m}_c$ is the maximum flow rate obtainable, the predicted mass flow rate is the smallest of the two.

Summarized, the assumptions for this model are:

- Steady state flow in one dimension
- Incompressible liquid phase
- The free gas quality is constant, (frozen flow) across the choke
- Adiabatic flow
- No losses up until vena contracta

As slip model included in ρ_e, Schüller et al. modified Chisholm's expression from Equation (14) to:

$$k_{modCh} = \sqrt{1 + x_G \left(\frac{\rho_L}{\rho_G} - 1 \right)} \left(1 + \xi e^{-\beta x_G} \right) \tag{49}$$

where $\xi = 0.6$ and $\beta = 5$ are constants were tuned to experimental results. Equation (49) is used for all mass fractions.

The integral of momentum density with respect to pressure was solved numerically, using Gauss-Legendre integration, by Selmer-Olsen [17]. When it comes to gas expansion, this is assumed to follow Equation (28) on page 12, the same as Sachdeva et al, with n given in Equation (29).

4 Data Sets for Model Testing

The models described in Section 3 below were tested against two different sets of data; one from a multiphase test loop facility, and one set of field data.

4.1 Porsgrunn Data Set

This data set, from a test facility in Porsgrunn, [14, 15] consists of 508 data points, most of which are from three-phase flow, where water, oil and gas all are present, but there are also several points that are gas-only or liquid-only. For the latter case, the composition varies from water-only through a mixture of oil and water to oil-only. The fluid is oil and gas from the Njord field and the Kårstø terminal respectively, mixed with salt water. Measured flow rates range between $0.05\,kg/s$ (only gas) and $13\,kg/s$ (only water), with gas mass fractions of $0 - 0.3$ or close to one. The fluid properties were observed at separator conditions, therefore, mass fractions and gas density for upstream conditions had to be calculated using specially adapted equations. [14]. When calculating the gas density, the ideal gas law was utilized, (that is, Equation (24) with $Z = 1$.) The measured pressures are denoted P_1 for upstream and P_3 for downstream pressure.

The test facility where the data were measured was set up horizontally so that the flow is undisturbed a length of six meters upstream of the choke. The pressure drop over the choke was recorded for given volumetric flow rates. It was mainly the upstream pressure that varied, while the downstream pressure was held almost constant from one test to another. [14]

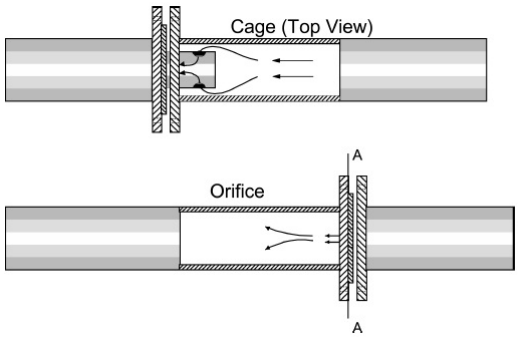

Figure 5: Sketch of cage and orifice choke that were used in the Porsgrunn data set Fig. 3, [14]

Two different choke geometries were used in the testing process; orifice and cage, with three different openings each; $11\,mm$, $14\,mm$ and $18\,mm$. A sketch of their geometry can be found in Figure 5. The pipe diameter before and after the choke is $77.9\,mm$.

As was described in Section 3, the multiphase choke models included in this report consider liquid as one phase only and does not separate between water and oil. The liquid properties for this data set will therefore be weighted averages for oil and water properties, following the equations below:

$$\rho_L = (1 - WC)\rho_o + WC\rho_w \tag{50}$$

$$C_{P,V} = \frac{x_o C_{P,V\,o} + x_w C_{P,V\,w}}{x_o + x_w} \tag{51}$$

The water cut WC, is the ratio of the volumetric flow rate of water to the volumetric flow rate of liquid, which can be expressed as $x_w\rho_o/\left(x_w\rho_o + x_o\rho_w\right)$. The heat capacities, $C_{P,V}$, are weighted by mass fractions.

4.2 Field Data

The field data [4] consists of 87 data points from the Ekofisk area in the 1980s. Of fluid properties, only oil and gas density, oil volumetric flow rate and GOR at standard conditions are given. It was therefore necessary to convert these properties and values to flow conditions for the upstream pressure given. Since the production well from which the measurements come was classified as an oil well, [1] the Black Oil Model, described in Standing [18] was thought to be adequate for this purpose. Because the composition was unknown, the pseudo-critical pressure and temperature had to be estimated. This was done using correlations suggested by Standing [2] The Z-factor was then estimated using Yarborough and Hall's equations [8, 19]. There was no information about water production, therefore the water phase was ignored and the liquid phase consists of oil only.

The values for heat capacities for this particular oil and gas are also unknown. But because these properties normally do not vary a lot hydrocarbon gases and liquids, this was not thought to be a large source of error, and the same values as for the Porsgrunn data set have been used.

Because this is data from a field in production, many of data points are very similar, in both pressure and mass fractions. The gas mass fractions lie between 0.3 and 0.95, thus filling an empty area from the Porsgrunn data. However, these are very high amounts of gas when considering the applicability of the Black Oil Model, and x_G is an important input parameter to the choke models.

The pressures are also generally higher than those from Porsgrunn. The measured mass flow rates range between $3\,kg/s$ and $35\,kg/s$, through three different choke openings: $13\,mm$ $(32/64\,inch)$, $22\,mm$ $(56/64\,inch)$, and $38\,mm$ $(96/64\,inch)$. As will be shown in figures later, it is relatively easy to see which data points belong to which opening. Also the upstream pressure do not vary very much for one opening. Because the gas mass fractions are rather similar, there are sharp distinctions between the mass flow rate through the choke opening areas: the cluster with the lowest mass flow rate are the data points for the smallest choke opening and the largest flow rates from the largest choke opening.

The upstream and downstream pipe diameter was not known for this data set. This is probably not a big issue, because the choke opening is so much smaller that it will dominate a term like $1/A_1^2 - 1/A_2^2$. Where the upstream or downstream area is needed for calculations, such as in Al-Safran and Kelkar's pressure recovery equation, the diameter $d_2 = 10\,cm$ has been used, because this is a standard size in the oil industry. [4]

The downstream pressure is measured at the separator location, which means that there is probably a considerable distance from the choke to where P_3 was measured. If so, there may have been pressure loss due to wall friction after the choke. Given that this is production data from a platform, it can be assumed that the distance between the choke and separator is some tens of meters, not more. This means that the pressure loss is in the order of magnitude of kilo pascal, which is little compared to the upstream pressure and the pressure drop across the choke. It was attempted to create a function of the form $\Delta P_{friction} = constant \times \dot{m}/\rho_m$ to find a more correct downstream pressure. But when applying this, with different values for the constant, and running the data set through

the models, the results were absolutely not better than when using the given separator pressure as P_3. Therefore, it was decided to use the separator pressure.

5 Results

The choke models for prediction of mass flow rate described in Section 3 were programmed in MATLAB®[11]. Among the built-in functions in MATLAB's library that were used were `mean` and `std` to calculate the statistical parameters described in the following section. The function `fzero`, which finds the root of a continuous function, was a great help in the iteration procedure to find the critical pressure.

Being primarily for two-phase flow, none of the models that differ between critical and critical flow, are able to give a proper prediction for the critical pressure for liquid-only flow. This may not be surprising, as theory dictates that for incompressible flow, the critical velocity is practically infinite. To avoid this situation, the calculation of y_c or P_{2c} was skipped for liquid-only data points and flow regime was set to sub-critical. $x_L = 0$ was not a problem for any models.

5.1 Evaluation Criteria

Three statistical parameters were chosen for evaluation and comparison of the choke models; mean relative error, E_1 in Equation (52), mean of absolute relative error, E_2 in Equation (53) and the standard deviation, σ in Equation (54). [3]

$$mean\,relative\,error:\ E_1 = \frac{1}{N}\sum_{i=1}^{N}\left(\frac{\dot{m}_{calc,i} - \dot{m}_{meas,i}}{\dot{m}_{meas,i}}\right) \times 100(\%) \tag{52}$$

$$mean\,of\,absolute\,relative\,error:\ E_2 = \frac{1}{N}\sum_{i=1}^{N}\left|\frac{\dot{m}_{calc,i} - \dot{m}_{meas,i}}{\dot{m}_{meas,i}}\right| \times 100(\%) \tag{53}$$

$$standard\,deviation:\ \sigma = \sqrt{\frac{1}{N-1}\sum_{i=1}^{N}\left[\left(\frac{\dot{m}_{calc,i} - \dot{m}_{meas,i}}{\dot{m}_{meas,i}}\right) - \frac{E_1}{100}\right]^2} \times 100(\%) \tag{54}$$

$\dot{m}_{calc}$ is the value predicted by the respective choke model, while $\dot{m}_{meas}$ is the observed mass flow rate.

The mean relative error describes the difference between predicted mass flow rate and the measured mass flow rate, and can take on both positive and negative values. If predictions are far from the measured value, but evenly distributed between over-predictions and under-predictions, this error will be close to zero, even though each prediction is rather wrong. The standard deviation says something about the amount of spread among the relative errors, but if all predictions are for example $20 - 25\,\%$ too high, the standard deviation will be low. E_2, the mean of absolute relative error, combines the attributes of E_1 and σ in that it will only be low if the error for each data point is small. For this reason, the discharge coefficient was tuned in order to minimize E_2. [10]

In figures, the error on the y-axis is the difference between the predicted and measured mass flow rate divided by the measured mass flow rate.

5.2 The Bernoulli Equation With Two-Phase Multiplier

Applied to the Porsgrunn Data Set

Figure 6a shows a graph of the calculated values for the mass flow rate compared to what was measured for the Bernoulli Equation with ρ_m and Chisholm's and Simpson et

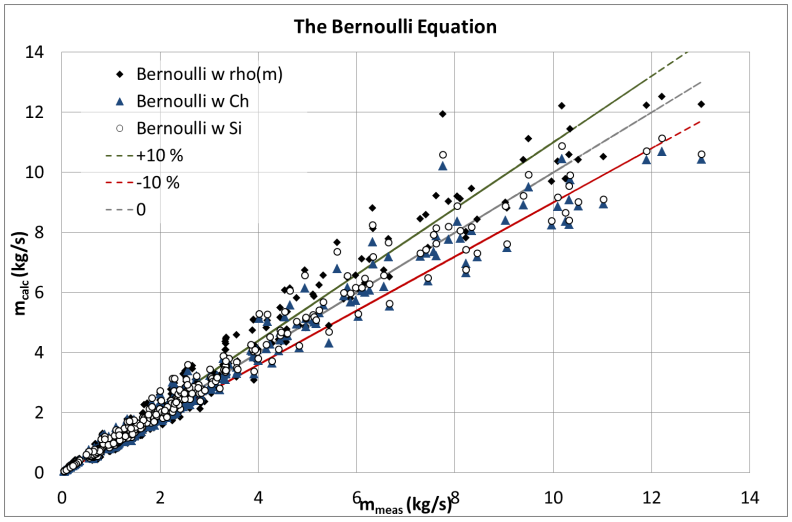

(a) Calculated vs. measured mass flow rate

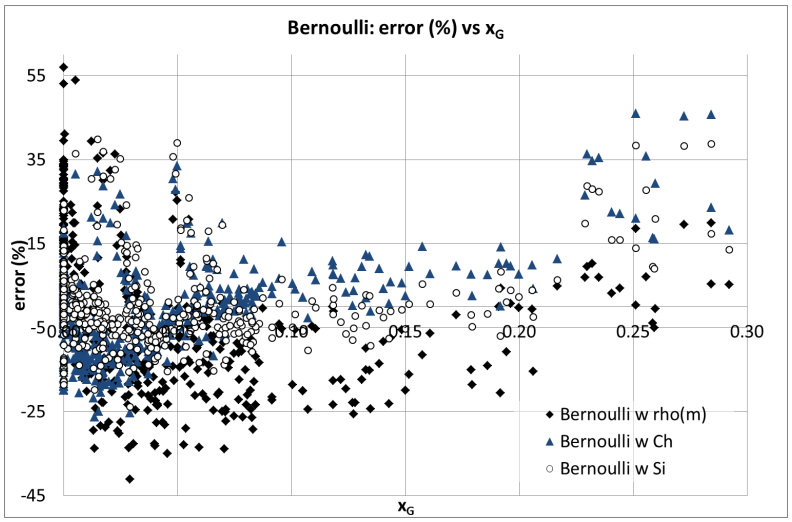

(b) Error vs x_G

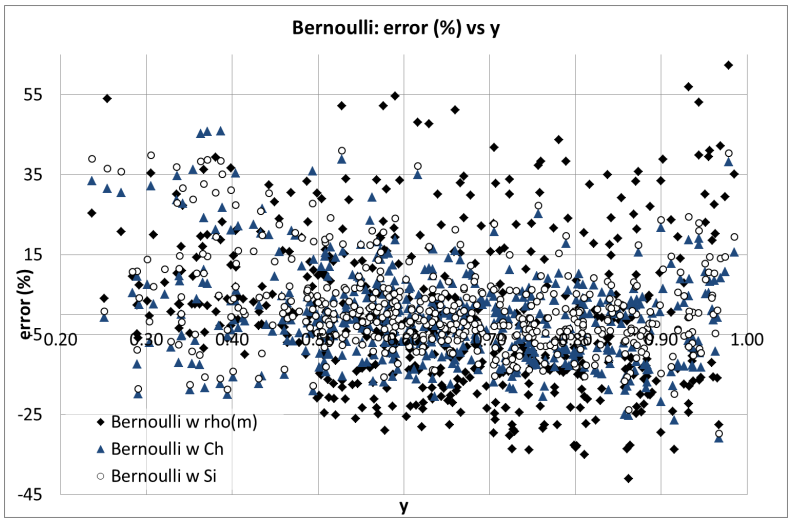

(c) Error vs $y = P_2/P_1$

Figure 6: Error distribution for the Bernoulli Equations, Porsgrunn data set (see also Appendix A on page 79)

al.'s two-phase multipliers. The discharge coefficients are tuned to minimize the relative absolute error and are summarized in Table 1 with the statistics given in Table 2.

Table 1: Discharge coefficients for the Bernoulli equations

(a) C_D-values for cage choke, Porsgrunn data set

Choke opening:	$11\,mm$	$14\,mm$	$18\,mm$
Bernoulli (ρ_m)	0.66	0.86	0.69
Bernoulli w $\Phi_{TP,Ch}$	0.63	0.66	0.59
Bernoulli w $\Phi_{TP,Si}$	0.64	0.69	0.61

(b) C_D-values for orifice choke, Porsgrunn data set

Choke opening:	$11\,mm$	$14\,mm$	$18\,mm$
Bernoulli (ρ_m)	0.68	0.82	0.74
Bernoulli w $\Phi_{TP,Ch}$	0.62	0.62	0.63
Bernoulli w $\Phi_{TP,Si}$	0.63	0.65	0.64

(c) C_D-values for field data

Choke opening:	$12\,mm$	$22\,mm$	$38\,mm$
Bernoulli (ρ_m)	0.48	0.53	0.72
Bernoulli w $\Phi_{TP,Ch}$	0.46	0.56	0.66
Bernoulli w $\Phi_{TP,Si}$	0.47	0.54	0.67

First of all, all three versions of the Bernoulli Equation give surprisingly good results. It seems that Simpson et al.'s Φ_{TP} is slightly better than Chisholm's, in spite of a much simpler slip model. However, looking at Figure 6b, it is clear that all three versions struggle when the gas mass fraction increases. Alone, without any slip model or two-phase multiplier, the Bernoulli Equation has more scatter in the results than with a Φ_{TP}. Slip is included in the two-phase multipliers, but could also be inserted directly into the Bernoulli Equation by the use of two-phase density ρ_{TP} or momentum density ρ_e. As was shown in Section 3.1, combining the momentum density with Simpson et al.'s slip model is the same as combining Chisholm's two-phase multiplier with Simpson et al.'s slip model, which again is the same as Simpson et al.'s original two-phase multiplier. The results of other possible combinations are summarized in Table 3. The corresponding C_D-values can be found in Appendix B.

Best results are produced by Simpson et al.'s Φ_{TP}, but also here the predictions drastically worsens as the gas mass faction increases. It is therefore possible that this trend is caused by the assumption of constant gas density.

Because none of the versions of the Bernoulli Equation differ between sub-critical and critical flow, it was expected that for low values of $y = P_2/P_1$, they would predict too high flow rates. From Figure A.3c, this is not as visible as might have been expected.

Applied to the Field Data

All three versions of the Bernoulli Equation give almost the same predictions for this data set, as can be seen in Figure 7 and from Table 11.

From the Porsgrunn data set, it was seen that the quality of predictions was dependent on gas mass fraction. This data set has in general much higher x_G than the Porsgrunn

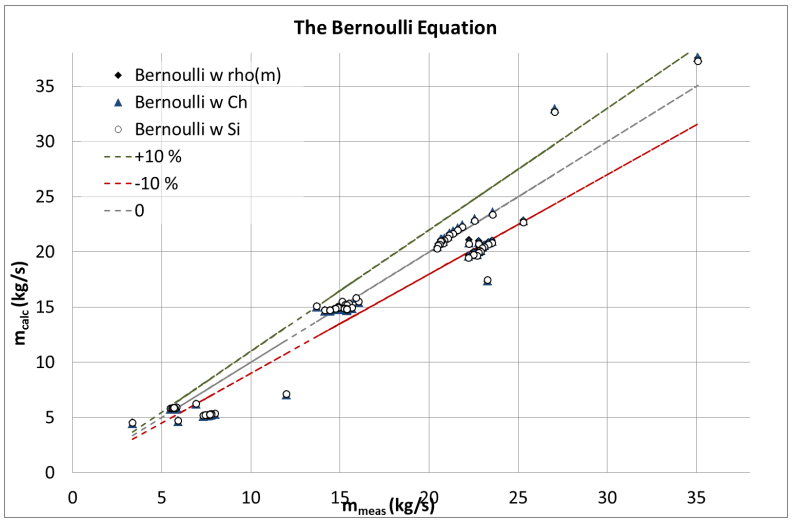

(a) Calculated vs. measured mass flow rate

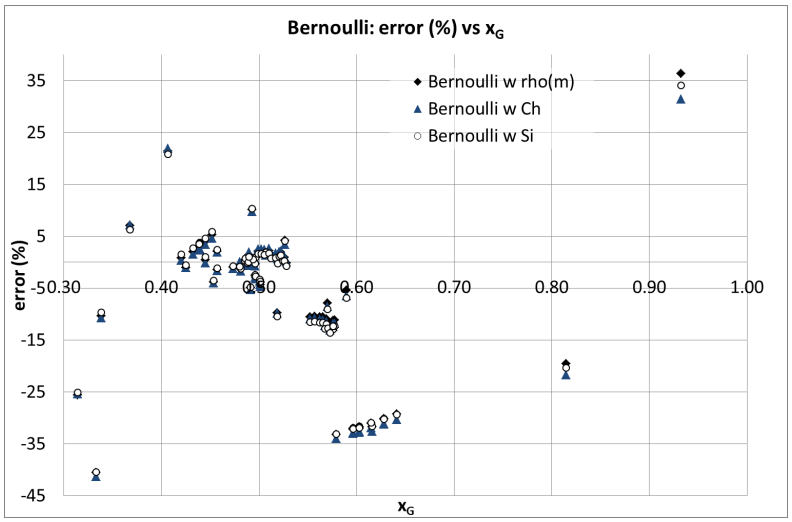

(b) Error vs x_G

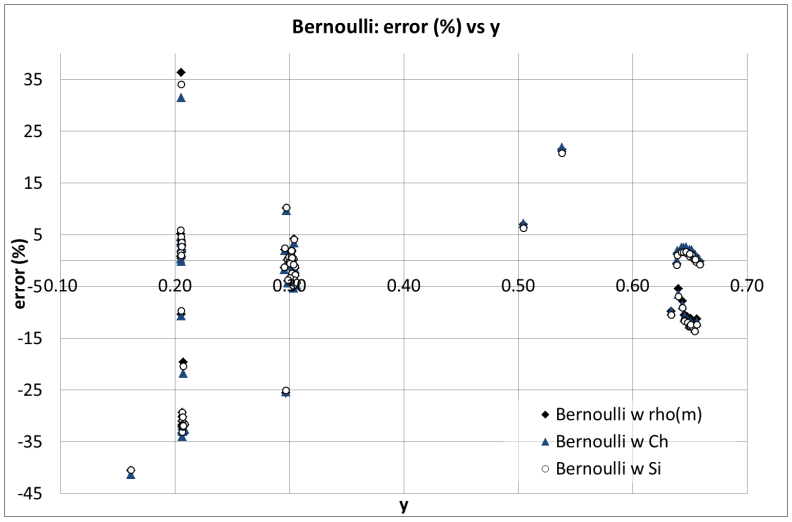

(c) Error vs $y = P_2/P_1$

Figure 7: Error distribution for the Bernoulli Equations, field data

data set, but they do not cover a wide range of values for each choke opening, therefore it is difficult to see if there is a trend in the error distribution in Figure 7b. There are, however, some very good predictions in the area $0.4 < x_G < 0.6$. In Figure 7c, it is especially visible which data points belong to which choke opening. The lump of points around $y_{actual} \approx 0.2$ belong to the $12\,mm$ choke opening, the ones around $y_{actual} \approx 0.3$ have choke opening of $22\,mm$ and the last group that spans a somewhat wider area are from largest, $38\,mm$, choke opening. From this, it can also be seen that the predictions are best for the $22\,mm$ choke opening, while there is much more scatter for the smallest opening. This is the case for all three versions of the Bernoulli Equation.

Table 2: The Bernoulli Equation Statistics (%)

	Porsgrunn Data			Field Data		
	E_1	E_2	σ	E_1	E_2	σ
Bernoulli (ρ_m)	−0.322	15.299	19.131	−6.407	9.508	13.614
Bernoulli w $\Phi_{TP,Ch}$	−0.288	9.006	11.930	−6.834	9.707	13.706
Bernoulli w $\Phi_{TP,Si}$	1.352	7.871	11.091	−6.560	9.636	13.573

In spite of a slightly higher standard deviation, it is the Bernoulli Equation with homogeneous mixture density that gives the best E_1 and E_2 in Table 2. Simpson et al.'s two-phase multiplier is the one with the lowest standard deviation. Summarized in Table 3, none of the other combinations are better than $\Phi_{TP,Si}$ for this data set.

Table 3: Different combinations for the Bernoulli Equations with Φ_{TP} and k

	Porsgrunn Data			Field Data		
Different combinations	E_1	E_2	σ	E_1	E_2	σ
Bernoulli w ρ_{TP} and k_{Ch}	1.742	10.239	13.715	-6.800	9.895	13.796
Bernoulli w ρ_{TP} and k_{Si}	1.427	12.885	17.065	-6.779	9.769	13.818
Bernoulli w ρ_e and k_{Ch}	-0.507	9.011	11.936	-6.834	9.707	13.706
Bernoulli w $\Phi_{TP,Si}$ and k_{Ch}	-17.905	26.333	30.866	-6.928	10.308	14.510

5.3 Asheim's Model

Applied to the Porsgrunn Data Set

The results from Asheim's model are not particularly good. E_2 and standard deviation in Table 5 show that it is not better than the Bernoulli Equation with $\Phi_{TP,Si}$, even though the mean relative error is one of the best so far. The values for the discharge coefficients, which can be found in Table 4 do not display the expected increase in value by decrease in choke opening, but the middle sized opening is the one with with highest C_D.

During calculation, Z is set to be one, which is an assumption that was made when calculating upstream gas density, (see Section 4.1 on page 19).

Figure 8 shows that the error distribution follows a very steep curve for small gas mass fractions, but this trend seems to flatten out as x_G increases above 0.05. The difference between predicted and measured mass flow rates varies from $-40\,\%$ to $80\,\%$, where the highest errors occur for data points that are almost single-phase flow, either liquid or gas.

Asheim's model is the model that predicts the most data points to be critical flow, but from Figure 8c, there seems to be a trend, although weak, where the predicted mass

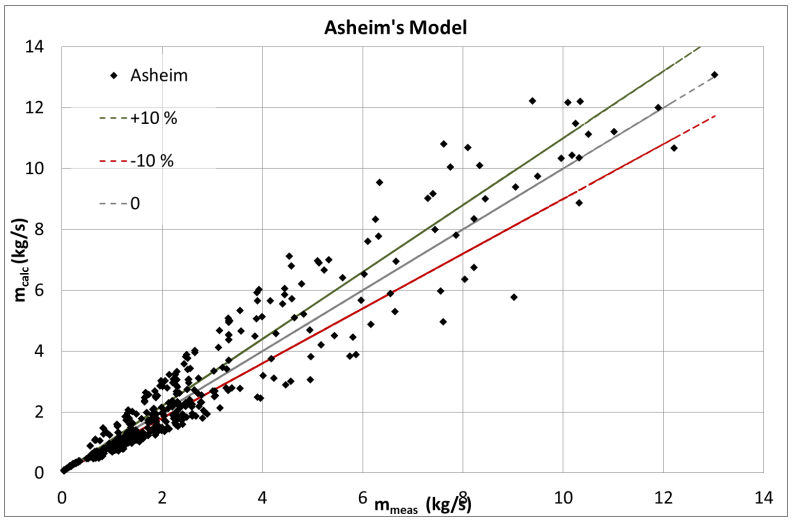

(a) Calculated vs. measured mass flow rate

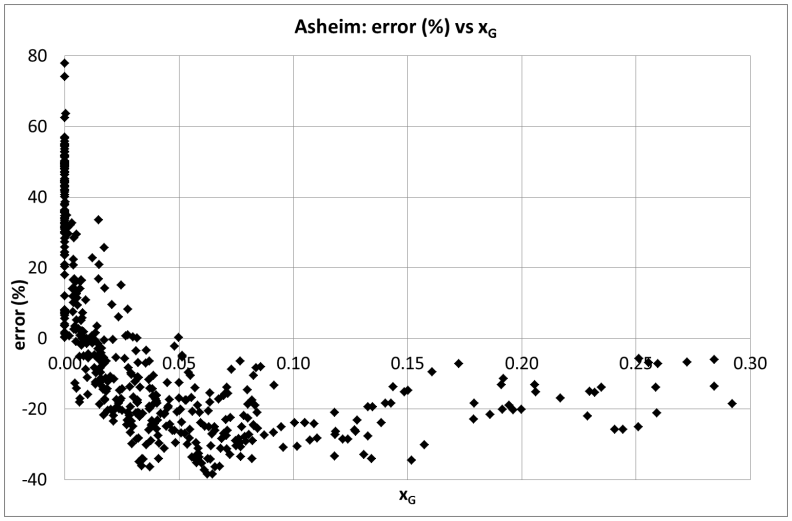

(b) Error vs x_G

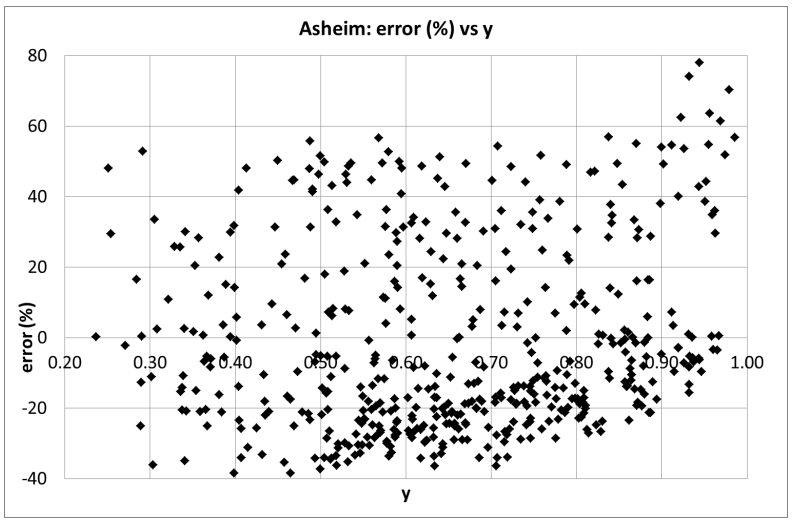

(c) Error vs $y = P_2/P_1$

Figure 8: Error distribution for Asheim's model, Porsgrunn data set
see also Appendix A on page 79

flow is too high for high pressure ratios (that is, little difference between upstream and downstream pressure) and too low for low pressure ratios.

Applied to the Field Data

The Z-factor that was calculated from the Yarborough and Hall method, when properties were converted from standard conditions to production conditions was also used when calculating mass flow rates with Asheim's model. The molar mass was then found by rearranging Equation (24). Results are shown in Figure 7 and Table 5. They are very similar to what was predicted by the Bernoulli Equation with two-phase multiplier.

Again, the greatest dispersion is seen around the $12\,mm$ choke opening, in Figure 9c. It seems that Asheim's model is not giving better results than the best of Bernoulli Equation for this data set either, even though approximately two thirds of data points are predicted to be critical flow, see Table 6. These data points belong to the smallest and middle sized choke opening, with only critical flow data points for the largest choke opening.

5.4 The Sachdeva et al. Model

Applied to the Porsgrunn Data Set

The results for the Sachdeva et al. model found in Figure 10 are not very different from those of Asheim's model. This should not be surprising, as the models are very similar. However, this model does give better results for both E_2 and standard deviation, summarized in Table 5 on page 40. The C_D-values can be found in Table 4. The same curve in the error distribution for low gas mass fractions that was present in Asheim's model, is also visible here, in Figure 10b. All in all, the Sachdeva et al. model is slightly better than Asheim's model in almost every point, but the improvement is not very large.

Applied to the Field Data

Also for this data set, the Sachdeva et al. model gives similar predictions as Asheim's, as can be seen in Figure 11. For the Porsgrunn data set, it was little but noticeable better, but in this case the situation is almost turned around. At least, the advantage it had over Asheim's model is much less visible, both when comparing graphs and from the error analysis in Table 5. The values for the discharge coefficients are given in Table 4. The tuned C_D-values for Sachdeva et al.'s model are lower than those tuned for Asheim's model, both for this set of data and the Porsgrunn test facility data set, although the resulting predictions for Sachdeva et al.'s model are not always lower than those from Asheim's model. This is especially illustrated for the largest choke opening, by comparing Figure 9c and Figure 11c, or Figure A.6c in Appendix A on page 79.

5.5 Al-Safran and Kelkar's Model

While the other models were quite straight forward to program, Al-Safran and Kelkar's model presented a challenge because there are two different expressions for k; one to be used with sub-critical flow and another for critical flow. It is difficult to know which expression to use when calculating the critical pressure ratio y_c. Therefore, two values of y_c was calculated; one using k_{Si} and another value with k_{modCh}. If the observed y was

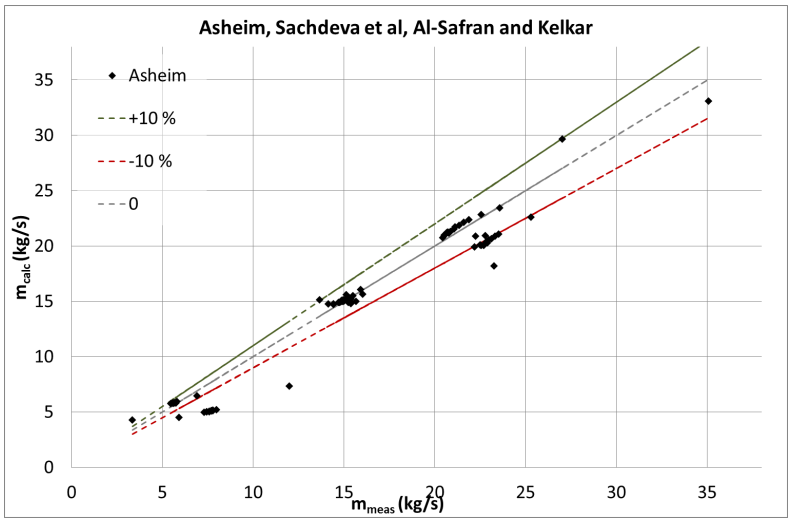

(a) Calculated vs. measured mass flow rate

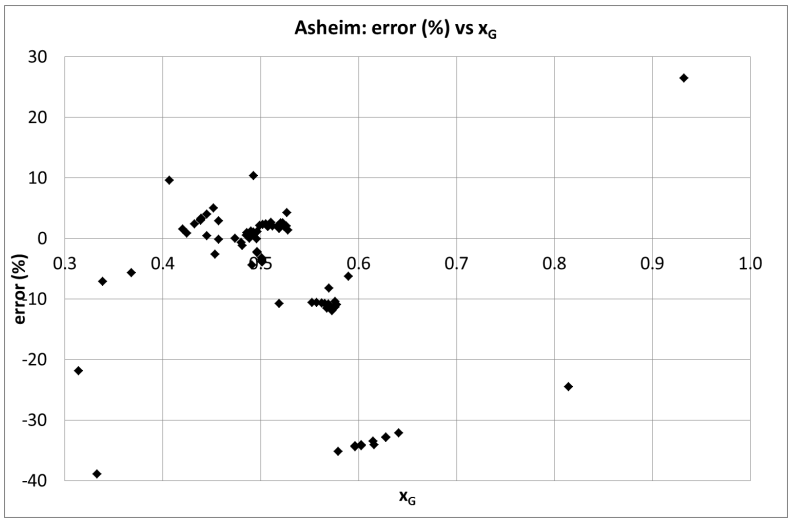

(b) Error vs x_G

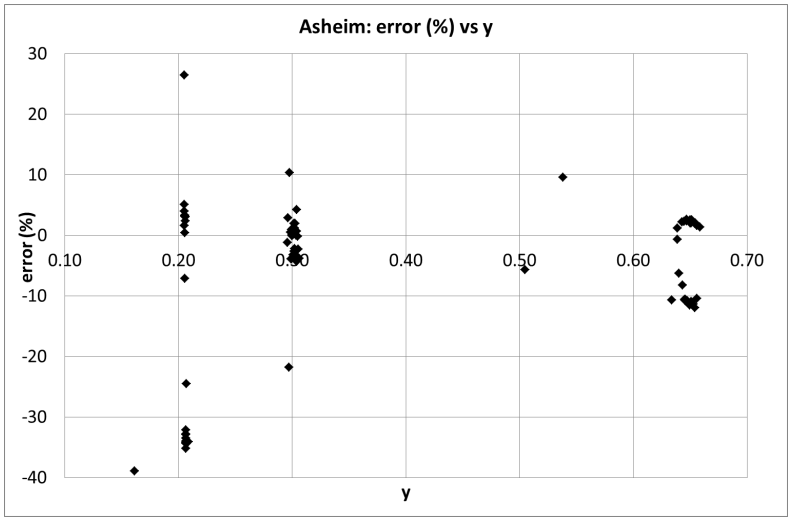

(c) Error vs $y = P_2/P_1$

Figure 9: Error distribution for Asheim's model, field data

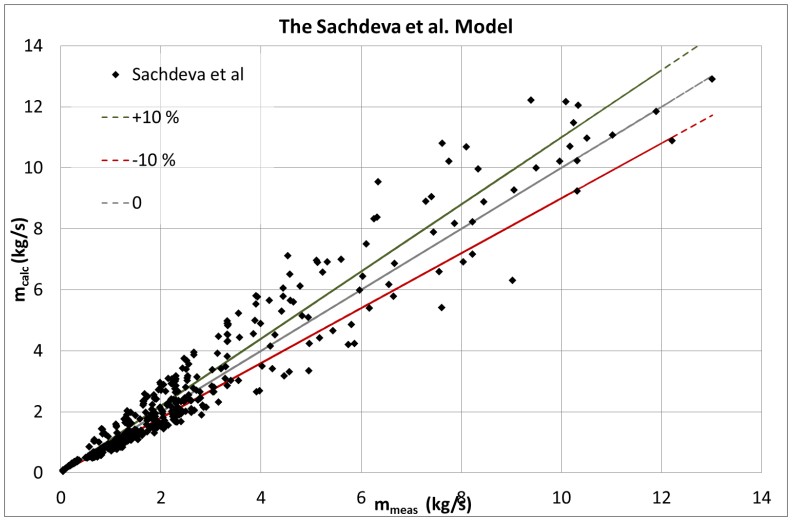

(a) Calculated vs. measured mass flow rate

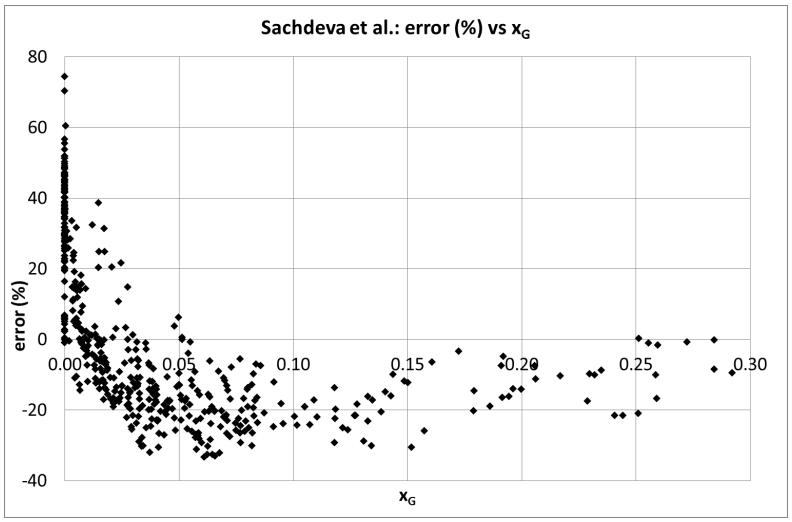

(b) Error vs x_G

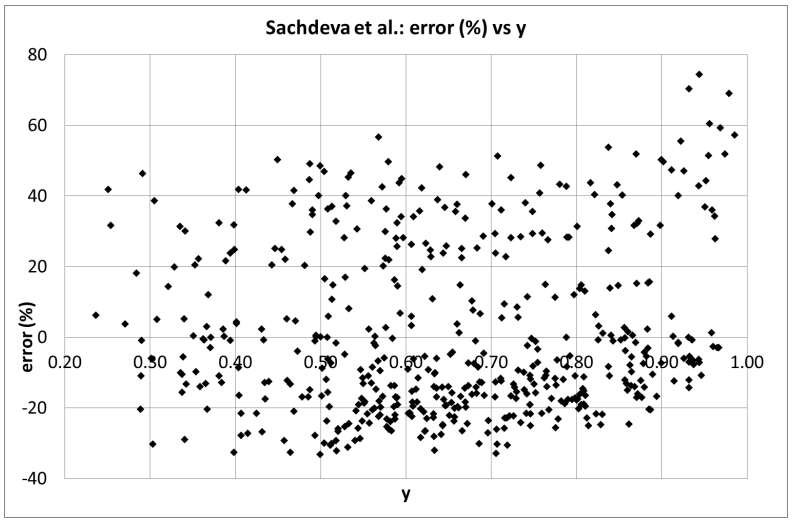

(c) Error vs $y = P_2/P_1$

Figure 10: Error distribution for the Sachdeva et al. model, Porsgrunn data set (see also Appendix A on page 79)

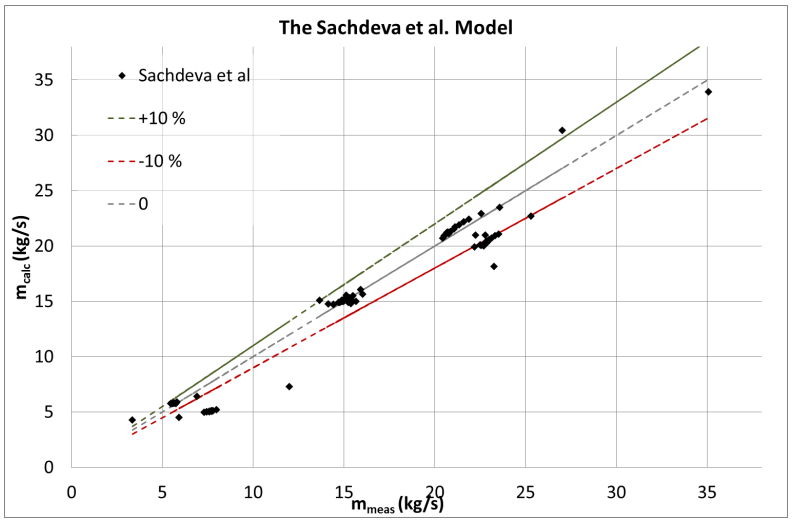

(a) Calculated vs. measured mass flow rate

(b) Error vs x_G

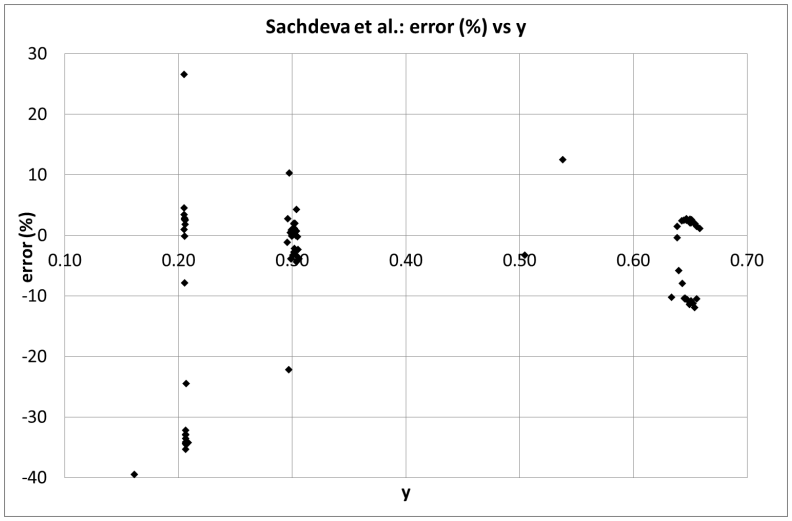

(c) Error vs $y = P_2/P_1$

Figure 11: Error distribution for the Sachdeva et al. model, field data

either lower or higher than both y_c-values, the case is clear for which kind of flow regime there is. Then one can go back and use the appropriate expressions for either sub-critical or critical flow and calculate the mass flow rate accordingly. [9]

However, because k_{modCh} is expected to be larger than k_{Si}, $y_c(k_{modCh})$ will be lower than $y_c(k_{Si})$, as can be seen in Figure 16 on page 40. The solid red line is the y_c-value calculated with k_{Si}, whereas the dotted red line represents y_c when using k_{modCh}. In some cases encountered, the observed y fell in-between these two. Comparing the observed y to the y_c assuming critical flow will cause the model to predict sub-critical flow, while compared to the y_c assuming sub-critical flow the result should be critical flow. In these cases, the average of the two flow rates is used as prediction. For the Porsgrunn data set, this occurs 20 (out of 508) times, but for the field data it was not an issue.

Applied to the Porsgrunn Data Set

This is the first model presented here that takes both phase slippage and pressure recovery into account. Therefore, it is expected to be the best so far. The results shown in Figure 12 show that it gives better results than Asheim and Sachdeva et al.'s model, in spite of some inconsistent data points. Nevertheless, the model still does not give better results than the Bernoulli Equation with Simpson et al.'s Φ_{TP}. In Figure 12b, there can still be discerned a curve in the error distribution with respect to x_G, although it is not so distinct as for Asheim and Sachdeva et al.'s models. In many ways, it is more similar to the error distribution of the Bernoulli Equation with Simpson et al.'s Φ_{TP}.

The values for discharge coefficients are found in Table 4 and the statistics are summarized in Table 5.

In three out of six cases, the C_D-values are larger than unity. Except for the largest choke opening, there is also less difference between the values for cage choke and orifice choke with the same opening for this model than for the other models. In fact, Asheim's model and the Sachdeva et al. model both have a difference of 0.9 between the C_D for cage and orifice choke for the $11\,mm$ and $14\,mm$ openings, while only $0.2 - 0.3$ for the largest opening. For Al-Safran and Kelkar's model it is opposite: the largest difference is found for the largest openings; 0.9, while for the two others, the difference is no more than 0.6.

The pressure recovery lies around P_2 being $80 - 99\,\%$ of the measured downstream pressure.

Applied to the Field Data

The results are shown in Figure 13 and Table 5. This was the statistically best model for the Porsgrunn data set, but does not stand out in the same positive way when looking at this set of data. But again, there is little difference between the results from this model and the previous models.

As the model includes A_3, in Equation (37), not knowing A_3 could be a source of error, especially for the largest choke opening. By adjusting A_3 and trying different values between $8\,cm$ and $15\,cm$, then retuning C_D, it was seen that for the two smallest choke openings, the C_D-values were unchanged, while for $38\,mm$ opening, there was a difference. However, the mean of absolute relative error was in fact lowest for $d_3 = 10\,cm$, with the corresponding $C_D = 1.20$, as given in Table 4. This would suggest that $d_3 = 10\,cm$ is a reasonable assumption, and not a large source of error.

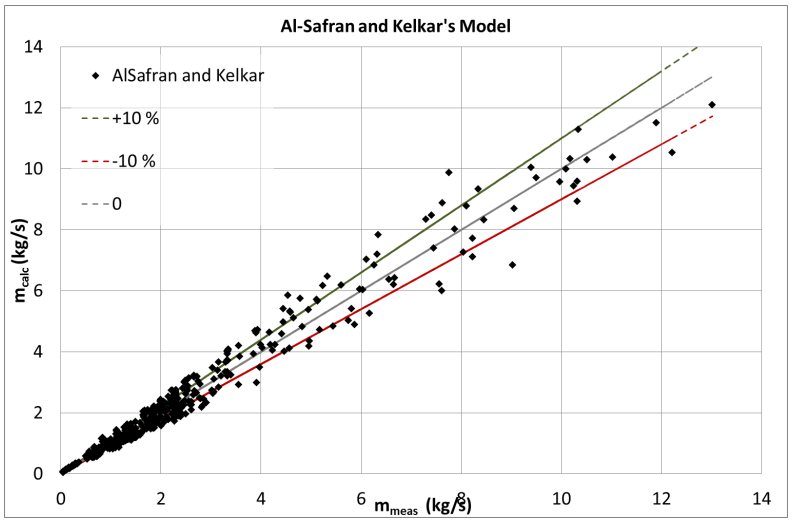

(a) Calculated vs. measured mass flow rate

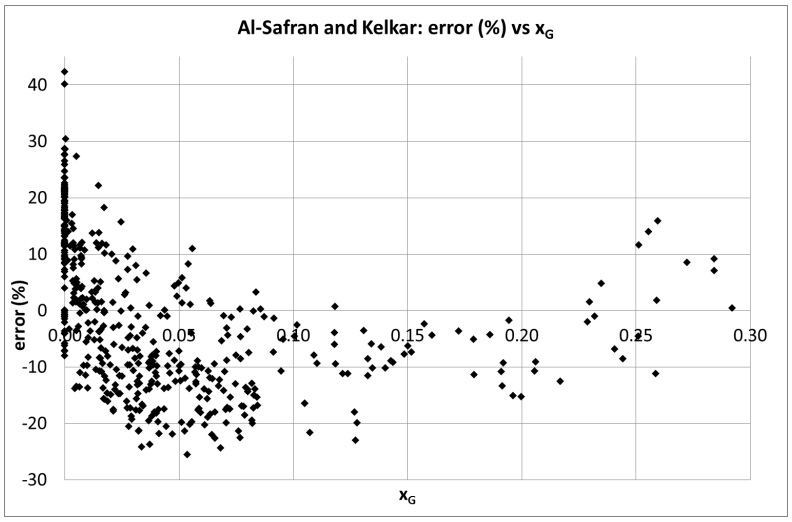

(b) Error vs x_G

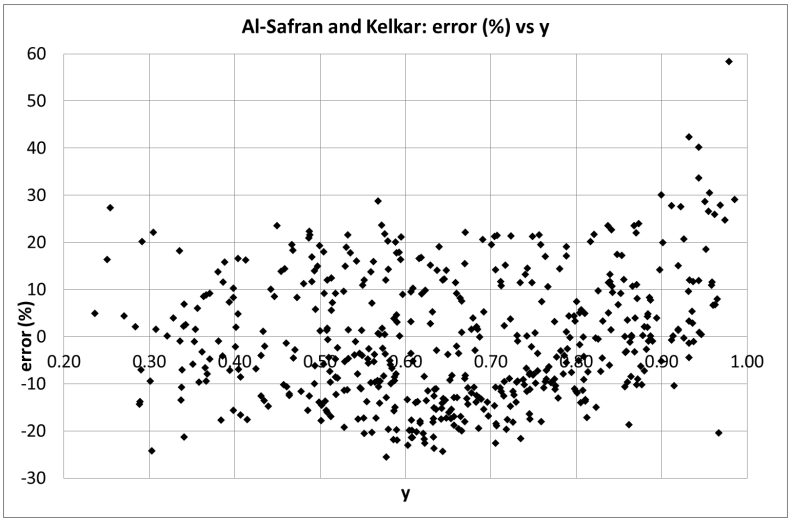

(c) Error vs $y = P_2/P_1$

Figure 12: Error distribution for Al-Safran and Kelkar's model, Porsgrunn data set (see also Appendix A on page 79)

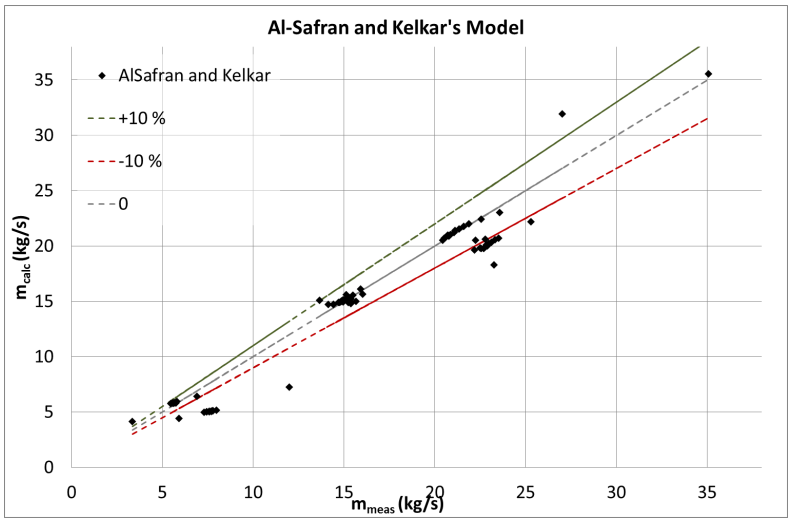

(a) Calculated vs. measured mass flow rate

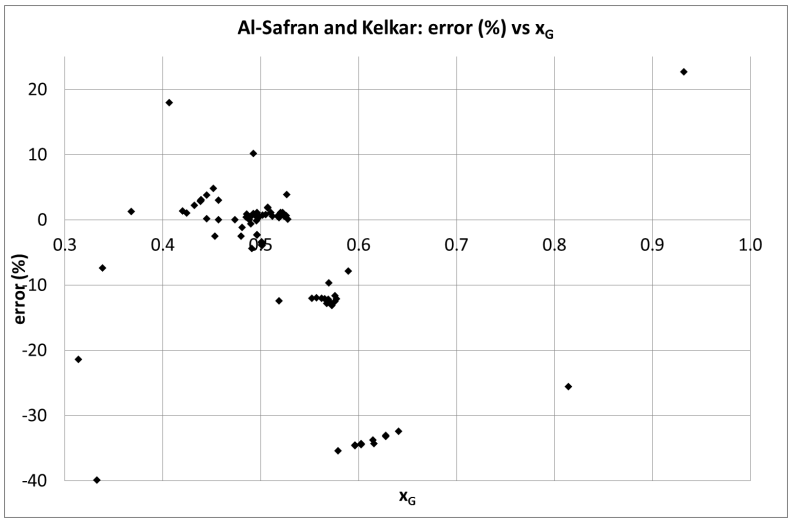

(b) Error vs x_G

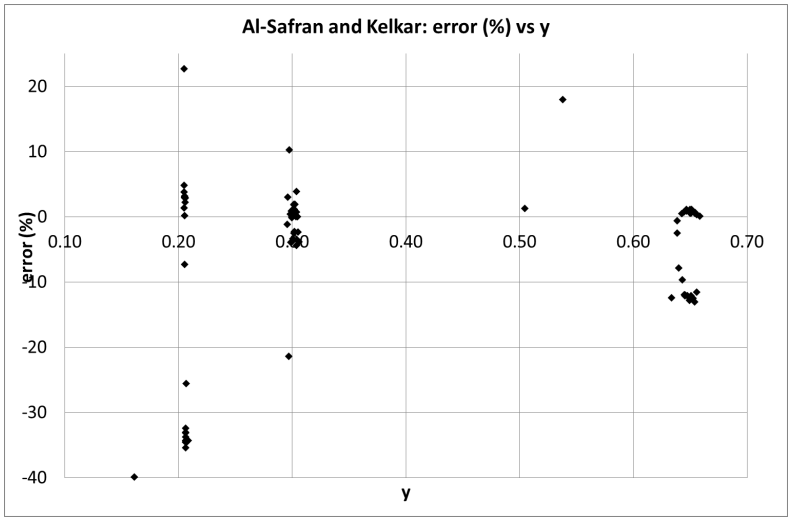

(c) Error vs $y = P_2/P_1$

Figure 13: Error distribution for Al-Safran and Kelkar's model, field data

In spite of having high C_D-values, all of them above unity, most of the predictions are lower. This is especially true for the largest choke opening, where the model for pressure recovery will have highest impact on the prediction. For the two largest choke openings, the pressure recovery is between 10 and 20 %, while for the smallest choke opening, it lies relatively stable at $8 - 9$ % of the measured downstream pressure.

5.6 The Original Hydro Model

Applied to the Porsgrunn Data

Figure 14 shows the results for the Hydro Model. Especially Figure 14b is an improvement from the previous models, and any trend is difficult to see. From Table 5, it is better than Al-Safran and Kelkar's model and even the Bernoulli Equation with Simpson et al.'s two-phase multiplier.

When it comes to the error distribution with respect to y, however, there seems to be a trend for the model to predict too high mass flow rates for small pressure drops and too low flow rates for high pressure drops.

The C_D-value, given in Table 4 decreases as the choke opening increases, both for cage and orifice chokes. This is the only model for which the discharge coefficients are in a descending order, quite the opposite of theory.

When it comes to pressure recovery, the Hydro Model predicts this to be less than Al-Safran and Kelkar's model, with an average of 3 %. The absolute highest pressure recovery of 18 % is predicted for the data point with the highest pressure drop across the choke.

This set of data was used by Schüller et al. [14, 15] when modifying Chisholm's slip model, by tuning ξ and β. For the Hydro Model with Chisholm's original expression, see Section 6.4 on page 47.

Applied to the Field Data

The field data all come from one choke geometry, which is thought to be suitable for the long model of the Hydro Model, but the data set was also run through the short model, for comparison. As can be seen in Figure 15, the two versions, with different C_D-values, gave very similar results. Statistically, the long model seems to give marginally better results than the short. However, the Hydro Model is actually the model to produce the worst statistics, see Table 5 for this data set. The difference between this and the other models is not very large, though.

Although the pressure recovery predicted by the Hydro Model is less than what Al-Safran and Kelkar's model predicts, the difference is smaller for this data set than it was for the Porsgrunn data set. On average, P_2 is 90 % of the measured downstream pressure.

5.7 Summary

One of the most interesting things to observe is that the Bernoulli Equation with $\Phi_{TP,Si}$ gives very good results for both data sets. Even the simpler Bernoulli Equation with ρ_m is better than the more complicated models of Asheim and Sachdeva et al..

The Hydro Model is the one to give best results for the Porsgrunn data. It has the advantage that the slip model is tuned especially towards this data set. But also Al-Safran and Kelkar embrace this modified version of Chisholm's slip model and keep the

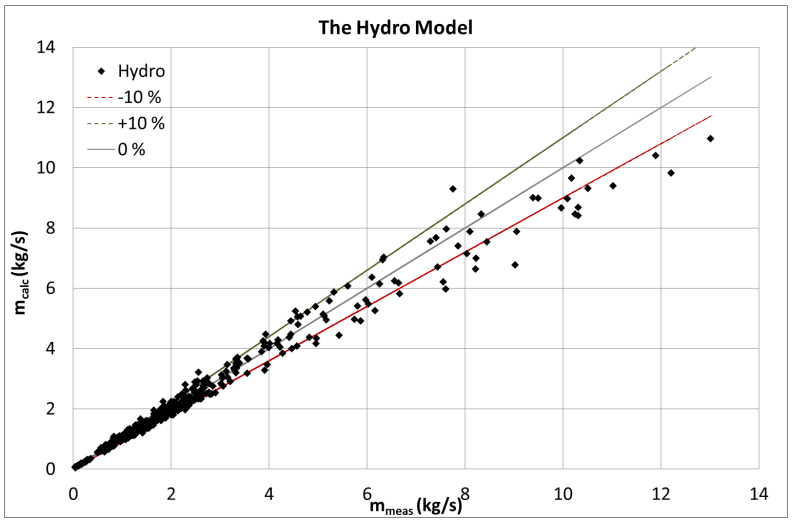

(a) Calculated vs. measured mass flow rate

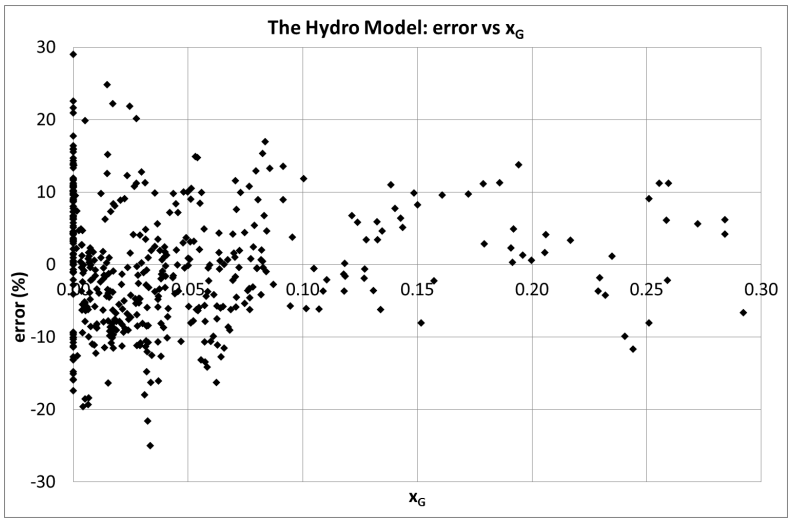

(b) Error vs x_G

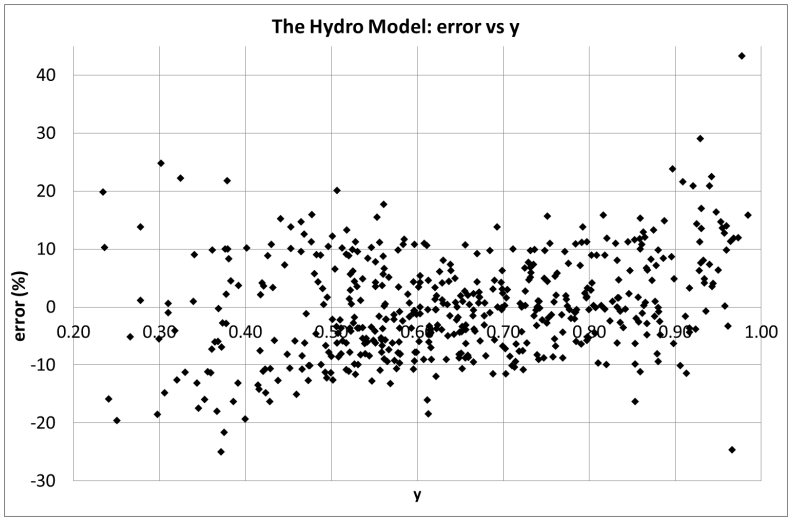

(c) Error vs $y = P_2/P_1$

Figure 14: Error distribution for the Hydro Model, Porsgrunn data

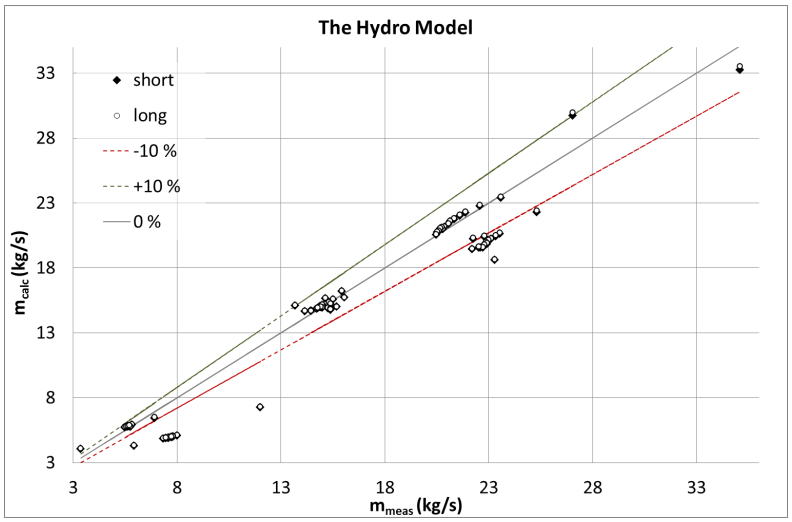

(a) Calculated vs. measured mass flow rate

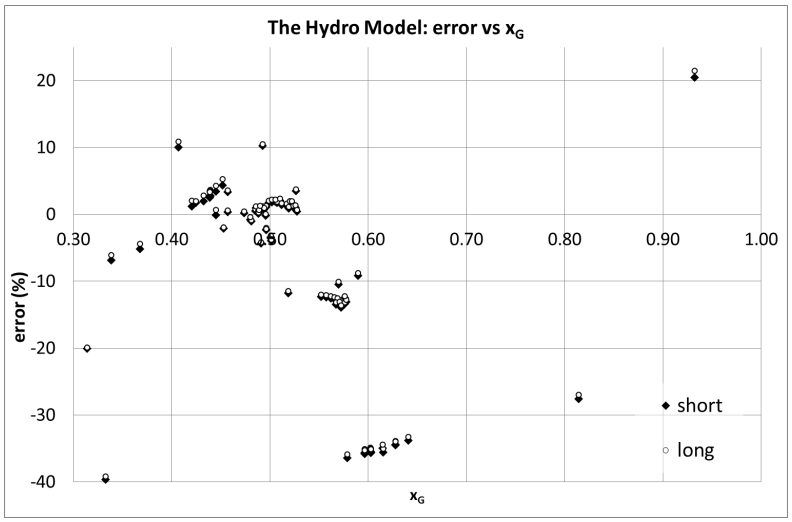

(b) Error vs x_G

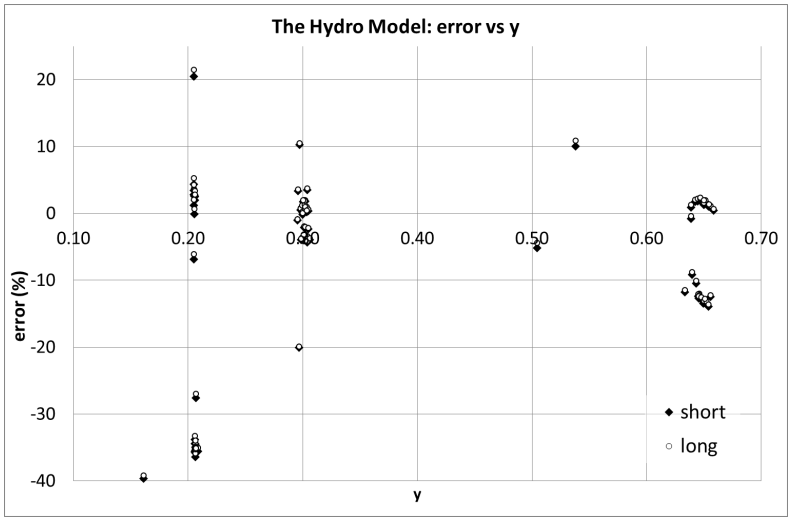

(c) Error vs $y = P_2/P_1$

Figure 15: Error distribution for the Hydro Model, field data

same constants when they develop their model for critical flow. [3] This suggests that the modification is an improvement more generally, not just for the Porsgrunn data set.

When applied to the field data, however, neither Al-Safran and Kelkar's model or the Hydro Model perform very well, and the situation is turned around: apart from the Bernoulli Equation with $\Phi_{TP,Si}$, the models that give best results for the Porsgrunn data set are the worst for the field data, and vice versa. There are many critical points for the field data, therefore k_{modCh} with its two constants the two constants ξ and β probably influence the results also for Al-Safran and Kelkar's model. Thus, the models that use k_{modCh}, are the two worst. It would therefore be interesting to see if changing the slip model can improve these results, which will be further discussed in Section 6.4 on page 47.

For the Porsgrunn data set, it is possible to see a development in error distribution, if there is any, for both gas mass fraction and pressure ratio, as the data points are spread over a wider range of properties. The field data are clumped into three groups, for each choke opening, and it is therefore more difficult to discover any trends. But they are actual production data, and it is useful to see how the models handle, for example, the higher pressure and less controlled circumstances they represent.

When it comes to the field data, there seems to be little doubt about whether there is critical or sub-critical flow. For the Porsgrunn data set, however, the models range from predicting 114 out of 508 critical flow data points in Asheim's, to only 40 in the Hydro Model.

Table 4: Discharge coefficients for Asheim's, Sachdeva et al.'s and Al-Safran & Kelkar's and Hydro models

(a) C_D-values for cage choke, Porsgrunn data set

Choke opening:	11 mm	14 mm	18 mm
Asheim	0.94	1.00	0.81
Sachdeva et al.	0.90	0.98	0.81
Al-Safran & Kelkar	1.03	1.09	0.91
The Hydro Model	0.49	0.48	0.42

(b) C_D-values for orifice choke, Porsgrunn data set

Choke opening:	11 mm	14 mm	18 mm
Asheim	0.85	0.91	0.79
Sachdeva et al.	0.81	0.89	0.78
Al-Safran & Kelkar	0.98	1.03	1.00
The Hydro Model	0.66	0.66	0.64

(c) C_D-values for field data

	12 mm	22 mm	38 mm
Asheim	0.92	1.04	0.99
Sachdeva et al.	0.82	0.93	0.91
Al-Safran and Kelkar	1.11	1.23	1.20
Hydro Model, long	0.56	0.64	0.56
Hydro Model, short	0.78	0.87	0.78

Figure 16 shows hos the critical pressure ratio, $y_c = P_{2c}/P_1$, varies with gas mass fractions, all other properties unchanged for the different models. In accordance with

Table 5: Statistics (%) for Asheim's, Sachdeva et al.'s, Al-Safran & Kelkar's and Hydro's models

	Porsgrunn Data			Field Data		
	E_1	E_2	σ	E_1	E_2	σ
Asheim	-0.740	22.377	26.574	-6.827	9.636	13.764
Sachdeva et al.	1.366	19.973	24.139	-6.867	9.593	13.818
Al-Safran & Kelkar	-0.664	11.268	13.536	-7.281	9.702	13.849
Hydro Model, long	0.067	6.993	8.859	-7.423	9.982	14.056
Hydro Model, short				-7.626	9.973	14.081

Table 6: Critical points, predicted by Asheim, Sachdeva et al., Al-Safran and Kelkar, the Hydro Model

	Porsgrunn Data Set	Field Data
Asheim	114	59
Sachdeva et al.	105	59
Al-Safran and Kelkar	83*	59
The Hydro Model	40	59**

* +20 in-between critical and sub-critical
** both long and short

theory, the critical pressure ratio drops toward zero as the gas mass fraction approaches zero. As the Hydro Model gives the lowest y_c, it is not surprising that it is the model to predict fewest critical points.

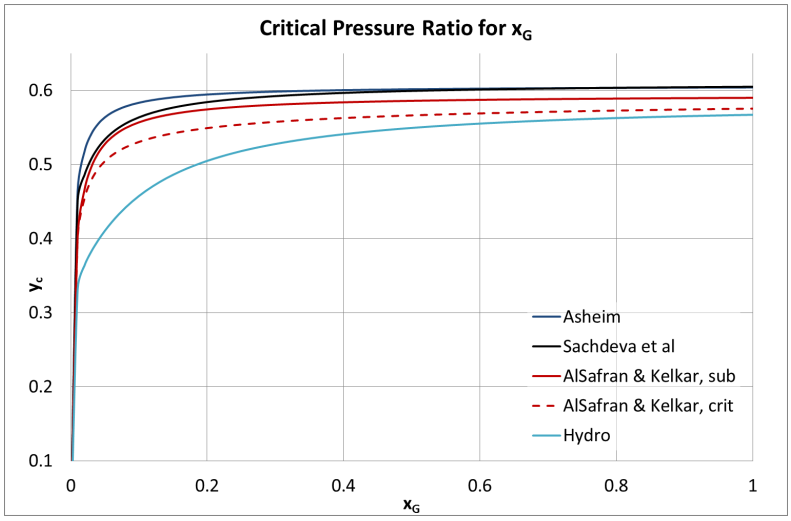

Figure 16: How $y_c = P_{2c}/P_1$ varies with x_G

6 Modifying The Hydro Model

In this section, several features of the Hydro Model will be looked at separately, in order to discover their importance and effect on the final results. As was seen from Figure 14c, the model as a tendency to predict too high mass flow rates for high pressure ratios and too low mass flow rates for low pressure ratios. Figure 17a shows some of the same issue, but in a different way, where the predictions for most sub-critical data points are too high, and the closer to critical the data point is, the lower is the predicted value. The aim of this section is to find a way to remove this trend without worsening the results, and simplify or verify parts of the model.

A possible solution to the problem could be to decrease the curvature of the $\dot{m}_{calc}\, vs.\, P_2$ curve as shown in Figure 3 on page 11 in a way that the maximum point is moved upwards and to a lower pressure, but without changing the the sub-critical prediction too much. If the diagonal trend in Figure 17a is evened out, the predictions can be tuned down with the discharge coefficient.

The features that will looked at in the following sections are pressure recovery, the numerical integration of $1/\rho_e$, density calculation of a two-phase fluid, slip model and gas expansion.

6.1 Pressure Recovery

The only reason why two iteration procedures are necessary in the Hydro Model is the inclusion of pressure recovery. This makes it a lot more time consuming than any of the other models presented here. Therefore, it would be interesting to see how much improvement this additional time and actually gives.

Figure 18 shows a graph of how substantial the pressure recovery is for the Porsgrunn data set. P_2 is never less than 80 % of P_3, most of the time more than 90 %. Dropping the pressure recovery in the model could result in a considerable difference in the mass flow rate predictions, but it is hoped that the discharge coefficient could absorb some of it. The main conscern is therefore the border between sub-critical and critical flow.

Running the Hydro Model for the Porsgrunn data set without pressure recovery, where $P_2 = P_3$, and not using Equation (45) or (46), yielded the results given in Table 7 and Figure 19, after retuning C_D.

Table 7: The Hydro Model without pressure recovery: statistics

The number in parenthesis is change from the original value in Table 5

	Porsgrunn data			Field data		
	E_1	E_2	σ	E_1	E_2	σ
Hydro, long	-0.122 (+0.055)	6.820 (-0.173)	8.651 (-0.208)	-8.162 (+0.739)	9.979 (-0.003)	14.027 (-0.029)
Hydro, short				-7.985 (+0.359)	10.002 (+0.029)	13.920 (-0.161)

The results are absolutely not worse than with pressure recovery, at least not for the Porsgrunn data set. Although the average relative error has increased somewhat in magnitude, the standard deviation and average absolute relative error have both decreased, which means that there is now less spread among the errors. From Figure 19c, not includ-

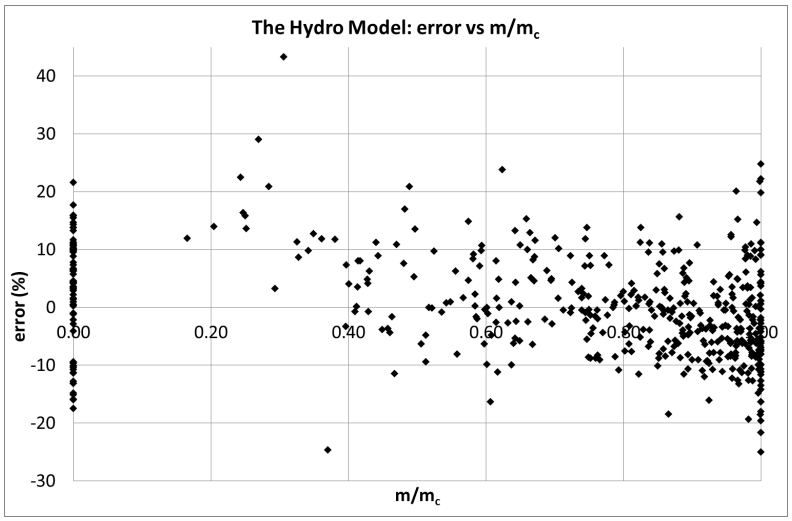

(a) Error vs. $\dot{m}_{calc}/\dot{m}_{c(calc)}$

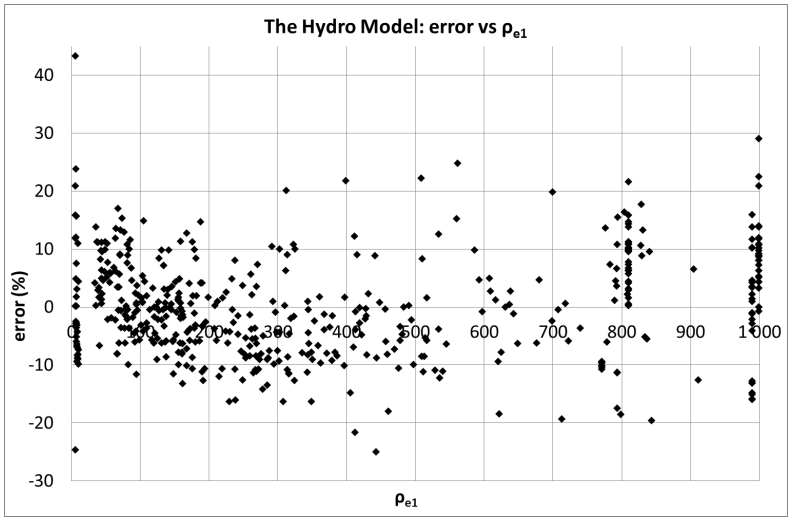

(b) Error vs. ρ_{e1}

Figure 17: The original Hydro Model error distribution

ing the pressure recovery seems to help a bit in evening out the targeted trend explained above.

The C_D-values are almost unchanged, which is another sign that pressure recovery does not have a great impact on the flow rate predictions. That the little change there is, is an increase rather than a decrease is also sensible, because without pressure recovery the pressure difference across the choke is smaller, and predicted the mass flow rate with the same C_D will also be smaller.

For the field data, it does not seem so obvious that pressure recovery is unnecessary. Also for this data set the standard deviation decreases, although very little. Graphs similar to Figure 19 for the field data can be found in Appendix A. Especially E_1 increases in magnitude, but with less than half a percentage point for the short model. The C_D-values for the different choke openings both increase and decrease for both long and short model, which is unexpected.

MATLAB®'s built-in function `tic toc` makes it easy to measure the time the Hydro Model needs to calculate mass flow rates for all 508 data points in the Porsgrunn data set. Taking the average over 100 runs, when including pressure recovery, it took 6.01 seconds

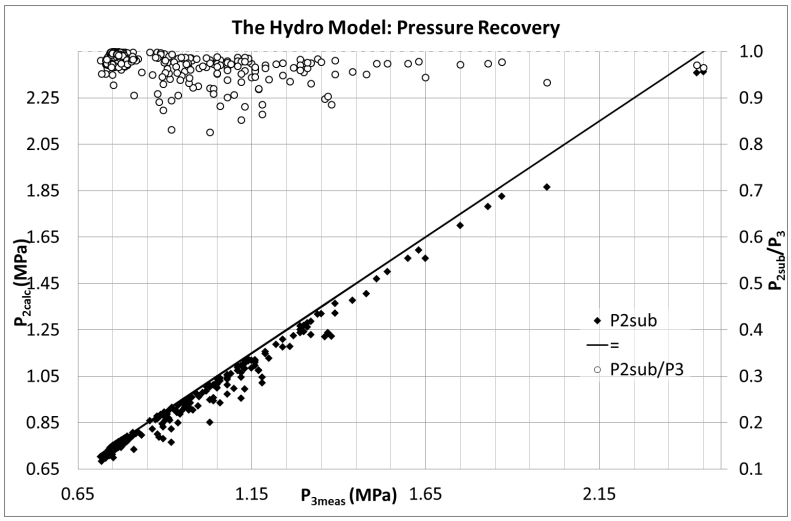

Figure 18: The Hydro Model: Pressure Recovery, Porsgrunn data set

Table 8: The Hydro Model without pressure recovery: C_D

The number in parenthesis is change from the original value in Table 4

(a) C_D-values for the Porsgrunn data set

	11 mm	14 mm	18 mm
Cage (Hydro, long)	0.49 (-)	0.48 (-)	0.43 (+0.01)
Orifice (Hydro, short)	0.67 (+0.01)	0.66 (-)	0.65 (+0.01)

(b) C_D-values for the field data

	12 mm	22 mm	38 mm
Hydro, long	0.55 (-0.01)	0.63 (-0.01)	0.57 (+0.01)
Hydro, short	0.78 (-)	0.86 (-0.01)	0.80 (+0.02)

to go through the data set. Without pressure recovery, the average run time was reduced to 3.58 seconds.

All in all, skipping the pressure recovery from the Hydro Model seems to be an acceptable option. It greatly simplifies the model, both when it comes to computational time and complexity. Continuing without it, also makes it easier to change other features within the model.

The one iteration that is left, finding the critical pressure, can be done in two ways. Either, Equation (44) can be differentiated and set equal to zero to find the P_{2c} corresponding to the maximum mass flow rate, or one can continue to use the iteration $\dot{m}^2{}_{1-2} - \dot{m}_c^2 = 0$.

6.2 Merging the Long and Short Submodels

Removing the pressure recovery term in the Hydro Model simplifies the model more than just removing one iteration: The only difference between the long and short model lies in calculation of $\dot{m}_{2-3}$, where the long model uses A_2 as the flow area in the choke, while the short model uses $A_{vc} = C_D A_2$. This causes the sub-critical mass flow rates for the long and short versions to be slightly different, and depending on which model is used,

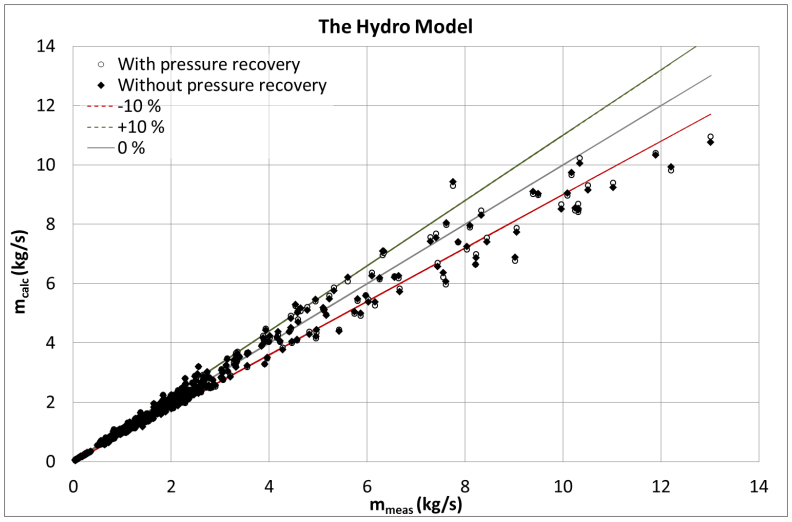

(a) Calculated vs. measured mass flow rate

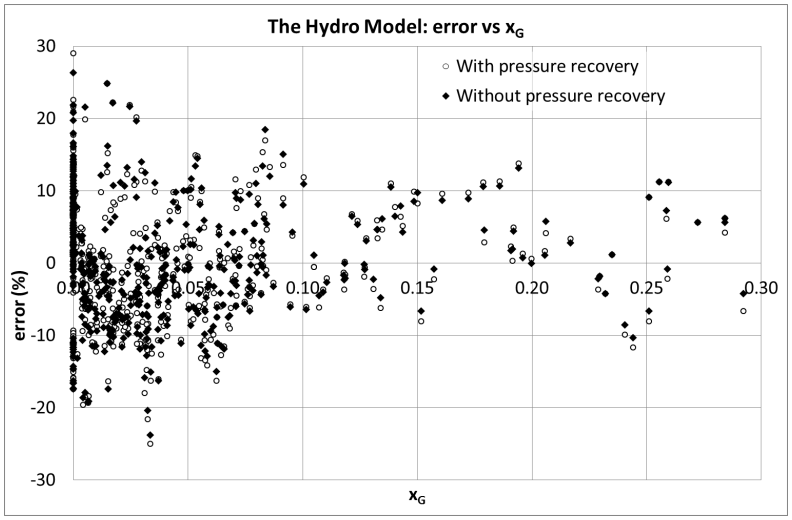

(b) Error vs x_G

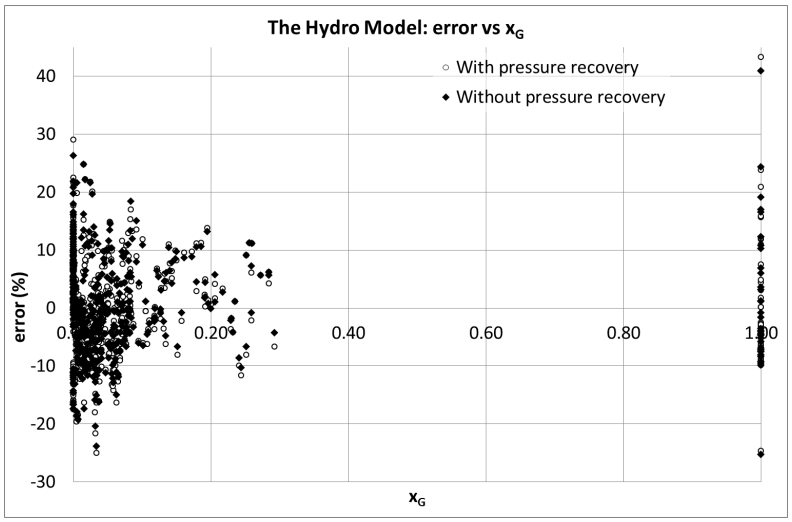

(c) Error vs $y = P_2/P_1$

Figure 19: Error distribution for the Hydro Model without pressure recovery, Porsgrunn data

the prediction for sub-critical or critical flow could be different. However, when Equation (45) and (46) are no longer in use, the long and short models are identical. This can be shown better by rearranging Equation (43) into:

$$\dot{m}_{1-2}^2 = \frac{2\int_{P_1}^{P_2} \frac{1}{\rho_e} dp}{\frac{1}{A^2\rho_{e1}^2} - \frac{1}{A_2^2\rho_{e2}^2}\left[\left(\frac{1}{C_D} - 1\right)^2 + 1\right]} \quad (long) \tag{55}$$

and then comparing the expressions for C_D, by writing:

$$C_{D,short}^2 = \frac{1}{\left(\frac{1}{C_{D,long}} - 1\right)^2 + 1} \tag{56}$$

That this actually is the case, can be seen from the C_D-values for the field data in Table 8, where the same data set has been run through both models. Putting the discharge coefficients for the long model into Equation (56), the C_D for the short model, within rounding margin, is obtained. The reason for the difference in the error measurements in Table **??** are thought to be due to the fact that C_Ds are tuned to two decimal points, which is not as exact as Equation (56). Calculating C_D for the short model from the discharge coefficients for the long model and rerunning the short model, produces identical results for long and short versions of the Hydro Model.

As it has been suggested to neglect pressure recovery, there is only need for one model henceforth. This simplifies the Hydro Model even further, making the difference between including pressure recovery or not larger. Neglecting pressure recovery not only reduces the number of iterations from two to one, but also makes it unnecessary to have one model for long contractions and another for short. Discharge coefficients should continue to be tuned separately for orifice and cage chokes, though, because of their different geometry.

The new C_Ds for cage geometry chokes and statistical parameters are summarized in Table 9-11 on page 60 and onwards.

6.3 The Density Integral

The integral of momentum density

$$\int_{P_1}^{P_2} \frac{1}{\rho_e} dP = \int_{P_1}^{P_2} \left(\frac{x_G}{\rho_G} + k_{modCh}\frac{x_L}{\rho_L}\right)\left(x_G + \frac{x_L}{k_{modCh}}\right) dP \tag{57}$$

is a complicated expression as k_{modCh} (or k_{Ch} or k_{Si} if those should be used) also includes ρ_G. Selmer-Olsen developed a numerical integration formula to integrate it, using the Gauss-Legendre method. It calculates the momentum density separately, so another slip model could be substituted for k_{modCh}. Also, another expression for the density could be used with the formula.

6.3.1 Verification in MATLAB®

MATLAB has a large library of built-in functions that simplifies programming. Among others, the some of them can integrate user-defined functions by numerical integration, where the user can choose between several different numerical integration algorithms. A few of these were chosen to compare to the formula used in the Hydro Model, both in

order to get an impression of its accuracy and see if another version would improve, or worsen, the predictions.

From Figure 2 on page 6, it is seen that the momentum density, therefore also $1/\rho_e$ should be similarly smooth. Then MATLAB's `quadl` seems appropriate, as it is suitable for smooth functions and gives higher accuracy than adaptive Simpson quadrature (`quad`). `quadl` uses adaptive Lobatto quadrature. `quad` and `quadgk` (using adaptive Gauss-Kronrod, it is suitable for high accuracies and also infinite intervals, although the latter will not be an issue here) [11] were also included, for comparison.

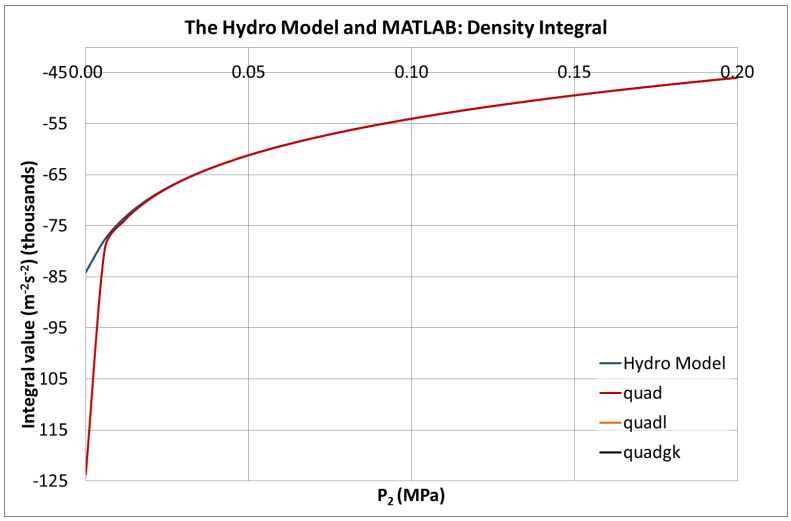

Figure 20: The Hydro Model: Density integral, the original vs MATLAB methods `quad`, `quadl` and `quadgk` are so similar that their lines are on top of each other $P_1 = 2.91\,MPa$ and $x_G = 0.28$

The values of the density integral for some numerical integration formulaes are shown in Figure 20. Around atmospheric pressure, the difference between the original integral and `quadl` is 0.0001 %, and as P_2 increases, the difference becomes even less. Only for so low downstream choke pressures that they are only theoretically interesting, is there a maximum difference of 5 % between the numerical method used in the Hydro Model and what MATLAB functions calculate. When running the Hydro Model with `quad`, `quadl` or `quadgk`, the differences in mass flow rates or P_{2c} are not observable.

From these observations, it seems that because the momentum density follows a smooth, monotonously increasing curve, the results are not particularly sensitive for which numerical integration method is being used.

6.3.2 Trapezoidal Method Approximation

When it was discovered that all three MATLAB functions and the original integration formula gave as good as identical results, it was thought that it may be possible to simplify the integral even further, by utilizing the very simple trapezoidal method. Figure 23 suggests that the inaccuracy of approximating $1/\rho_e$ by a straight line, as the trapezoidal method does, may give adequate results. It is feared, however, that especially for large pressure drops, the inaccuracy may be too high a price to pay for the simplicity.

Introducing a trapezoidal approximation into Equation (44) and retuning C_Ds give the results for the Porsgrunn data set shown in Figure 22 and Table 10. This was noticeably

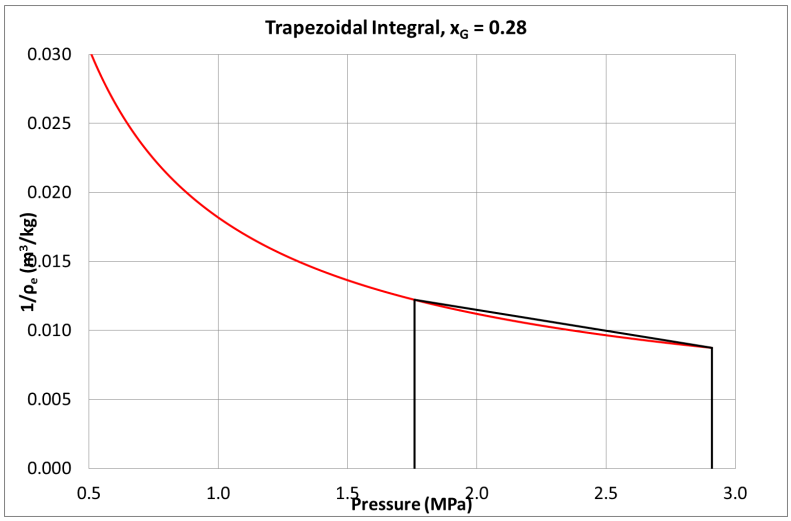

Figure 21: The Hydro Model, sketch of trapezoidal approximation for density integral

worse, especially for y, where the trend in over-predicting the mass flow for low pressure drops and under-predicting the ones for high pressure drops is aggravated.

As can be seen from Figure 23, the trapezoidal approximation lifts the original $\dot{m}_{calc}$-curve, before retuning the C_D. This is in accordance with Figure 20 where it can be seen that the trapezoidal method overestimates the actual integral, making the absolute value in the nominator larger than for the original integration formula. Retuning C_D, the curve is lowered closer the original again, and it should be noted that the shape of the curve has not changed much between P_1 and the maximum point.

For the Porsgrunn data set, the trapezoidal approximation the the density integral noticeably worsened the results compared to the original integration formula, especially when looking at the standard deviation. Neither the results from the field data shows any positive change. As a result, the original numerical integration formula should be kept.

6.4 Density Average and Slip Model

The momentum density ρ_e was chosen because its derivation is based on momentum flux, which makes it suitable for use in the momentum equation. But as was seen in Figure 2, there is clearly a difference between the different densities. When changing expression for density and slip, MATLAB's `quadl` was used to calculate $\int (1/\rho)\, dP$ to be sure that the integral calculation was not influenced by the original ρ_e and k_{modCh}. Also, whenever substituting another slip model or density equation, a new expression for $\frac{d}{dP}(1/\rho)$ has to be calculated.

6.4.1 Homogeneous Density

Results from Section 5 suggests that slippage between the gaseous and liquid phases is an important part of any model. To better see the significance of slip in the Hydro Model, it was run once without any slip. The homogeneous density that was used for this is given in Equation (8) on page 4. When assuming gas and liquid to flow with the same velocity in modeling, the gas must take up a larger portion of the flow area in order to produce the same gas flow rate as when the gas is allowed to flow faster than the liquid phase. This causes the homogeneous density to be lower than both two-phase density and momentum

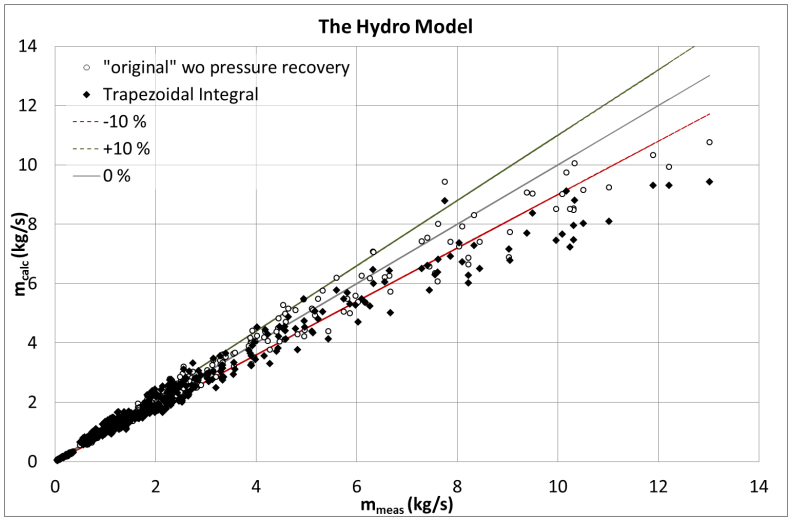

(a) Calculated vs. measured mass flow rate

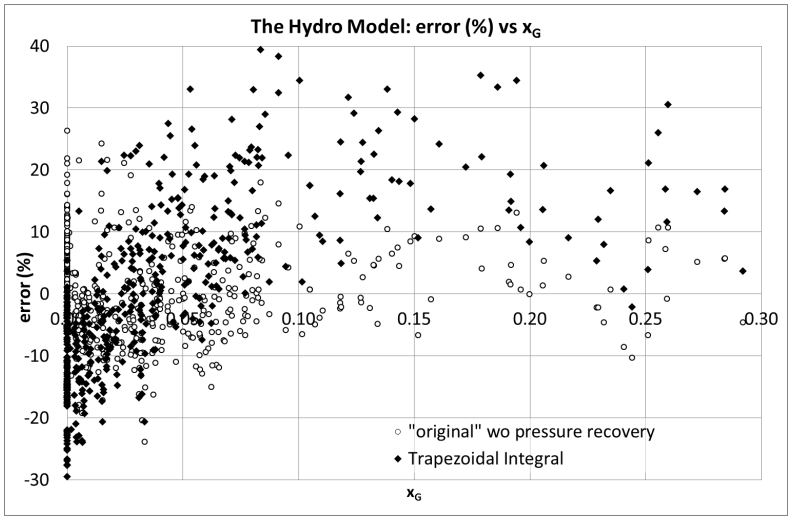

(b) Error vs x_G

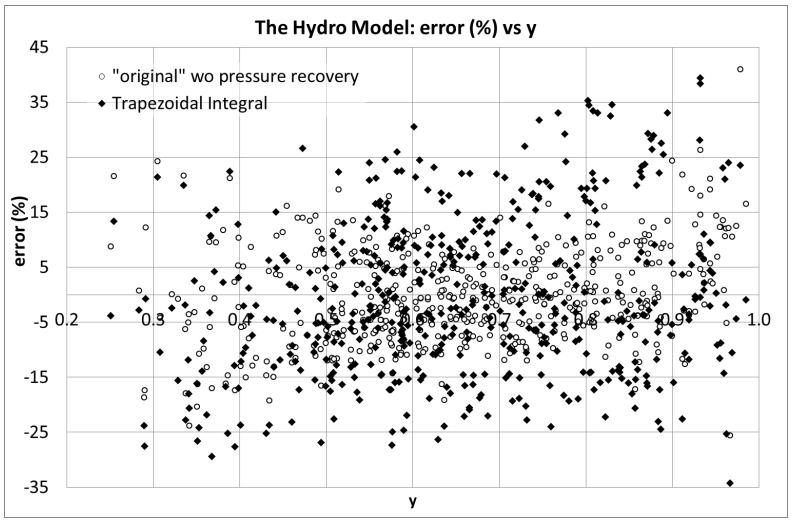

(c) Error vs $y = P_2/P_1$

Figure 22: Error distribution for the Hydro Model with trapezoidal approximation in integral, Porsgrunn data

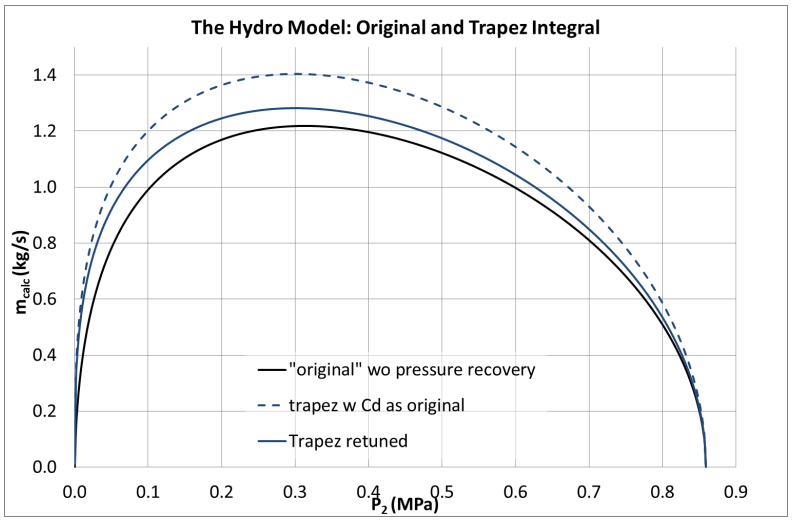

(a) From the Porsgrunn data set, $x_G = 0.01$ and $P_1 = 0.86\,MPa$

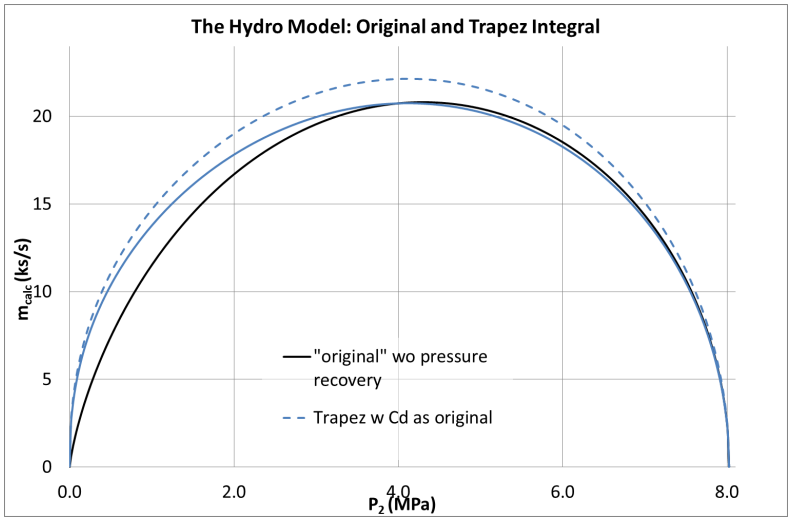

(b) From the field data, $x_G = 0.59$ and $P_1 = 8.02\,MPa$

Figure 23: The Hydro Model: $\dot{m}_{calc}$ vs P_2 for trapezoidal approximation to density integral

density, and reduces the amount of mass that can flow through an area per time unit.

The results for the Porsgrunn data set are shown in Figure 24. It can be seen that the curve, or sudden drop in the error distribution with respect to gas mass fraction, in Figure 24b, is comparable to the error distribution for Asheim and Sachdeva et al.'s models, which do not include slippage either. There is a lot more spread in the results without slip, although there seems to be approximately as many over-predictions as under-predictions (low E_1). There are also more data points that are predicted to be critical now than when including a slip model. The C_D-values in Table 10 are considerably higher than when including slip.

In Figure 24c, there seems to be two layers of data points in the horizontal direction, where the upper layer consists of data points that are over-predicted, and the bottom layer of mostly under-predicted data points. From Figure 2, it is seen that the homogeneous density is much lower than the original momentum density. Therefore, when using, and integrating ρ_m, a lower value will result, leading the retuned C_D to be higher than the original in order to bring the prediction up again. However, for data points within the same choke opening and geometry category, the same C_D has to be used for single-phase

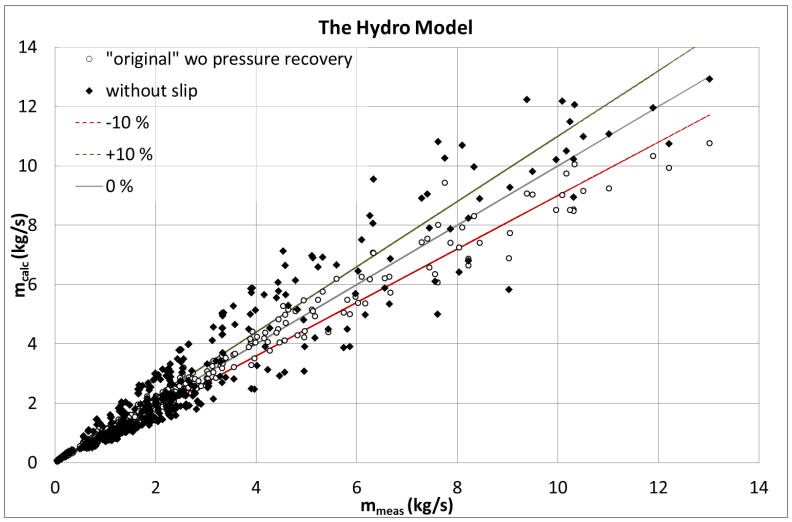

(a) Calculated vs. measured mass flow rate

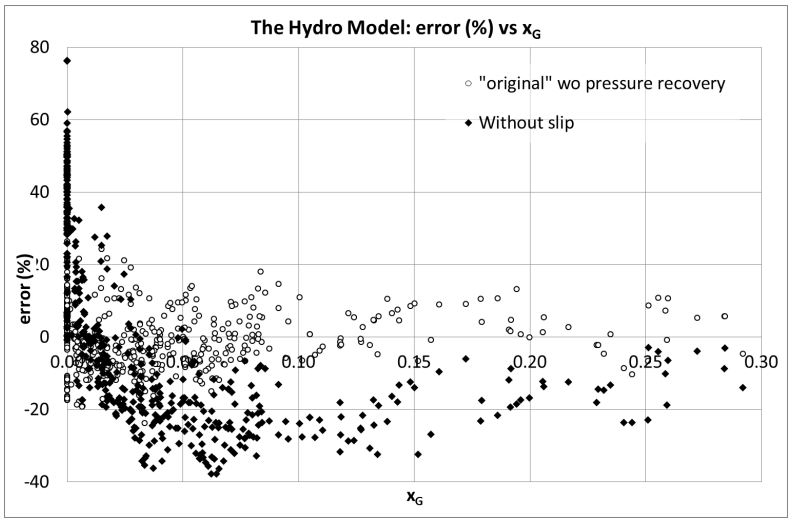

(b) Error vs x_G

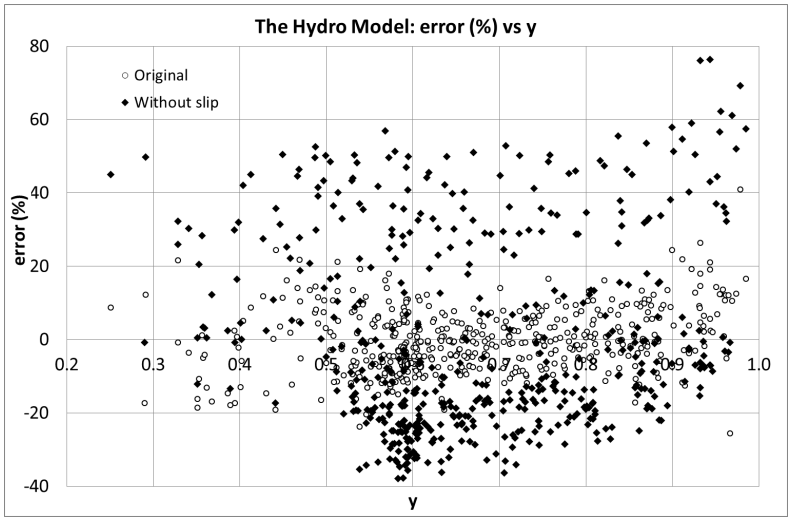

(c) Error vs $y = P_2/P_1$

Figure 24: Error distribution for the Hydro Model without slip

and multiphase flow. As a consequence, the upper layer in Figure 24c is made up almost solely single-phase flow data points, either gas-only or liquid-only, because the new C_D is too high. But the C_D-value is still too low for the multiphase data points, leading them to make up the bottom layer. The general trend of a diagonal line from low pressure ratios up to high pressure ratios, is still present, though.

From this, it seems that slippage is a very important part of the Hydro Model.

6.4.2 The Slip Models

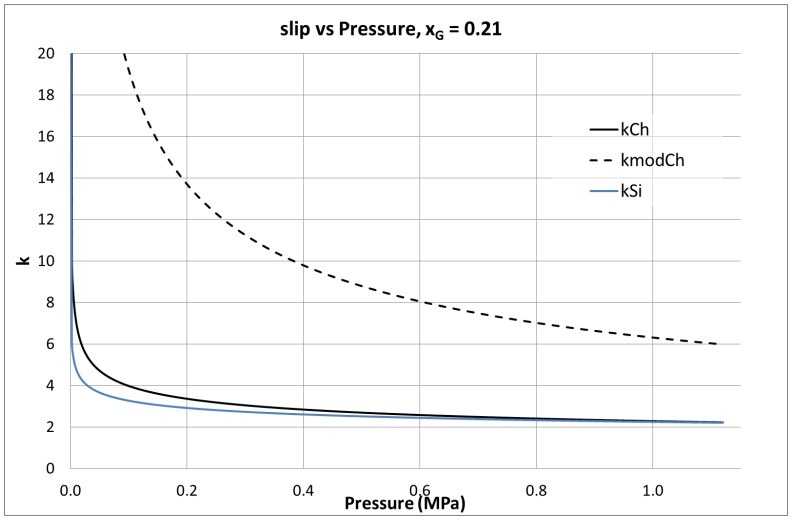

(a) Slip vs pressure

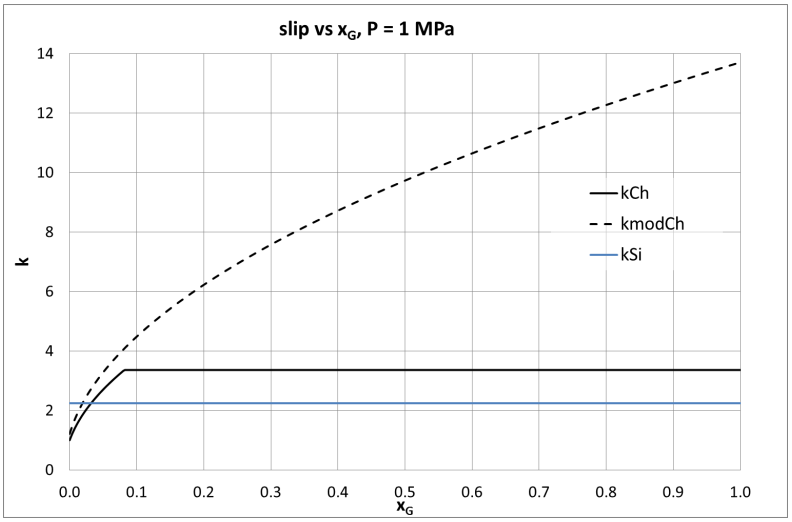

(b) Slip vs x_G

Figure 25: Three slip models

There are three different slip models that have been presented here: Chisholm in Equation (14), Simpson et al. in Equation (16), and modified Chisholm in Equation (49). The two latter includes at least one factor that can be tuned; in k_{Si} there is a and modified Chisholm has ξ and β, which have been tuned to the Porsgrunn data set and are purely experimental. Simpson et al.'s $a = 1/6$ has a more physical meaning, as that is the only value of the constant for which Equation (23) on page 10 is true for $\Phi_{2P,Si}(k_{Si})$ as well.

How the slip models change with pressure and gas mass fraction, are shown in Figure 25. For a given x_G, the modified Chisholm slip model always give the highest slip, while Chisholm and Simpson et al. are very close to each other as the pressure increases. This is also the case for other pressures: k_{Ch} lies a little above k_{Si}, but where they meet depends on x_G. The less gas there is, the steeper is the beginning of the curve. Also, the lines of k_{Ch} and k_{Si}, will eventually cross so that $k_{Ch} < k_{Si}$ for high pressure. As can be seen in Figure 25a, the slip decreases as the pressure increases. This is because under higher pressure, the fluid will become more and more homogeneous, and there is expected to be less slip [14].

Figure 25b shows clearly where where the Lockhart-Martinelli parameter becomes less than one, and from there on and higher gas mass fractions, the slip is constant for both Chisholm's and Simpson et al.'s slip models. The modified Chisholm model, however, continues to increase until it reaches a maximum value at $x_G = 1$. This absolute maximum will fall out of the equation for two-phase density, though, but the high slip for when very little liquid is present, will effect the calculations.

6.4.3 Two-Phase Density

The two-phase density in Equation (4) on page 4 is repeated here:

$$\frac{1}{\rho_{TP}} = \frac{\frac{x_G}{\rho_G} + k\frac{x_L}{\rho_L}}{x_G + kx_L}$$

From Figure 2, it was seen that the two-phase density is in general always the highest density expression, when looking at change with both pressure and x_G. As the pressure increases the difference between two-phase density and momentum density also increases, but not so fast as for lower pressures. In ρ_{TP}, slip has to be included, both times multiplied by x_L so that if $x_L = 0$, it does not matter which slip model is used.

In Figure 27, the predicted mass flow rates with varying choke pressure are drawn for different densities and slip models. The discharge coefficient is not tuned, to better see the effect of the slip models on the predicted mass flow rate. As expected, because the mixture density is highest, it also gives some of the highest predicted $\dot{m}$ for a given downstream pressure, and $\rho_{TP}(k_{modCh})$ being the highest of all. The higher the maximum point on the predicted mass flow rate curve is, the further it is shifted towards a lower P_{2c} as well. The incontinuity in the curves with k_{Ch} is where the Lockhart-Martinelli parameter causes a change in the expression for slippage. The figure also shows that the highest slip gives the highest mass flow prediction, which is logical.

Predictions for the Porsgrunn data set are shown in Figure 26, and the statistics in Table 9 suggest that the two-phase density may not be as good as using the momentum density with modified Chisholm as slip model. This comes as no surprise, given that the expression for the momentum density should be the ideal to use in the momentum equation, from which the Hydro Model and the other models presented here, are deduced. However, the improvement from not including slip at all, to include slip by using the ρ_{TP} is large; both standard deviation and average absolute relative error is halved for any of the three slip models.

Shifting the critical pressure to a lower value and lifting the whole $\dot{m}_{calc}$-curve was thought to even out the trend of over-predictions for high pressure ratios and under-predictions for low pressure ratios, but it does not seem that using two-phase density instead of momentum density is the way to do it.

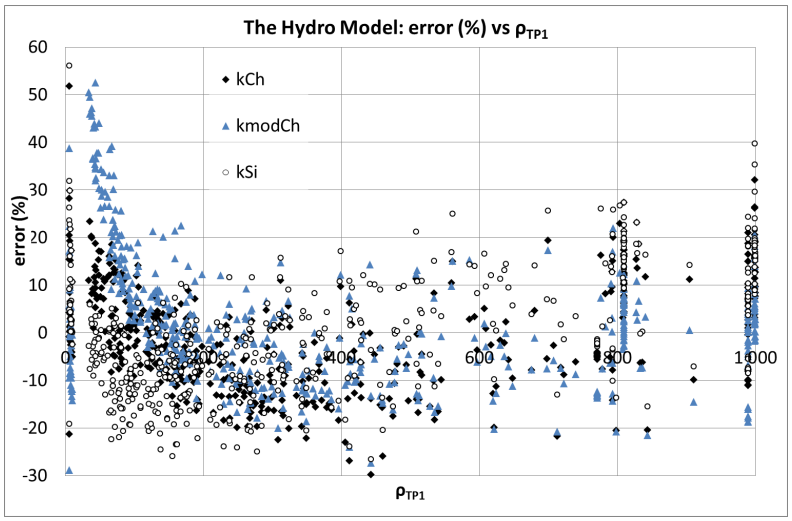

(a) Error vs ρ_{TP}

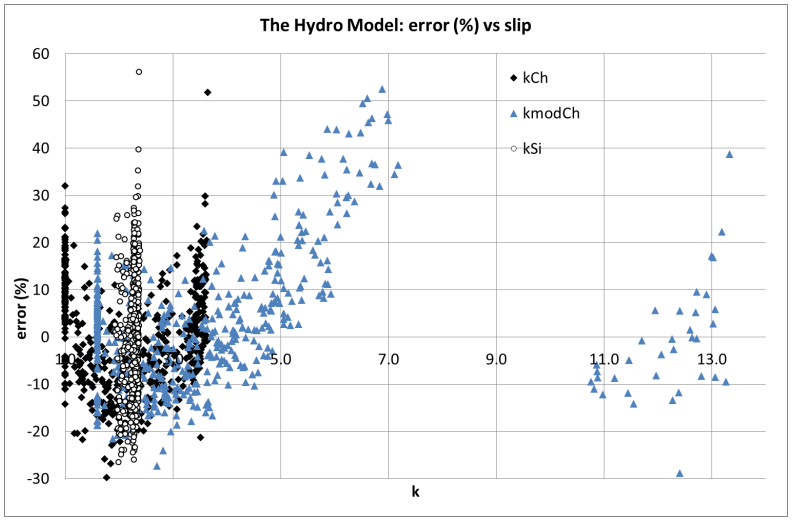

(b) Error vs slip

Figure 26: Error distribution for the Hydro Model with ρ_{TP} and different slip models, Porsgrunn data set

See also Appendix A

The best of the slip models with mixture density is k_{Ch}, with $E_2 = 9.362\,\%$ for the Porsgrunn data set. A reason why the performance for k_{modCh}, compared to the other slip models is not so good, could be that it contains two factors that have been tuned. Albeit, they have been tuned to fit the Porsgrunn data set, but within the original Hydro Model which uses the momentum density, not two-phase density. From Figure 26b, it can be seen that as the slip from k_{modCh} increases past that of Chisholm's model, the over-prediction also increases sharply, suggesting that it would have been better to set a maximum slip, like Chisholm has done. The very high slip values, where $k_{modCh} > 10$, are for cases with $x_G \approxeq 1$, and therefore the slip has little or nothing to say for the predicted mass flow.

6.4.4 Momentum Density

Equation (12) is repeated:

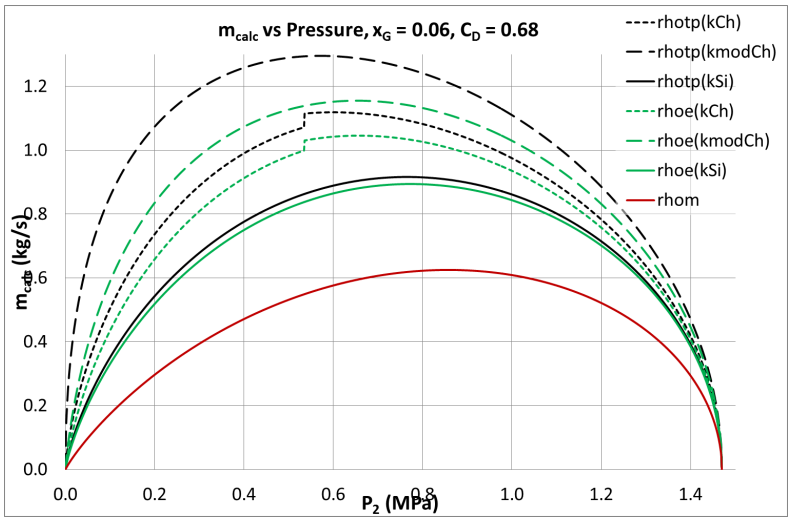

Figure 27: $\dot{m}_{calc}$ vs P_2 for different densities and slip models

$$\frac{1}{\rho_e} = \left(\frac{x_G}{\rho_G} + k\frac{x_L}{\rho_L}\right)\left(x_G + \frac{x_L}{k}\right)$$

Again, any slip model could be used with the momentum density. In the Hydro Model, there is originally made use of the momentum density and a modified version of Chisholm's slip model. The main difference between momentum density and two-phase density is the way in which slip is incorporated. ρ_e is divided by another factor, where ρ_{TP} is multiplied by one, and in this factor in ρ_e, x_L is divided by the slip, while in the factor in ρ_{TP}, x_L is multiplied by the slip.

Because ξ and β have been tuned to the Porsgrunn data set, it would be expected that using ρ_e with k_{modCh} will give better results than ρ_e with k_{Ch}, which it also did, as can be seen in Table 9, where ρ_e with k_{modCh} is almost at the top of the table ("wo. pressure recovery"). Results are shown in in Figure 28 and 29. and Appendix A.

Also for momentum density, Simpson et al.'s slip model has slightly higher errors than the others, even though Chisholm's k does not always depend on x_G either. The trend for $k_{modCh} > 4$ that was very clear when using two-phase density is not present here. The error distributions for k_{Ch} and k_{Si} are more or less the same for momentum density as they were for two-phase density.

Even though there is not a great difference in the errors calculated, Figures 26a and 28a suggest that the momentum density is more appropriate than two-phase density because the errors are more evenly distributed for momentum density and the steep line for low mixture densities is not seen.

6.5 Gas Expansion

Another thing to look at, that may help correct the trend in Figure 17a, is the model for how the gas expands. Originally in the Hydro Model, gas is expected to expand polytropicly, using an exponent that is a weighted average of liquid and gas heat capacities.

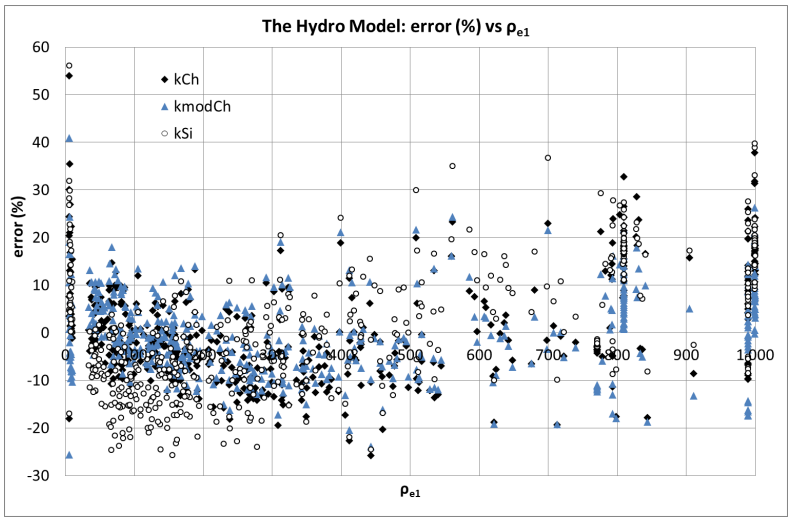

(a) Error vs ρ_{e1}

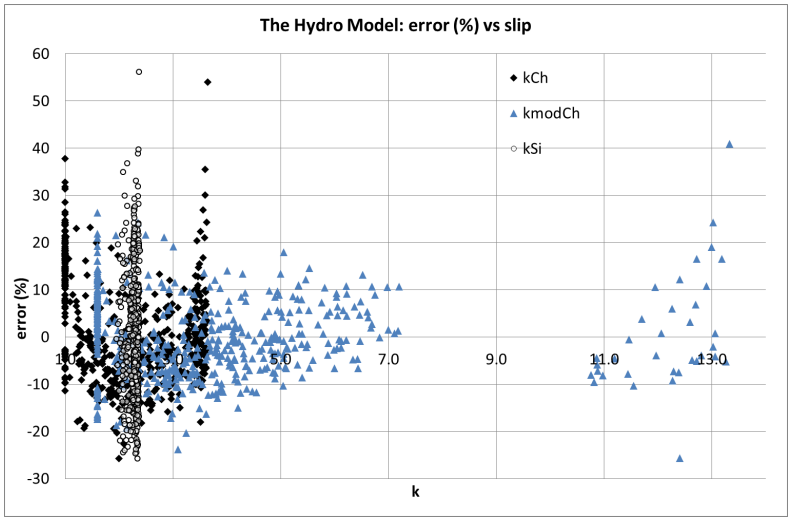

(b) Error vs slip

Figure 28: Error distribution for the Hydro Model with ρ_e and different slip models, Porsgrunn data set

6.5.1 Constant Gas Density

To see the effect of gas expansion, the Hydro Model was first run and tuned for the case of constant gas density. This can be done in several ways: the ones looked into here is using ρ_{G1} all the way through, and using an average of ρ_{G1} and ρ_{G3}, setting

$$\rho_G = const = \frac{\rho_{G1} + \rho_{G3}}{2} \tag{58}$$

where ρ_{G3} is calculated by Equation (28) on page 12. Using P_2 should be avoided because the density is an input parameter, while P_2 is considered unknown in the beginning. That the density is constant does not mean that there is no slip, but as the slip is a function of mass fractions and gas density, it will remain constant in all positions over the choke. With density and slip independent on pressure, the relationship between $\dot{m}_{calc}$ and P will be linear, and a higher pressure drop will give higher mass flow.

The results for the Porsgrunn data set are shown in Figure 30. As can be seen from Table 12, there are no data points that are predicted to be critical, and this is in accordance

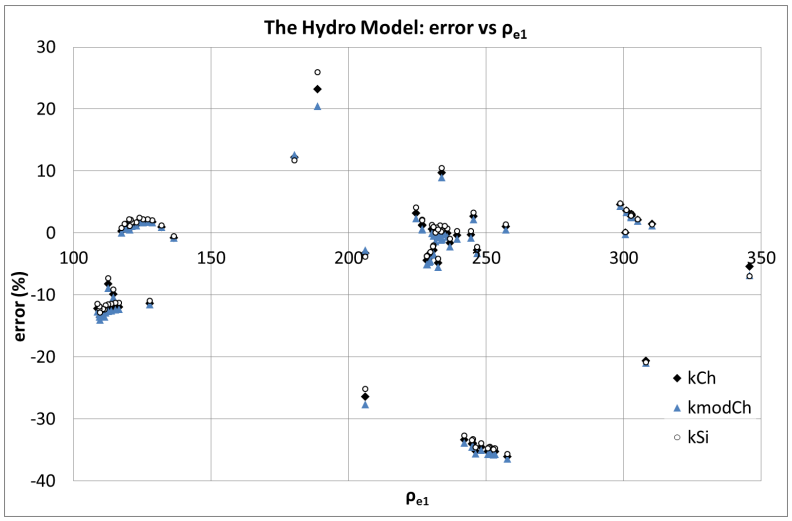

(a) Error vs ρ_{e1}

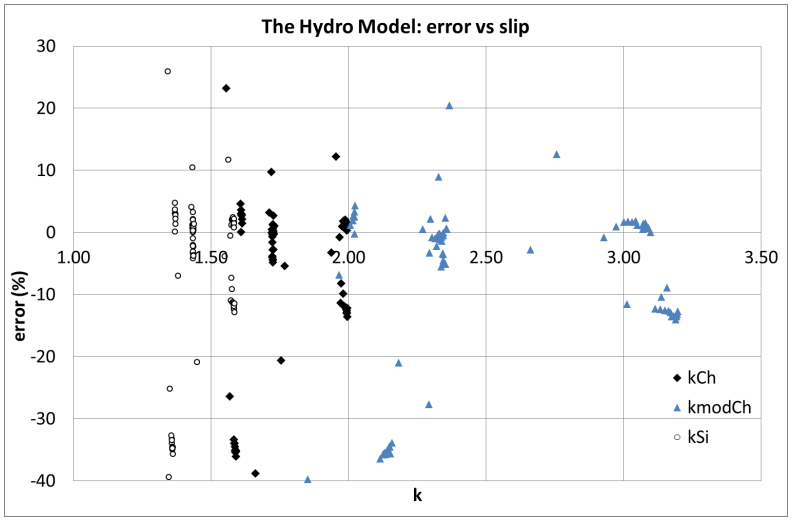

(b) Error vs slip

Figure 29: Error distribution for the Hydro Model with ρ_e and different slip models, field data

with theory; critical flow can only occur in a compressible fluid, and now the gas is considered to be incompressible as well as the liquid.

The results for both the data sets are surprisingly good for the fluid density to be kept constant. There is more spread than when including gas expansion, especially when using ρ_{G1}, but for the average gas density, the results are better than for substituting k_{Ch} for k_{modCh} in the Porsgrunn data.

When it comes to the field data, the difference is little, both between the two methods of calculating constant gas density and other alternatives that have been tested out. What has changed most, is the C_D-values in Table 10, they have all dropped quite a lot. This may be be related the pressure drop. For each choke opening, and by that, for each C_D-value, almost all the points have the same upstream pressure and the same pressure drop, and therefore the C_D can better be tuned to the situation. When using ρ_{G1} all the way, the gas density is higher than it should at the choke, and as compensation C_D is lowered. This fits well with the observations, especially because the smallest choke opening has the largest pressure drop, $y \approx 0.2$, and also the lowest C_D, while the largest choke opening

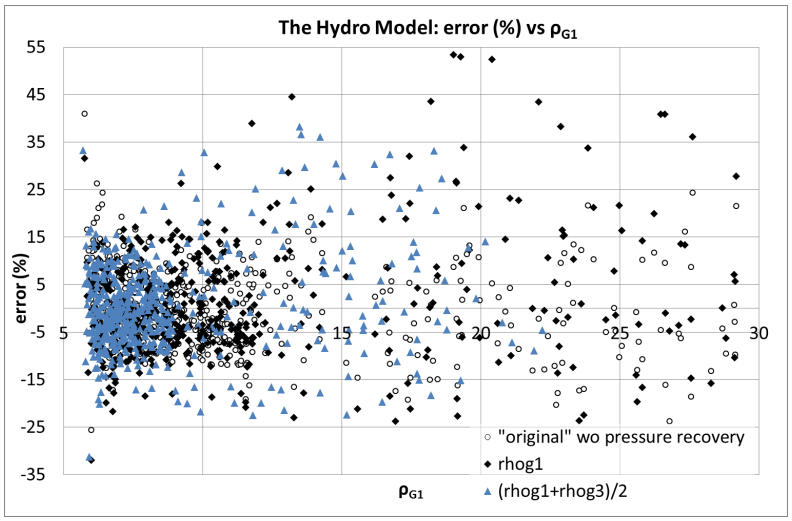

(a) Error vs. ρ_{G1}

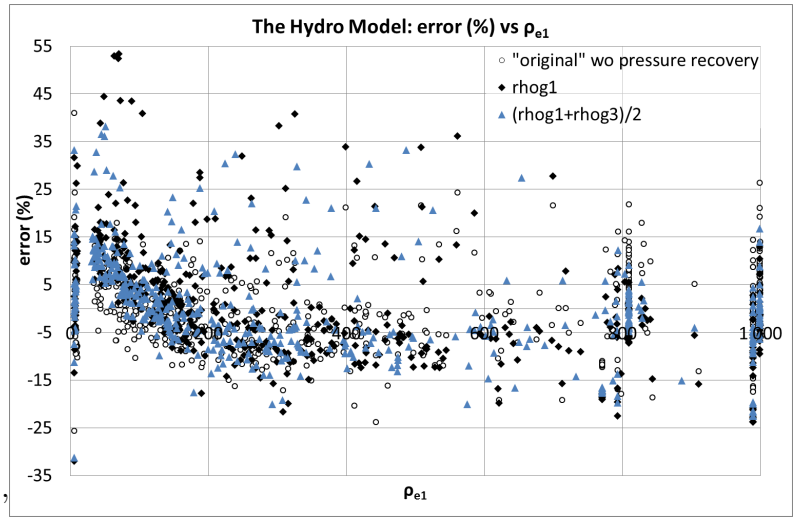

(b) Error vs. ρ_{e1}

Figure 30: Error distribution for the Hydro Model with constant gas density, Porsgrunn data set

See also Appendix A

has the smallest pressure drop and the highest C_D. This is also the case for the averaged density, but as expected, all C_Ds are now closer to their original value, most likely because the gas density is closer to what it should be at the choke.

6.5.2 n vs. κ

Originally in the Hydro Model, it has been assumed that when the gas expands, it is kept from cooling by receiving heat from the liquid so that the gas and liquid will always be at the same temperature. And because the liquid has higher heat capacity than gas, this temperature is assumed to be constant. Assuming adiabatic gas expansion, the model then predicts the gas to expand more than it would if it did not receive heat from the liquid. But the time for heat transfer between the phases is short, and it may be that it would be better to model the gas as cooling during the expansion, by using $\kappa = (C_P/C_V)_{gas}$ instead of n in Equation (28) so that

$$\rho_G = \rho_{G1} \left(\frac{P}{P_1} \right)^{1/\kappa} \tag{59}$$

Because $n \leq \kappa$, using κ will lead to less gas expansion. The results in the previous section, where it was shown that even with constant fluid densities, the predictions were not much worse, supports the idea of decreasing the modeled gas expansion. In addition, decreasing gas expansion is hoped to lessen the curvature in the $\dot{m}_{calc}$ vs. P graph. Figure 31 shows that κ does exactly that; moves the critical pressure to a lower value, and the critical mass flow rate to a higher value. A retuning of C_D brought the curve down a little again. The best thing with this change may be that the beginning of the curve, as seen from P_1, is unchanged.

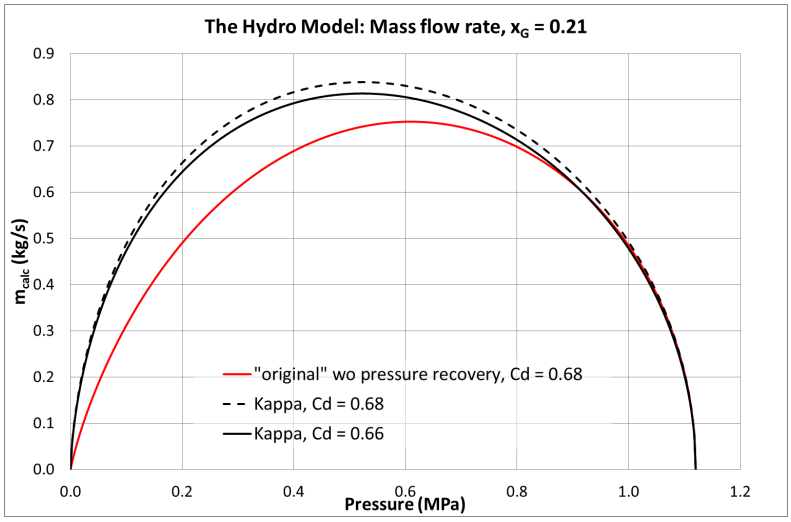

Figure 31: The Hydro Model: $\dot{m}_{calc}$ vs. P_2 for gas expansion using n and κ

The results for the Porsgrunn data set are shown in Figure 32. There is definitely some improvement in all but E_1. Originally (without pressure recovery), there were 12 data points, of 508, outside the range of error 20 %, but with κ, this number is reduced to seven; of which two are pure gas and the other five have $x_G < 0.03$. Even though the C_D-values are lower, most of the predictions are higher, except where there is single-phase flow. For cases with $x_G \approx 1$, $n \approx \kappa$, which means that the only change is a lower value of C_D, and the predictions are lowered. Figure 32a shows that the error trend for y is somewhat diminished. The $\dot{m}_{calc}/\dot{m}_{c(calc)}$ plot in Figure 32b shows a bit of the same thing, in that the trend of predicting too high flow rates for sub-critical points is leveled out. From Table 12, it can be seen that the number of critical points is almost halved from the original (still without pressure recovery) 25 to 13, which also indicates that the critical pressure has been lowered.

For the field data, an improvement of results was not obtained. While E_1 and E_2 are somewhat better, the standard deviation has increased. The number of critical flow data points remains unchanged at 57, suggesting that there is little doubt about whether a points is critical or not. Only two points differ in the highest and lowest prediction of number of critical points, when not looking at the incompressible gas cases.

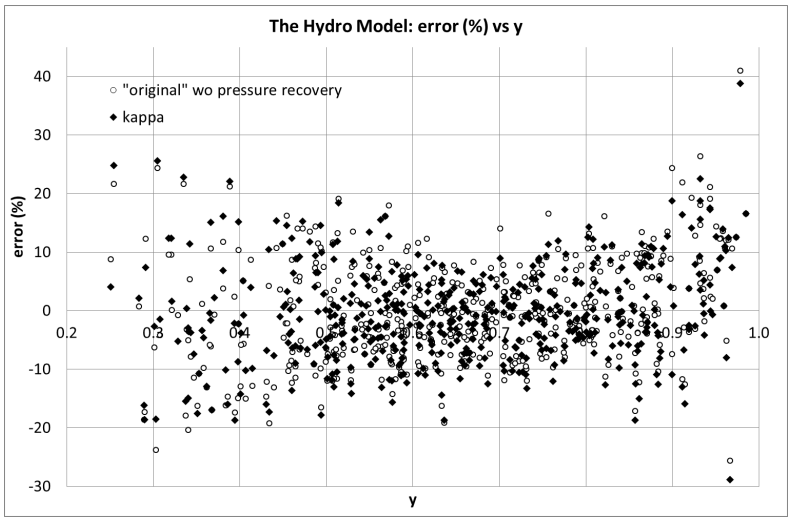

(a) Error vs. $y = P_2/P_1$

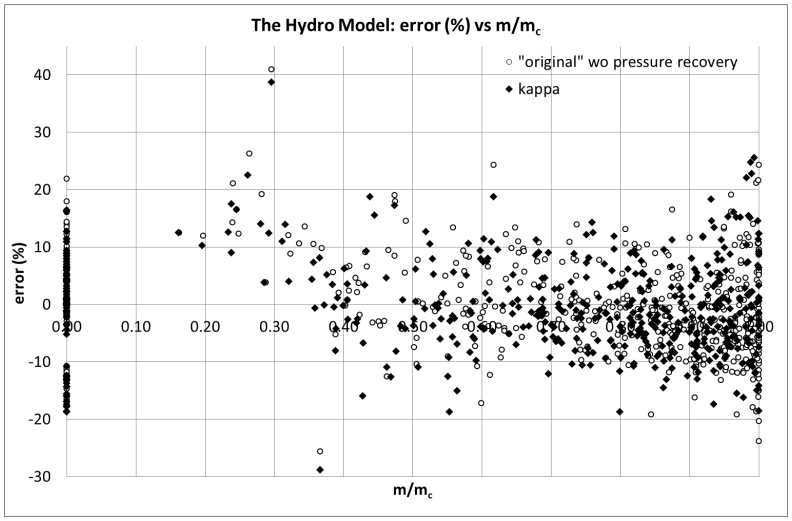

(b) Error vs. $\dot{m}_{calc}/\dot{m}_{c(calc)}$

Figure 32: Error distribution for the Hydro Model with κ, Porsgrunn data set
See also Appendix A

6.6 The Significance of the Term $1/A_1^2\rho_{e1}^2$

In the Bernoulli Equation with Φ_{TP}, Asheim, Sachdeva et al., and Al-Safran and Kelkar's models, the term containing u_1 have been ignored on the assumption that $A_2 \ll A_1$ and therefore $u_1 \ll u_2$ so that u_1 could be neglected. The Hydro Model has chosen to keep u_1 in the term $1/A_1^2\rho_{e1}^2$ in Equation (44) (and (43) when that is in use). But the upstream momentum density will always be higher than the downstream density, thus diminishing the importance of $1/A_1^2\rho_{e1}^2$ compared to $1/C_D^2A_2^2\rho_{e2}^2$ even further.

The field data have the highest choke opening compared to the assumed pipe diameter before. Setting $d_1 = 10\,cm$, a $38\,mm$ choke opening is 14.4 % of the upstream area. The pressure drop is in the range of $50 - 65\,\%$, which is the lowest pressure difference for this data set as well. These data points seem therefore to be where $1/A_1^2\rho_{e1}^2$ is most important. An overview of how large this term is related to $1/C_D^2A_2^2\rho_{e2}^2$ is given in Table B.3. The highest number is for the very last data point, where $1/A_1^2\rho_{e1}^2$ is 1.23 % of $1/C_D^2A_2^2\rho_{e2}^2$, something that translates to 0.6 % difference in predicted mass flow rate, and that is not

much.

Removing this term and retuning, there is no difference in C_Ds for either of the data sets, as can be seen in Table 10 and 11. For both data sets, the average relative error has increased a bit, while the other error parameters are almost the same or even slightly better than the original without pressure recovery. From this, it seems that the term $1/A_1^2\rho_{e1}^2$ has very little significance in the model.

6.6.1 Slip Upstream Choke

The Hydro Model has assumed no slip at position (1) in Figure 4 on page 16 and therefore $\rho_{e1} = \rho_m$ in Equations (43) and (44). But it has been shown above that slip is very important, therefore it is worth looking into whether including slip in position (1) and (3) will have any effect in the result, especially as it gives very little additional calculations. The change is not expected to be large, though, because the term $1/A_1^2\rho_{e1}^2$, does not influence the results a lot. Besides, adding slip in position (1) will also increase the momentum density at this point, thus maybe decrease the importance of the term even more.

Including slip in the momentum density upstream and downstream of the choke does not alter the results very much, as can be seen in Table 9. Again there is no change in the C_D-values for the Porsgrunn data set. For the field data, a small change was found for the middle-sized opening, where C_D increased with 0.1, but this did nothing to alter the result. E_1 and E_2 have become a little bit better, while the standard deviation was worsened, although not by much.

Even though slip is important, the significance of $1/A_1^2\rho_{e1}^2$ with or without slip, for the choke openings studied in this theses is negligible.

Table 9: The Hydro Model: different alternatives*: Statistics (%)

	Porsgrunn data			Field data		
	E_1	E_2	σ	E_1	E_2	σ
Original model	0.067	6.993	8.859	-7.626	9.973	14.081
Wo. pressure recovery	-0.231	6.817	8.636	-7.985	10.002	13.920
Trapezoidal approx. integral	-0.376	11.279	14.324	-7.671	10.100	14.047
No slip	0.267	22.161	26.387	-6.171	9.540	13.756
ρ_{TP} with k_{Si}	-0.463	10.459	12.824	-6.379	9.759	13.846
ρ_{TP} with k_{Ch}	-0.464	9.310	11.354	-7.086	9.822	13.953
ρ_{TP} with k_{modCh}	2.555	10.278	13.907	-7.399	9.737	13.576
ρ_e with k_{Si}	0.024	11.081	13.531	-7.024	9.779	13.956
ρ_e with k_{Ch}	1.025	8.815	11.222	-7.522	9.839	13.926
Constant ρ_{G1}	1.046	8.959	12.181	-6.353	9.698	13.755
Constant $(\rho_{G1} + \rho_{G3})/2$	0.525	7.563	10.147	-7.588	9.880	13.840
κ instead of n	-0.351	6.384	8.249	-7.639	10.004	14.149
Without $1/A_1^2\rho_{e1}^2$	-0.307	6.810	8.622	-8.191	10.022	13.865
Include k in ρ_{e1} and ρ_{e3}	-0.282	6.810	8.624	-7.663	9.942	14.093
The Hydro Model, revised	-0.430	6.327	8.225	-7.082	10.000	14.058

(*pressure recovery only in the original)

Table 10: The Hydro Model: C_D for different alternatives, Porsgrunn data set

(a) Cage; Discharge Coefficients

	$11\,mm$	$14\,mm$	$18\,mm$
Original model (long and short)	0.49	0.48	0.42
Without pressure recovery	0.69	0.68	0.60
Trapezoidal approx. integral	0.61	0.55	0.51
No slip	0.93	0.95	0.81
ρ_{TP} with k_{Si}	0.75	0.76	0.65
ρ_{TP} with k_{Ch}	0.73	0.71	0.62
ρ_{TP} with k_{modCh}	0.66	0.65	0.63
ρ_e with k_{Si}	0.77	0.78	0.66
ρ_e with k_{Ch}	0.76	0.74	0.64
Constant ρ_{G1}	0.62	0.62	0.56
Constant $(\rho_{G1} + \rho_{G3})/2$	0.63	0.64	0.58
κ instead of n	0.66	0.66	0.60
Without $1/A_1^2\rho_{e1}^2$	0.69	0.68	0.60
Include k in ρ_{e1} and ρ_{e3}	0.69	0.68	0.60
The Hydro Model, revised	0.66	0.66	0.60

(b) Orifice; Discharge Coefficients

	$11\,mm$	$14\,mm$	$18\,mm$
Original model (long and short)	0.66	0.66	0.64
Without pressure recovery	0.67	0.66	0.65
Trapezoidal approx. integral	0.57	0.52	0.57
No slip	0.85	0.91	0.79
ρ_{TP} with k_{Si}	0.70	0.73	0.72
ρ_{TP} with k_{Ch}	0.70	0.69	0.70
ρ_{TP} with k_{modCh}	0.63	0.63	0.64
ρ_e with k_{Si}	0.70	0.73	0.72
ρ_e with k_{Ch}	0.73	0.72	0.71
Constant ρ_{G1}	0.58	0.59	0.60
Constant $(\rho_{G1} + \rho_{G3})/2$	0.60	0.61	0.61
κ instead of n	0.64	0.64	0.64
Without $1/A_1^2\rho_{e1}^2$	0.67	0.66	0.65
Include k in ρ_{e1} and ρ_{e3}	0.67	0.66	0.65
The Hydro Model, revised	0.64	0.64	0.64

Table 11: Discharge Coefficients, field data

	$12\,mm$	$22\,mm$	$38\,mm$
Original model (short)	0.78	0.87	0.78
Without pressure recovery	0.78	0.86	0.80
Trapezoidal approx. integral	0.72	0.78	0.73
No slip	0.88	0.99	0.95
ρ_{TP} with k_{Si}	0.82	0.91	0.84
ρ_{TP} with k_{Ch}	0.79	0.88	0.78
ρ_{TP} with k_{modCh}	0.74	0.79	0.68
ρ_e with k_{Si}	0.82	0.92	0.86
ρ_e with k_{Ch}	0.80	0.89	0.83
Constant ρ_{G1}	0.46	0.53	0.64
Constant $(\rho_{G1} + \rho_{G3})/2$	0.53	0.60	0.68
κ instead of n	0.74	0.82	0.77
Without $1/A_1^2\rho_{e1}^2$	0.78	0.86	0.80
Include k in ρ_{e1} and ρ_{e3}	0.78	0.87	0.80
The Hydro Model, revised	0.75	0.82	0.78

6.7 The Revised Hydro Model

The first, and largest change, that can be made to the Hydro Model is removing the pressure recovery, thus almost halving the computational time. It has been seen that pressure recovery has very little importance and because C_Ds are tuned for each choke opening and geometry, they are adequate to account for the decrease in pressure drop as removing pressure recovery will lead to.

Also, it was found that κ was a better exponent than n to use for gas expansion, which may be due to little time for heat transfer across the choke. The term $1/A_1^2\rho_e^2$ could be be removed, without any cost to the accuracy of the predictions. When it comes to density, on the other, the momentum density seems to be the best density equation, at least among those tested in this thesis. As slip model, k_{modCh} should be kept as it is.

Summarized, the equations used in the Revised Hydro Model are:

$$\dot{m}_{1-2}^2 = 2C_D^2 A_2^2 \rho_{e2}^2 \int_{P_2}^{P_1} \frac{1}{\rho_e} dP \tag{60}$$

where the gas expands according to Equation (59) and the critical flow boundary calculated as $\dot{m}_{1-2} - \dot{m}_c = 0$ where $\dot{m}_c$ is as in Equation (47).

The result from applying Revised Hydro Model the Porsgrunn data set and field data are shown in Figures 33-34 and 35 respectively. It has been succeeded to even out the trend of too high predictions for high pressure drops and too low predictions for low pressure drops, but statisticly, the model has not been improved very much, especially not for the field data.

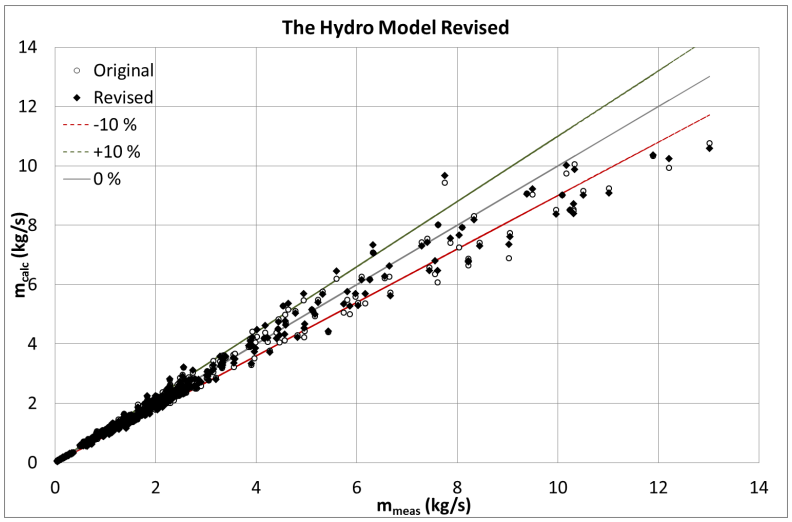

(a) Calculated vs. measured mass flow rate

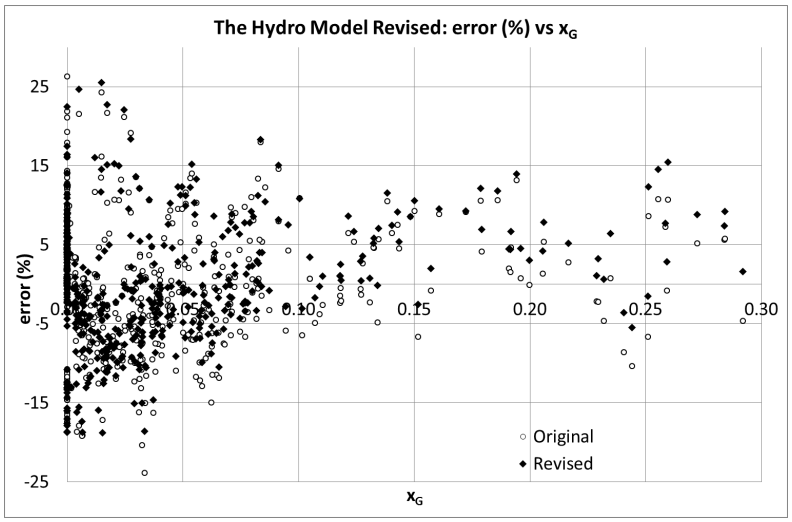

(b) Error vs. x_G

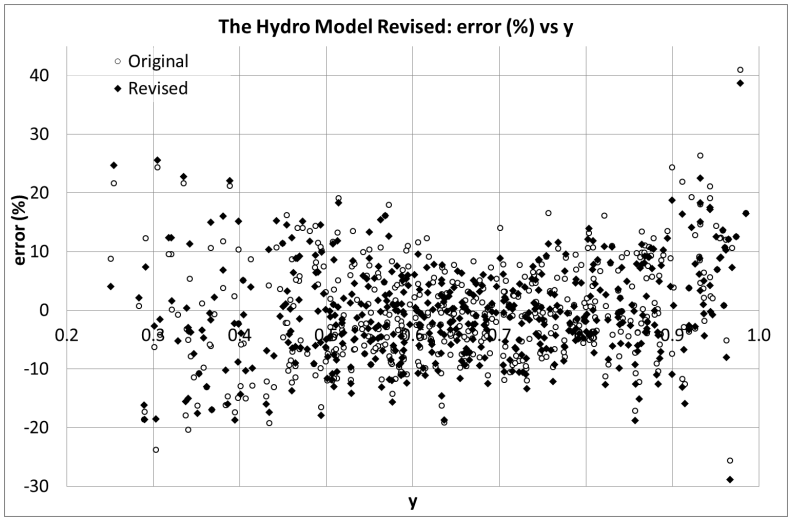

(c) Error vs. $y = P_2/P_1$

Figure 33: Error distribution for the Revised Hydro Model, Porsgrunn data set

Table 12: The Hydro Model: Number of critical points for different alternatives

	Porsgrunn data total: 508	Field data total: 87
Original model (long and short)	40	59
Without pressure recovery	25	57
Trapezoidal approx. integral	35	57
No slip	117	59
ρ_{TP} with k_{Si}	138	59
ρ_{TP} with k_{Ch}	131	59
ρ_{TP} with k_{modCh}	116	59
ρ_e with k_{Si}	53	58
ρ_e with k_{Ch}	38	58
Constant ρ_{G1}	0	0
Constant $(\rho_{G1} + \rho_{G3})/2$	0	0
κ instead of n	13	57
Without $1/A_1^2\rho_{e1}^2$	25	57
Include k in ρ_{e1} and ρ_{e3}	25	57
The Hydro Model, revised	13	57

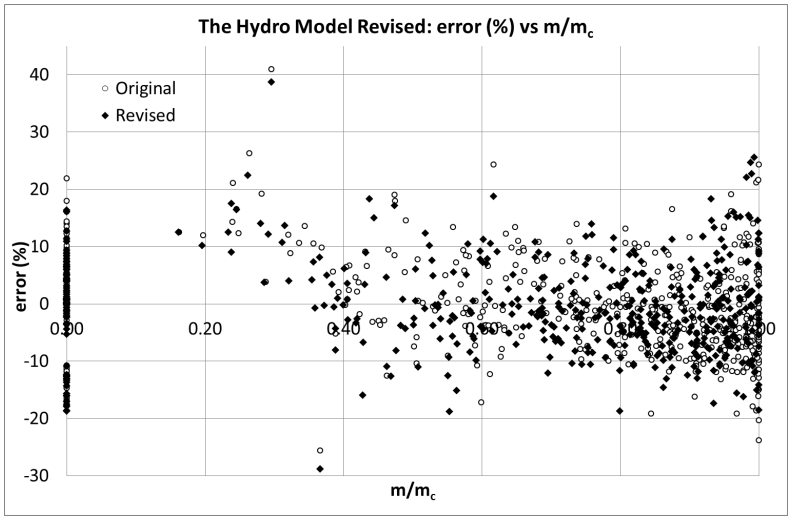

Figure 34: The Revised Hydro Model: error distribution vs. $\dot{m}_{calc}/\dot{m}_{c(calc)}$, Porsgrunn data set

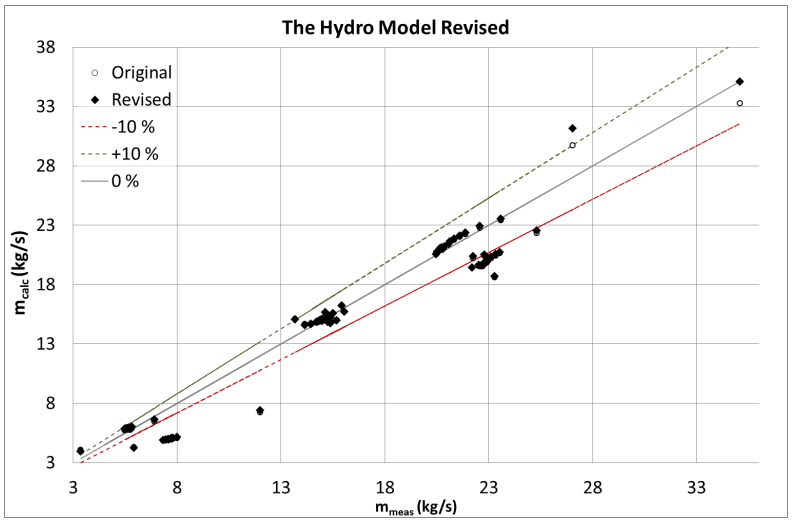

(a) Calculated vs. measured mass flow rate

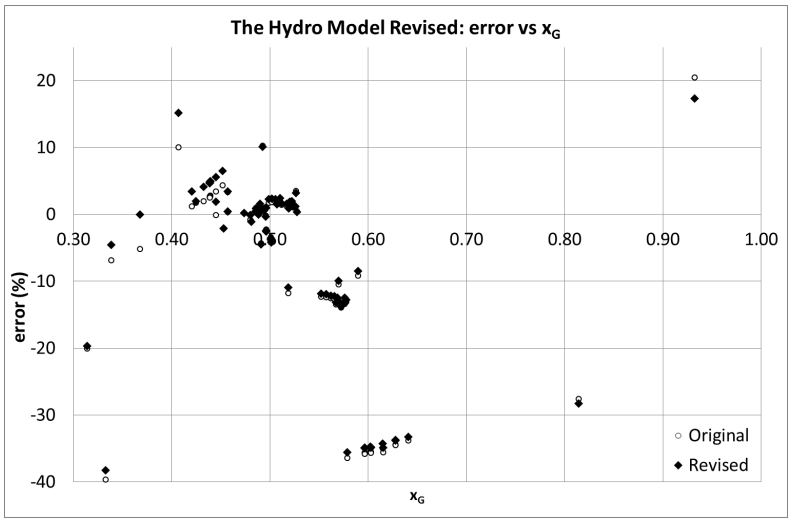

(b) Error vs. x_G

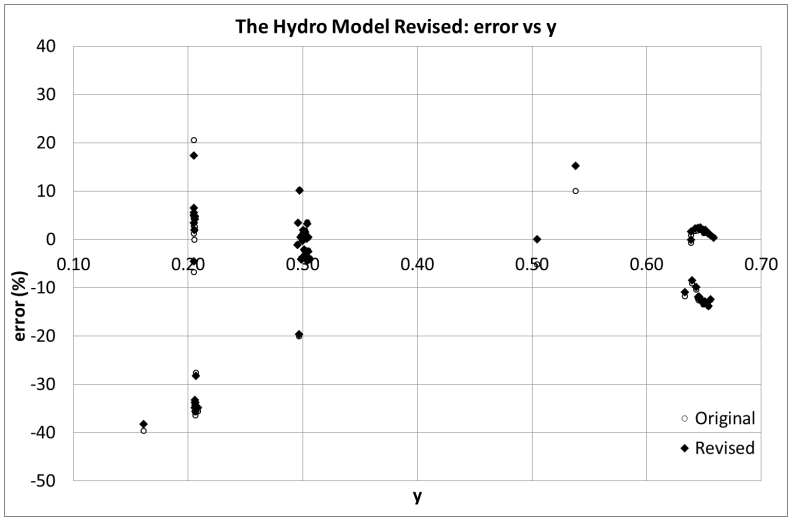

(c) Error vs. $y = P_2/P_1$

Figure 35: Error distribution for the Revised Hydro Model, field data

7 Discussion

7.1 Pressure Recovery

Two of five choke models presented above include pressure recovery from position (2) to (3) in Figure 1 on page 3; Al-Safran and Kelkar's model and the Hydro Model. This is means that the pressure drop is modeled as larger than for the models without pressure recovery, as $P_2 < P_3$, which would give a higher flow rate. This can be adjusted downwards again by tuning the discharge coefficient, though, so one of the main differences is related to the transition between sub-critical and critical flow. For the Hydro Model, the number of critical points for the Porsgrunn data set are reduced from 40 to 25 when removing pressure recovery. Looking closer at these particular points, there is no general trend of whether they have been improved or worsened by the removal of pressure recovery, only that the points that were under-predicted have become better while those that were over-predicted have become slightly more worse. But as has been discussed previously, there was originally a trend in the Hydro Model in predicting too low mass flow rates for high pressure drops and too low flow rates for low pressure drops, and by modeling fewer points as critical, some of these points are lifted upwards, both by being modeled as sub-critical and a higher discharge coefficient. This is probably the most visible reason for why the standard deviation for the data set as a whole has decreased a little when removing the pressure recovery.

Doing a quick run of Al-Safran and Kelkar's model without pressure recovery, summarized in Table B.4, shows the same thing, there are 19 fewer critical points. In addition, fewer data points fall in the region between critical and sub-critical flow, which should be considered as a good thing.

A question that might arise is whether the data points that became modeled as sub-critical when removing pressure recovery actually are critical or not. Looking at the predictions for the Bernoulli Equation with $\Phi_{2P,Si}(k_{Si})$, the results are surprisingly good. In the upper left of Figure A.3c, there are some data points that are thought to be critical because they are found at relatively high pressure drops and are predicted to be much higher that the the measured mass flow rate. That there are approximately of them, with an error of $> 25\,\%$, also supports the predictions for the Hydro Model without pressure recovery that says there are 25 critical points, compared to the 40 critical points when including pressure recovery.

Al-Safran and Kelkar's model and the Hydro Model predict very similar pressure recovery for the Porsgrunn data set. For the field data, the difference is larger, but the two models are still within $2.5\,\%$ of each other, the Hydro Model being the one to give least pressure recovery both times. This may be because Al-Safran and Kelkar's pressure recovery model is based almost entirely on downstream pipe area, which is an assumed value for the field data, and by that rather uncertain. However, given that the same assumption is made in both models, it may also be because the field data have in general higher choke openings relative to the (assumed) downstream area, and Al-Safran and Kelkar's pressure recovery equation is proportional to d_3. In the Hydro Model, the expression is more complex and depends for instance on C_D when using the short model, but not for the long. Although, as in logical, the Hydro Model also predicts higher pressure recovery for larger choke opening.

Looking at the mean relative error for each choke opening in Table 13, it can be seen that there is no particular trend for the error for high choke openings to be worse without pressure recovery. This supports the argument that a retuning of C_D is adequate to

adjust for the removal of the pressure recovery from the Hydro Model. Tables 10 and 11 also point in that direction. It can be seen that when removing pressure recovery, the discharge coefficient increases the most for the highest choke opening to account for the lessening in pressure drop. That this happens without increasing the standard deviation shows that pressure recovery seems to be unnecessary.

Table 13: Average relative error, E_1, (%) for each choke opening with and without pressure recovery

	Porsgrunn data set			Field data		
Choke opening:	$11\,mm$	$14\,mm$	$18\,mm$	$12\,mm$	$22\,mm$	$38\,mm$
Hydro Model, original	0.894	1.028	-1.213	-18.209	-0.712	-5.096
Hydro Model, wo pressure rec.	0.979	-0.208	-1.040	-18.121	-1.854	-4.994
Al-Safran & Kelkar, original	-1.591	0.486	-0.509	-17.309	-0.821	-4.717
Al-Safran & Kelkar, wo pres rec.	-1.227	0.387	0.528	-17.309	-0.821	-4.393

7.2 Gas Expansion

The Bernoulli Equation does not involve any form of gas expansion, yet it has a lower standard deviation and E_2 than Asheim, Sachdeva et al. and Al-Safran and Kelkar's model, when using Simpson et al.'s two-phase multiplier and slip model for the Porsgrunn data set. However, there seems to be an upwards trend in the error distribution for increasing gas mass fractions, see Figure 6b. When setting the gas density constant in the Hydro Model, in Figure A.13b, the same trend is observable. This suggest that it is the constant gas density that is the most influencing factor in causing this trend.

On the other hand, as seen in Table 9, the lack of gas expansion did not cause the statistical errors to increase as much as might have been expected. Using ρ_{G1}, which was seen to be slightly worse than the average of upstream and downstream gas density, E_1, E_2 and σ are still better than several of the density and slip combinations.

In the Sachdeva et al., Al-Safran and Kelkar and Hydro Model, the gas is assumed to expand polytropicly, with n as the polytropic exponent. Asheim, on the other hand, uses the gas law, and this is the only difference between Asheim's model and that of Sachdeva et al., as none of them include phase slippage. Given that the Sachdeva et al. model is slightly better than Asheim's model for as good as every point in the Porsgrunn data set, it seems that it is better to assume polytropic expansion rather than using the gas law. However, because it has been assumed that $Z = 1$ when finding the input gas density, this assumption has to be passed on to Asheim's model as using ρ_{G1} in Equation (24) will again give the Z-factor equal to unity. It is of course possible that a more accurate Z-factor could diminish the gap between Asheim's model and Sachdeva et al.'s model. For the field data, where Z has been calculated for upstream conditions based on the Black Oil Model, the gap between Sachdeva et al.'s model and Asheim's model is less, even with Asheim's model having the lowest standard deviation. It should be kept in mind, though, that there is very little difference between the predictions for any model for the field data.

In the Hydro Model, when changing from n to κ, both E_2 and σ decreased noticeably for the Porsgrunn data set, and the trend of predicting too high mass flow rates for low pressure drops and too low for high pressure drops is evened out. The lifting and left-shift of the $\dot{m}_{calc}$-curve in Figure 31 that is obtained by introducing κ is also what was wanted, and expected, to even out the trend. This seems to mean that the gas does not expand as

much as first assumed, and there can be several reasons for that. First of all, n assumes that there is heat transfer between the gas and liquid phase, which might not be case. The velocity across the choke, by Equation (2), is typically higher than $15\,m/s$ for the Porsgrunn data set, through a choke that is a few centimeters across, leaving very little time for heat transfer. In addition, there is limited space inside the choke, something that could also contribute to less expansion of the gas. Therefore, it seems reasonable that κ is a better parameter to control gas expansion than n.

7.3 Density and Slip

How gas expansion is assumed to happed is not the only aspect thought to influence the error distribution with respect to x_G. Also the slip model used has something to say. This is because phase slippage affects how the flow area is distributed between the gas and liquid phase so that the flow area of gas, α can be less and the same amount of gas can still be produced compared to a no-slip condition.

Removing slip from the Hydro Model, and by that using the same homogeneous density as Sachdeva et al. and Asheim, the curve in error distribution for x_G for the two latter models appears in the Hydro Model as well. In fact, without pressure recovery and slip, the Hydro Model is very similar to Sachdeva et al.'s model and the largest difference is the how the critical pressure is calculated. Sachdeva et al.'s model gives a higher critical pressure ratio and thus more critical data points, which causes the error distribution to be somewhat different. For the field data, where the two models predict the same number of critical data points, the statistical results are much more similar, but then most of the field data results are like this. Now, Al-Safran and Kelkar include slip in their model, and the curve in the error distribution for low x_G is still present there, although not quite so distinct. This could be caused by the model's inconsistent treatment of slip. First of all, as has been observed earlier, which slip model to be used depends on whether there is critical or sub-critical flow while the slip is also included in the expression that decides flow regime. Second, the slip is considered to be constant when integrating the momentum equation, even though the gas is assumed to expand polytropicly, and slippage is a function of gas density. For the field data, this may not be a large source of error for sub-critical flow as there is little variation in k_{Si} at choke conditions, see Figure 29b, but depending on the input data, it can have a more severe effect. For critical flow, when k_{modCh} is used, the variation is larger, and the error in keeping the slip constant is expected to be worse.

Given that the Hydro Model is the only one that does not have a curve in the error distribution for low x_G, it seems that this curve is caused by slip and how it is incorporated. The curve is most distinct for Asheim's and Sachdeva et al.'s model which do not include slip at all, somewhat lessened in Al-Safran and Kelkar's model which includes slip in calculation of $\dot{m}$ but not integration of $1/\rho_e$, and has disappeared in the Hydro Model which includes slip also in the integration.

From Table 9, it seems like phase slippage is the single most important aspect in the Hydro Model. Removing slip completely gave a lot worse results than any other density average and slip model combination. Not surprisingly, perhaps, is the momentum density considerably better than two-phase density with k_{Ch} or k_{modCh}. What is worth noticing is that $\rho_{TP}(k_{modCh})$ produces considerable worse results than when using the two-phase density with Chisholm's original slip model. This might be related to the two constants ξ and β that are tuned for use in the momentum density and the Porsgrunn data set, and

suggests that the constants are sensitive to the position of slip in the density equation as well. An issue is how much they vary for different situations and input data. For instance, it would be valuable to know if k_{modCh} with $\xi = 0.6$ and $\beta = 5$ will give better results than using k_{Ch} for any input data, or whether it would be better to use k_{Ch}, or possibly just Equation (14a) independent on the Lockhart-Martinelli parameter, if a tuning of ξ and β is not possible. It is difficult to answer this question by looking at the results from the field data, because there is so little variation in the results in general and the slip is almost constant for each choke opening, as will discussed further in the following section. However, Al-Safran and Kelkar embraces k_{modCh} for critical flow in their model as well, suggesting that it might be better than k_{Ch}.

Al-Safran and Kelkar's model and Chisholm's slip model have illustrated two important things when it comes to changing parameters midway. Differentiation based on flow regime is difficult when the parameter itself is part of the expression that decided if there is critical flow or not. As good as all parameters are in some ways included in the criterion for critical flow, so this means that changing any parameter on the basis of flow regime should be avoided. Differentiating based on another criterion, on the other hand, seems possible. Which expression to use in Chisholm's slip model depends indirectly only on pressure as all models consider x_G, n or κ to be constants, and was possible to carry out in practice in the same manner as gas expansion is included in the models.

7.4 The Field Data

The results for the field data is almost the same for all models, no matter what changes are made. Even the removal of slip from the Hydro Model, which greatly impacts the results for the Porsgrunn data set, does not really change the error estimators for the field data considerably. If anything, the results are improved. For all models, there is a considerable difference in the predictions for the Porsgrunn data set, but for the field data, there is little variation, the standard deviation is always around $13 - 14\,\%$, with $9\,\% < E_2 < 10\,\%$ and E_1 sees the largest difference between $6 - 8\,\%$. This means that basically every model and version gives the same spread among the data points, and the magnitude of the predicted flow rate is tuned up and down with the discharge coefficient. That this varies a lot can be seen in Table 4 and 11.

The field data consists of many data points that are very similar to each other, especially within one choke opening and by that within each C_D. For example, all data points for the two smallest choke opening are predicted to be critical by all models, while all but one or two in the largest choke opening are sub-critical. In addition, the pressure drop and P_1 are little different for the data points within one choke opening. As can be seen from Figure 29b, also the slip is relatively constant for each choke opening. For each slip model, there can be seen three columns that happen to coincide with the choke openings. The only exception here is k_{modCh}, where the data points for the largest choke opening form an arch, around $k_{modCh} \approx 3$, more than a column, but the difference is still not very large.

Looking at any $\dot{m}_{calc}\, vs.\, \dot{m}_{meas}$-plot for this data set, the different choke openings are also easily discernible, where the smallest choke opening gives the smallest mass flow rate and the largest choke opening the largest mass flow rate.

Because the data points are so similar in pressure drop and gas density, the discharge coefficient is effectively tuned for each special case, leading the differences between the models to almost disappear. That, for instance, the Sachdeva et al. model and Asheim's

model do not include slip, can be accommodated for with a higher C_D than the Hydro Model, as can be seen in Table 4 and is also illustrated when removing the slip from the Hydro Model in Table 11. As long as the properties within each choke geometry and opening are relatively similar, the discharge coefficient seems to be a powerful tuning instrument that will give almost the same results independent on which model is used. Which model or version that is best seems therefore almost random, and might as well depend more on how well tuned C_D is, and whether adding a third decimal point would give other results.

Because of this, the field data used in this thesis are not ideal for evaluating a choke flow model, and more emphasis has been put on the Porsgrunn data set to see trends in error distribution and similar.

7.5 General

The Bernoulli Equation with $\Phi_{TP,Si}$ started out by giving good predictions with a relatively simple model. The two-phase multiplier that includes phase slippage is probably an important reason for that, as it was later seen in Al-Safran and Kelkar's model and the Hydro Model how important slip is. Change in gas density is not included, not even when calculating the slip, but this does not seem to be an issue until x_G approaches 0.25, where the Bernoulli Equation greatly over-predicts the flow rate. This area is also the area where there critical velocity is at its lowest, and it is possible that part of the reason for so high over-predictions in these data points are that they are in fact critical flow.

It is also interesting to see that for the different versions of the Bernoulli Equation in Table 1, the discharge coefficients are in the expected order from smallest to largest for the field data only, not for the Porsgrunn data set. For the more advanced models, the discharge coefficients do not follow any particular pattern. For the field data, the middle choke opening always has the highest C_D, and it is also the opening area with least spread in the data points. The altogether nine different C_Ds for every model or version of a model, three for the field data, and 2×3 for the Porsgrunn data set, are in most cases rather different from each other, especially the field data and Porsgrunn data set. This shows that it is difficult to recommend one general value. However, when using κ with the Hydro Model without pressure recovery, the C_D-values are the same for all orifice geometry chokes in the Porsgrunn data set, and two of the three cage geometry chokes. But for the field data, the discharge coefficients are different again. This may have something to do with the discharge coefficients of the field data being tuned a lot more to a particular pressure drop and slip, as discussed above, which affects the value more than changing n to κ. The reason for the discharge coefficients to be in an almost random order, and not higher for higher choke openings may have to do with the model not portraying actuality in exactly the right way.

Some of the discharge coefficients, especially for Al-Safran and Kelkar's model, are larger than unity. When thinking of C_D as the ratio of flow area to choke area, this seems very illogical, but also other factors play a part in the tuning process, for instance losses such as friction. But this is thought to lower the value, not increase it. Therefore it might be related to other parts of the model, for instance gas expansion, or slip model. For example, more gas expansion will give less mass per volume, thus leading to a lower mass flow rate than what actually flows through. The same is valid for a too low slip model.

That x_G is assumed to be constant is not considered to be a large drawback for any model. All but the original Hydro Model does not consider what happens after position

(2) in Figure 1, and it has previously been discussed how short a time the fluid spends passing through the choke. This means that there is also little time for mass transfer, and most flashing of gas could then be said to occur after the choke exit, in a location that is not included in the models.

Table 14: Summary: the best choke models' statistics

	Porsgrunn data set			Field data		
	E_1	E_2	σ	E_1	E_2	σ
The Bernoulli Equation w Φ_{TP}	1.352	7.871	11.091	-6.560	9.636	13.573
Asheim	-0.740	22.377	26.574	-6.827	9.636	13.764
Sachdeva et al.	1.366	19.973	24.139	-6.867	9.593	13.818
Al-Safran and Kelkar	-0.664	11.268	13.536	-7.281	9.982	13.849
The Hydro Model original	0.067	6.993	8.859	-7.626	9.973	14.081
The Hydro Model revised	-0.430	6.327	8.225	-7.082	10.000	14.058

7.6 Further Work

Although some conclusions have come of this thesis, there is still several things that should be further investigated, especially related to the modified version of Chisholm's slip model and generally more testing of the revised Hydro Model.

The constants $\xi = 0.6$ and $\beta = 5$ have been tuned, if not particularly to fit with, but with the help of the Porsgrunn data set that is used in this thesis. It was hoped that the field data could help in determining how much these can vary, if they are as different for different input data as the discharge coefficients are, or if they are relatively constant. However, that was not achieved, and a data set with more varying pressure drop, upstream pressure and gas mass fractions within each C_D, would be useful to find that out.

Another possibility that should be tested out is using only one part of Chisholm's original slip model, Equation (14a), for all gas mass fractions.

8 Conclusion

This thesis has evaluated five models for prediction of mass flow across a choke for two-phase flow. Of these five models, perhaps the best model is the Bernoulli Equation with Simpson et al.'s two-phase multiplier and slip model, because it gives good predictions for both data sets tested. This was a bit surprising because of the simplicity of the model and the lack of differentiating between critical and sub-critical flow.

When looking at different combinations of two-phase multipliers, density and slip models, it was discovered that $\rho_e(k_{Si}) = \rho_L/\Phi_{TP,Ch}(k_{Si}) = \rho_L/\Phi_{TP,Si}$, and it was also this combination that gave the best results for the Bernoulli Equation with two-phase multiplier. Simpson et al. and Chisholm are also names that are repeated among other authors, like Al-Safran and Kelkar and Selmer-Olsen et al.

Asheim's model and Sachdeva et al.'s model are also very similar, the only difference being that Asheim assumes gas expansion according to the gas law, while Sachdeva et al. models the gas expansion as adiabatic. It may seems adiabatic gas expansion is a little better, at least for one of the two data sets that were used for model evaluation in this thesis.

The Hydro Model gave the best predictions for the Porsgrunn data set, but was the worst for the field data. This shows how difficult it is to develop a general model. When it comes to the revision, there is not much difference between the original version and the revised version presented here. The largest change is the removal of pressure recovery, which approximately halves the run time without losing accuracy. This, however, did not improve the results for the field data very much, and the Revised Hydro Model is still the worst for this data set. The trend in error distribution that was originally seen, has been dimished by exchanging n for κ as gas expansion exponent.

In general, it seems that the models that account for slippage outperforms the models that do not. Because of this, slippage appears to be the single most important feature any multiphase flow choke model. Among the densities presented in this thesis, the momentum density ρ_e seems to be the one best suited for use with multiphase flow through a choke.

Nomenclature

Symbols

A	area, m^2
C_C	contraction coefficient, A_{vc}/A_2
C_D	discharge coefficient
C_L	heat capacity for liquid, J/kg
C_P	heat capacity at constant pressure for gas, J/kg
C_V	heat capacity at constant volume for gas, J/kg
CV	control volume
d	diameter, m
E_1	mean relative error
E_2	mean of absolute relative error
N	number of data points
k	slip ratio, u_G/u_L
M	molar mass, kg/mol
$\dot{m}$	mass flow rate, kg/s
n	polytropic exponent
P	pressure, Pa
Q	volumetric flow rate, m^3/s
R	universal gas constant, $8.3145\, J/molK$
T	temperature, K
u	velocity, m/s
WC	water cut
x	mass fraction, $\dot{m}_i/\dot{m}_{total}$
y	pressure ratio, P_2/P_1
Z	Z-factor for gas
α	void fraction, A_G/A
κ	heat capacity ratio, C_P/C_V
Φ_{TP}	two-phase pressure drop multiplier

ρ	density, kg/m^3
σ	standard deviation
χ	Lockhart-Martinelli Parameter

Subscripts

1	upstream of the choke
2	at the choke throat
3	downstream of the choke
1P	single-phase
TP	two-phase
c	critical
G	gas
L	liquid
act	actual (observed)
calc	calculated
meas	measured
e	momentum
m	homogeneous
o	oil
vc	vena contracta
w	water
Ch	Chisholm (slip model)
modCh	modified Chisholm (slip model)
Si	Simpson (slip model)

References

[1] The Norwegian Petroleum Directorate: Factpages. `http://factpages.npd.no/factpages/default.aspx`, April 2012.

[2] T. Ahmed. *Reservoir Engineering Handbook*, chapter 2: Reservoir-Fluid Properties. Gulf Professional Publishing, Elsevier, fourth edition edition, 2010.

[3] E. M. Al-Safran and M. Kelkar. Predictions of Two-Phase Critical-Flow Boundary and Mass-Flow Rate Across Chokes. *SPE Productions & Operations*, pages 249–256, May 2009. SPE 109243.

[4] H. A. Asheim. Personal communication, September–December 2011 and January 13, February 22-24, April 26 2012 . The Norwegian University of Science and Technology, Trondheim.

[5] D. Chisholm. Research Note: Void Fraction During Two-Phase Flow. *Journal of Mechanical Engineering Science*, 15(3):235–236, June 1973.

[6] D. Chisholm. *Two-phase flow in in pipelines and heat exchangers*. George Goodwin, London and New York and The Institution of Chemical Engineers, first edition, 1983.

[7] M. Fossa and G. Guglielmini. Pressure drop and void fraction profiles during horizontal flow through thin and thick orifices. *Experimental Thermal and Fluid Sciences*, 26:513–523, February 2002.

[8] K. R. Hall and L. Yarborough. A new equation of state for Z-factor calculations. *The Oil and Gas Journal*, pages 82–92, June 1973.

[9] R. K. Haug. Multiphase Flow Through Chokes. TPG 4510 Specialization Project at The Norwegian University of Science and Technology, January 2012.

[10] D. Ljungquist. Personal communication, February 2012. FMC Kongsberg Subsea, Asker, Norway.

[11] MATLAB. *Version 7.13.0.564 (R2011b)*. The MathWorks Inc., Natick, Massachusetts, 2011.

[12] B. R. Munson, D. F. Young, and T. H. Okiishi. *Fundamentals of Fluid Mechanics*. John Wiley & Sons, Inc, third edition, 1998.

[13] R. Sachdeva, Z. Schmidt, J. P. Brill, and R. M. Blais. Two-Phase Flow Through Chokes. In *61st Annual Technical Conference and Exhibition of the Society of Petroleum Engineers*, October 1986. SPE 15657.

[14] R. B. Schüller, T. Solbakken, and S. Selmer-Olsen. Evaluation of Multiphase Flow Rate Models for Chokes Under Subcritical Oil/Gas/Water Flow Conditions. *SPE Production & Facilities*, pages 170–181, August 2003. SPE 84961.

[15] R. B. Schüller, S. Munaweera, S. Selmer-Olsen, and T. Solbakken. Critical and Subcritical Oil/Gas/Water Mass Flow Rate Experiments and Predictions for Chokes. *SPE Production & Operations*, pages 372–380, August 2006. SPE 88813.

[16] S. Selmer-Olsen. Subsea Choke Flow Characteristics. Technical Report 92-2054, Det Norske Veritas Research, June 1993.

[17] M. Skottene and K. Holmås. Personal communication, January-June 2012. FMC Kongsberg Subsea, Asker, Norway.

[18] M. B. Standing. A Pressure-Volume-Temperature Correlation for Mixtures of California Oils and Gases. *API Drilling and Production Prac.*, pages 275–287, 1947.

[19] L. Yarborough and K. R. Hall. How to solve equation of state for Z-factors. *The Oil and Gas Journal*, pages 86–88, February 1974.

A Additional Figures

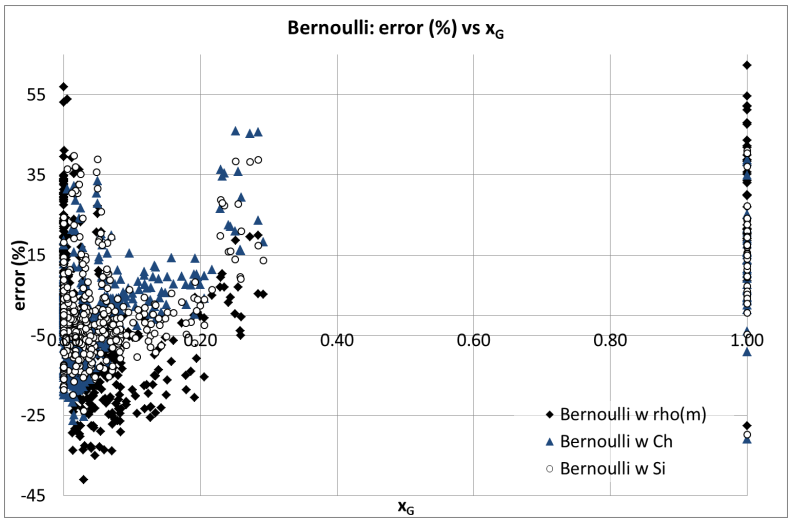

Figure A.1: Error vs. x_G for the whole range of x_G, Bernoulli Equations, Porsgrunn data set

as a supplement to Figure 6b

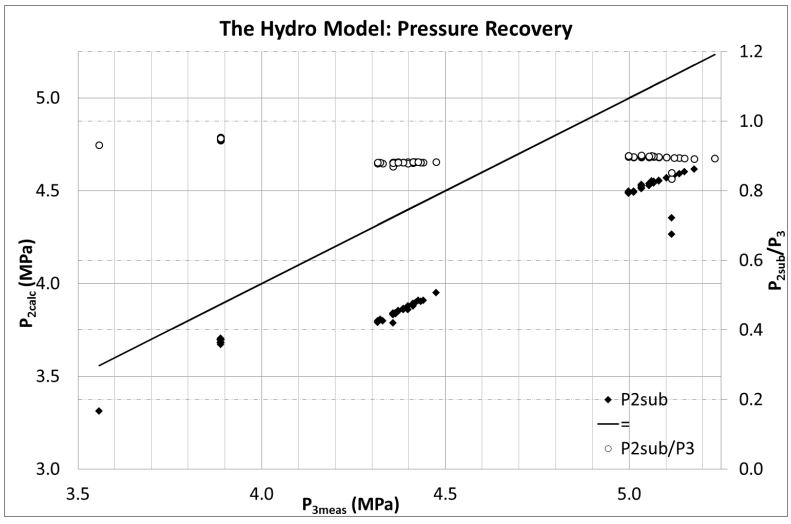

Figure A.2: The Hydro Model: Pressure recovery, field data

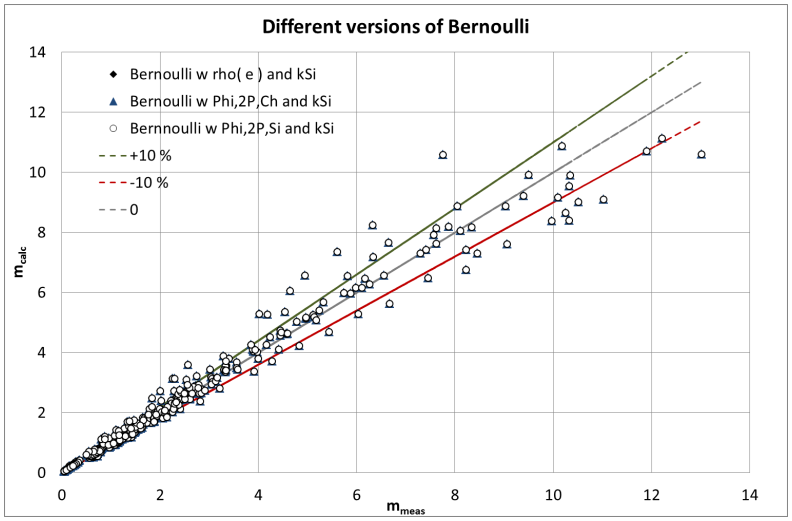

(a) Calculated vs. measured mass flow rate

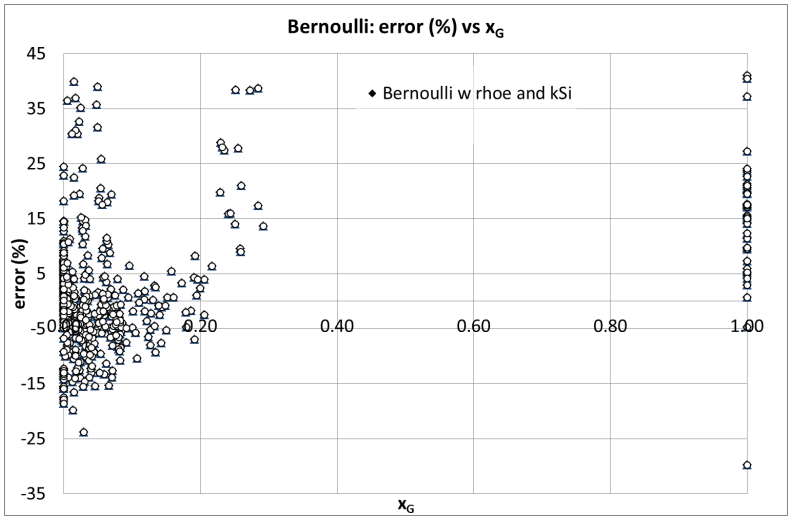

(b) Error vs. x_G for the whole range of x_G, the Bernoulli Equation with best results

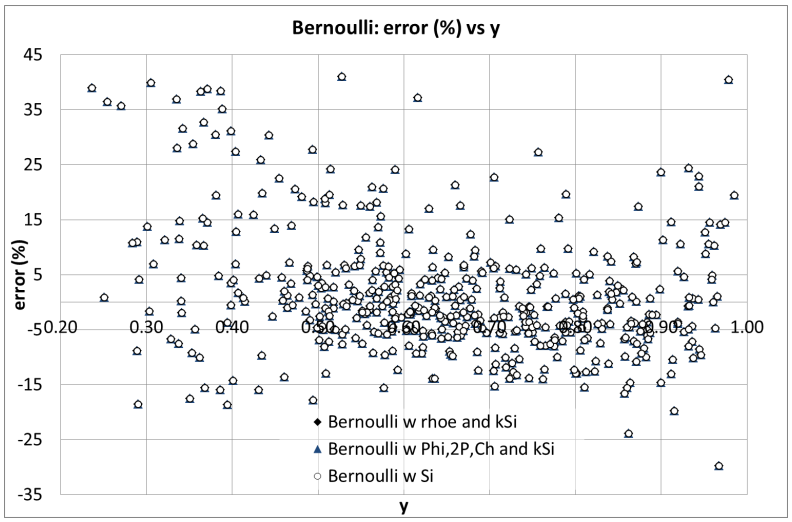

(c) Error vs $y = P_2/P_1$

Figure A.3: Error distribution for the Bernoulli Equation with best results, Porsgrunn data set

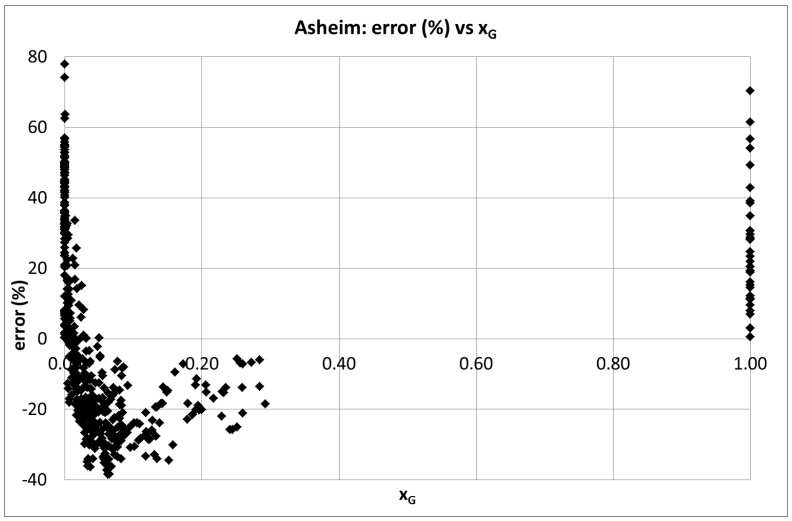

(a) Error vs. x_G for the whole range of x_G, Asheim's model, as a supplement to Figure 8b

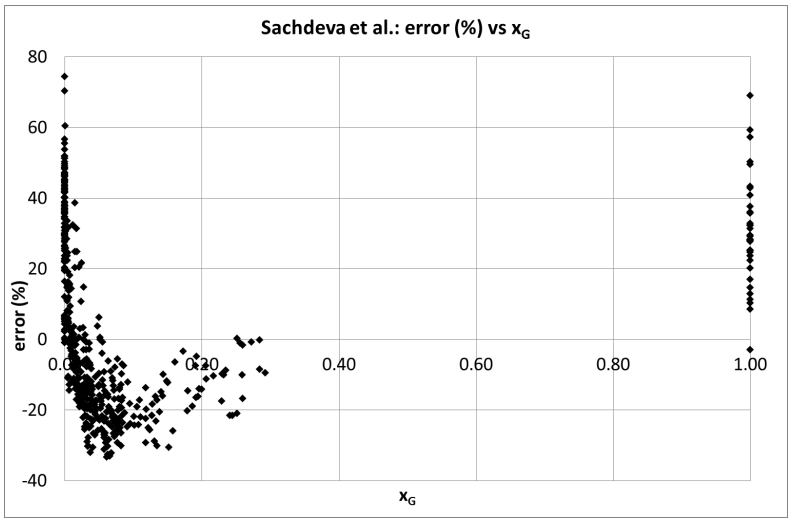

(b) Error vs. x_G for the whole range of x_G, the Sachdeva et al. model, as a supplement to Figure 10b

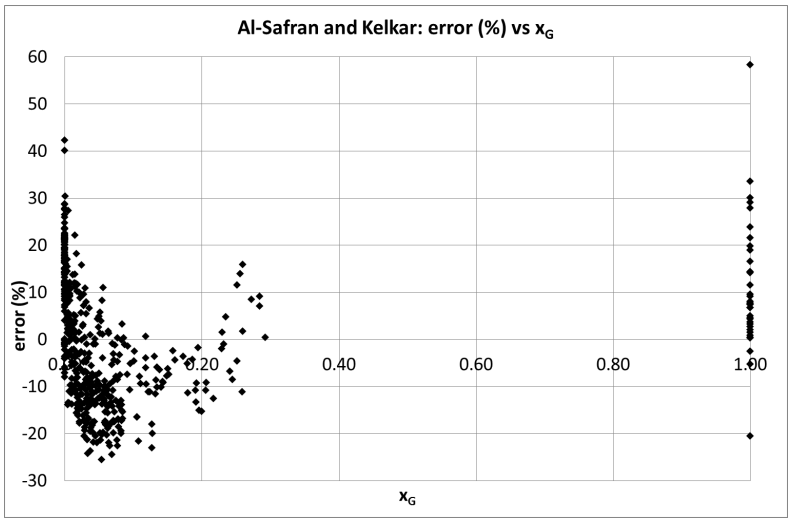

(c) Error vs. x_G for the whole range of x_G, Al-Safran and Kelkar's model, as a supplement to Figure 12b

Figure A.4: Error vs. x_G for Asheim's, Sachdeva et al. and Al-Safran & Kelkar's models, Porsgrunn data set

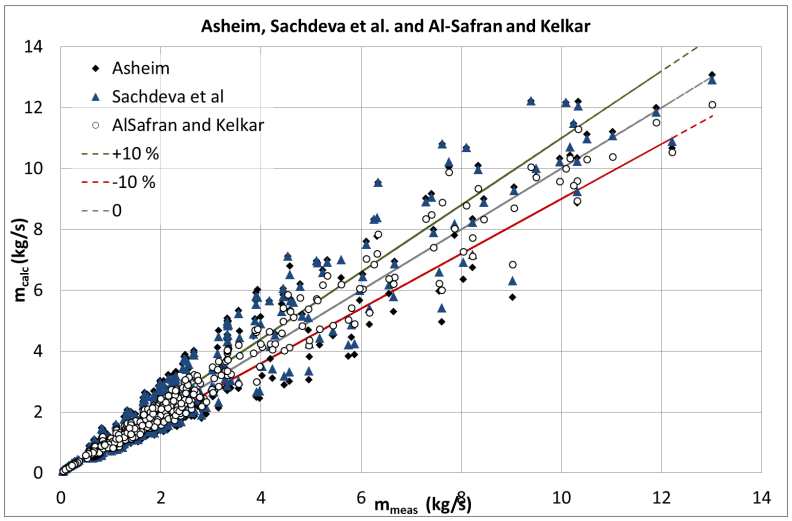

(a) Calculated vs. measured mass flow rate

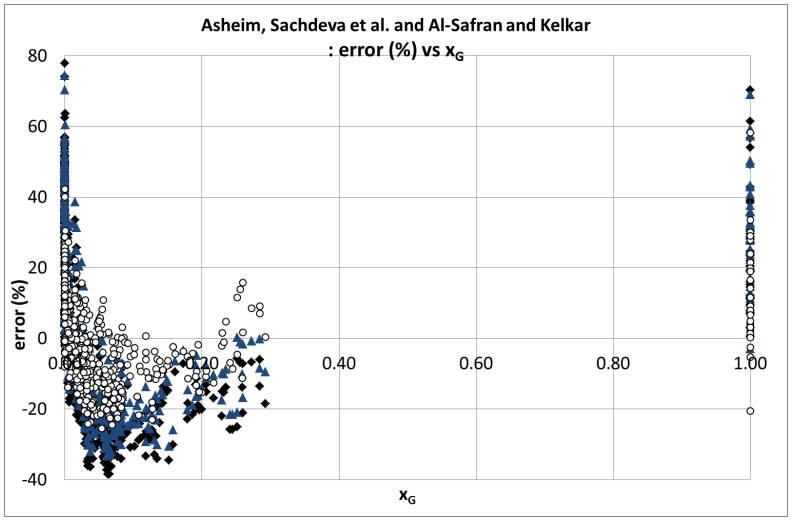

(b) Error vs. x_G for the whole range of x_G

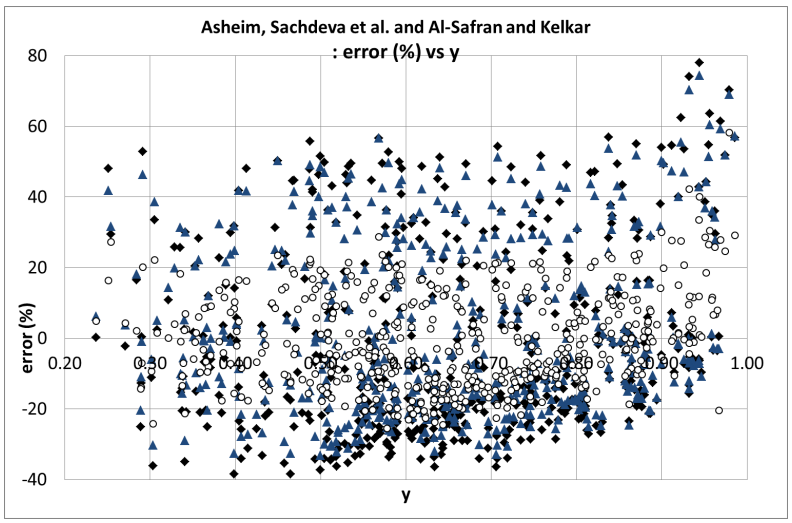

(c) Error vs $y = P_2/P_1$

Figure A.5: Error distribution for Asheim, Sachdeva, Al-Safran & Kelkar's models, Porsgrunn data set

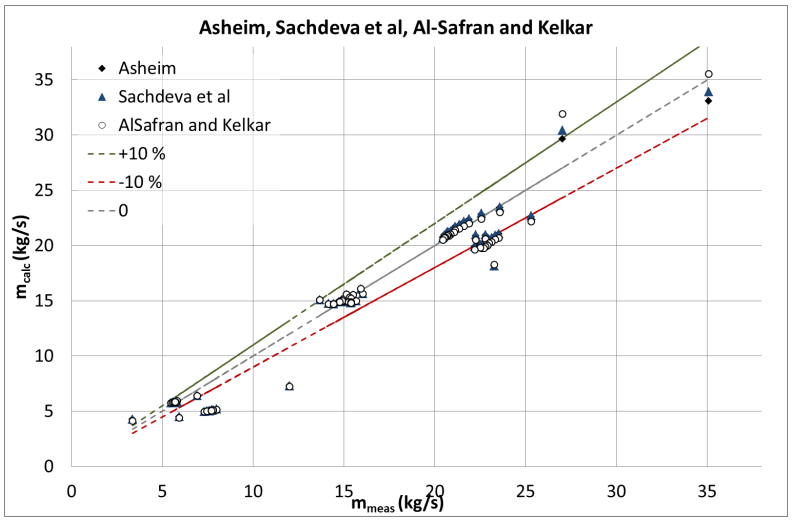

(a) Calculated vs. measured mass flow rate

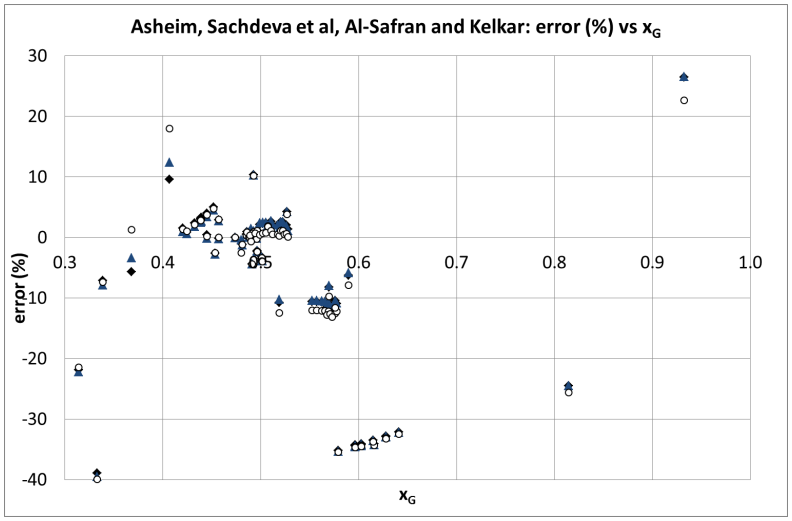

(b) Error vs. x_G

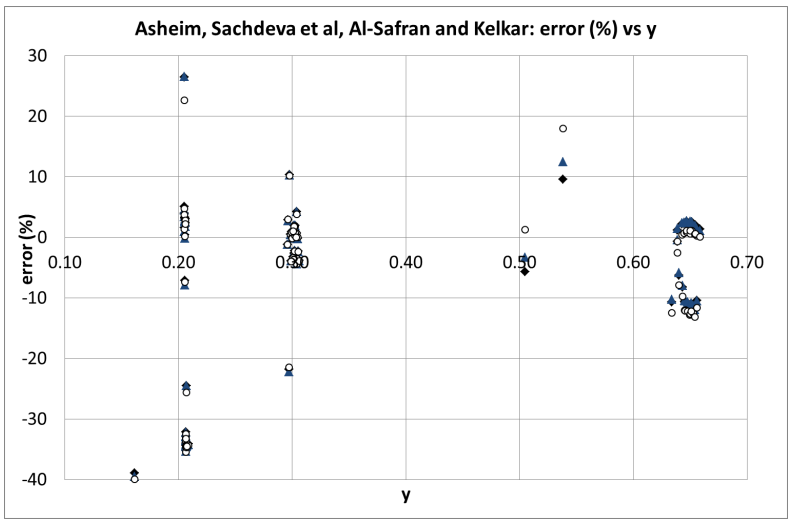

(c) Error vs $y = P_2/P_1$

Figure A.6: Error distribution for Asheim, Sachdeva, Al-Safran & Kelkar's models, field data

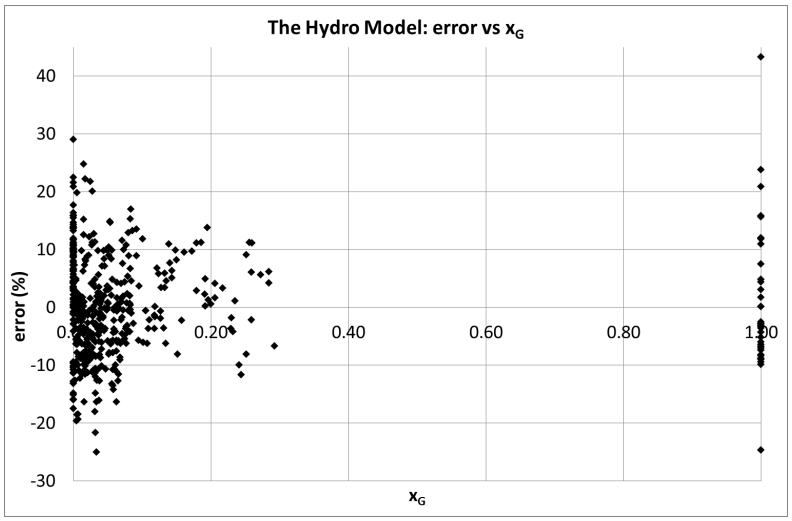

(a) The original model, as a supplement to Figure 14b

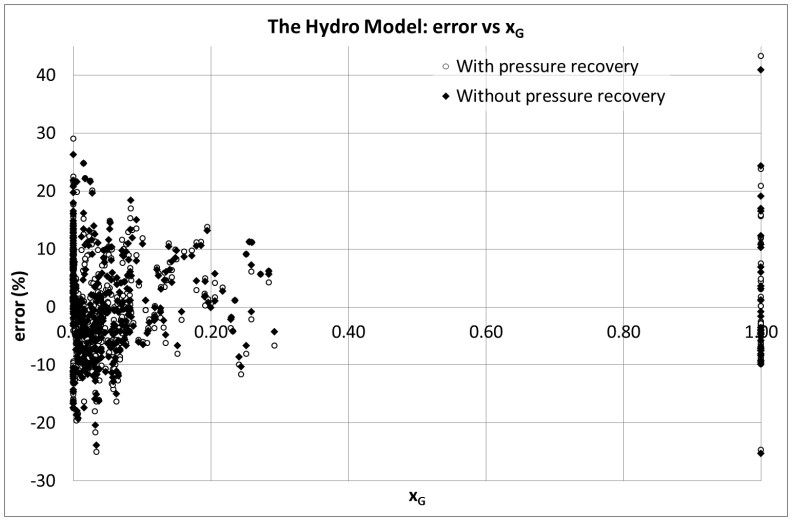

(b) Without pressure recovery, as a supplement to Figure 19

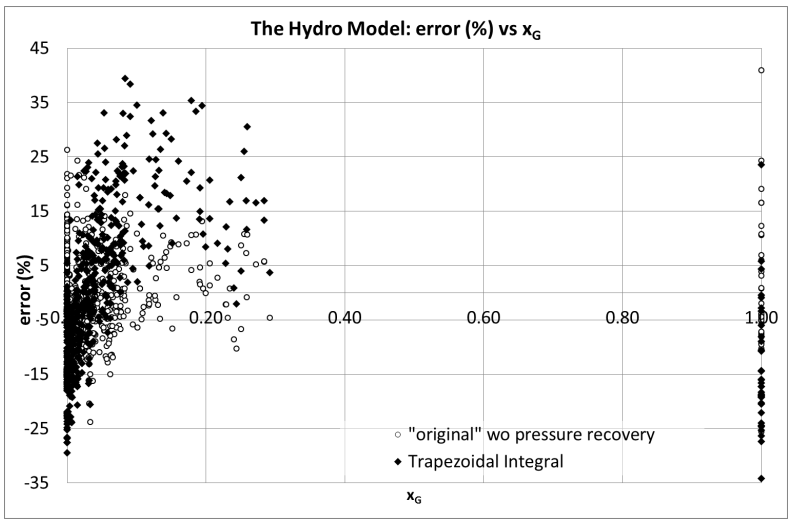

(c) Without pressure recovery, trapezoidal approximation for density integral, as a supplement to Figure 22b

Figure A.7: Error vs. x_G for the whole range of x_G, the Hydro Model, Porsgrunn data set

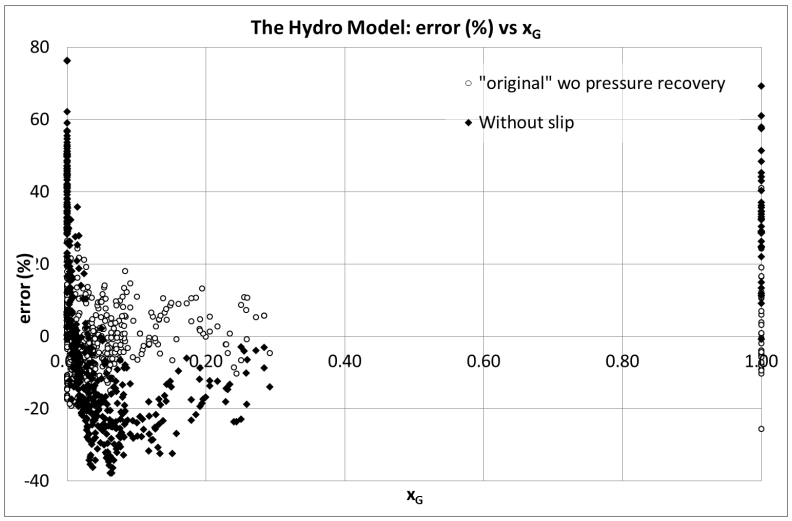

(a) Without pressure recovery, and no slip (ρ_{hom}) as a supplement to Figure 24b

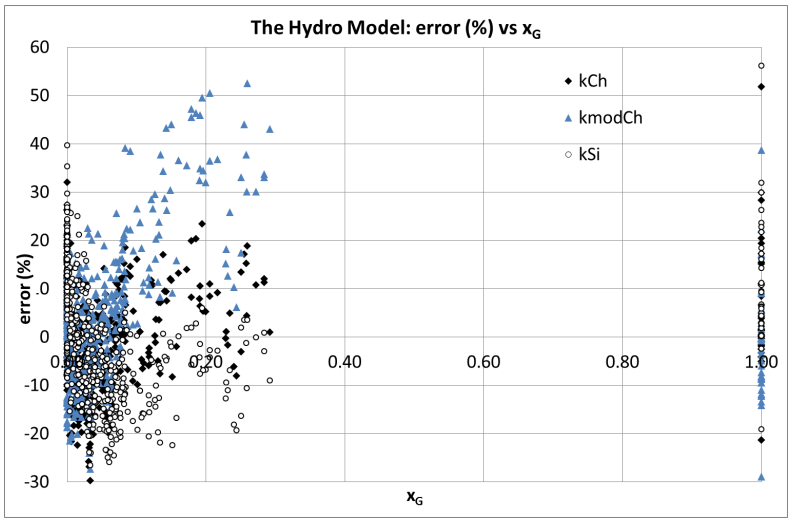

(b) Without pressure recovery, with ρ_{TP} and different slip models, as a supplement to Figure A.10b

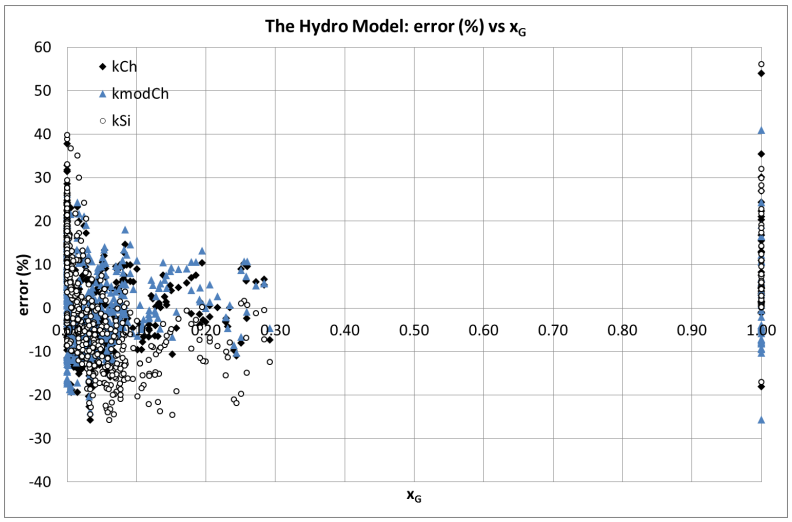

(c) Without pressure recovery, with ρ_e and different slip models, as a supplement to Figure A.11b

Figure A.8: Error vs x_G for the whole range of x_G, the Hydro Model, Porsgrunn data set

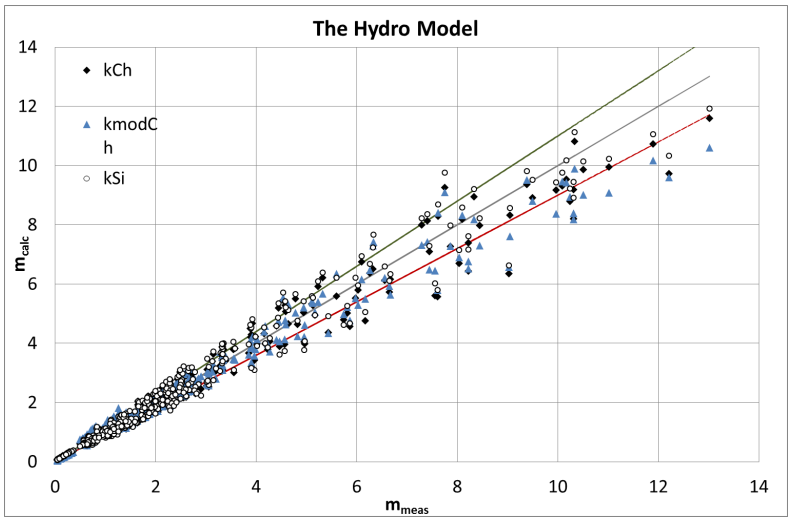

(a) Calculated vs. measured mass flow rate

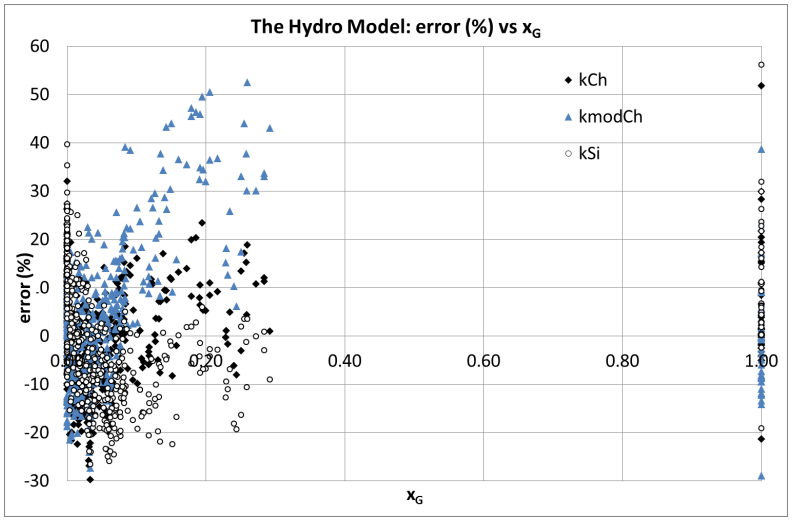

(b) Error vs x_G

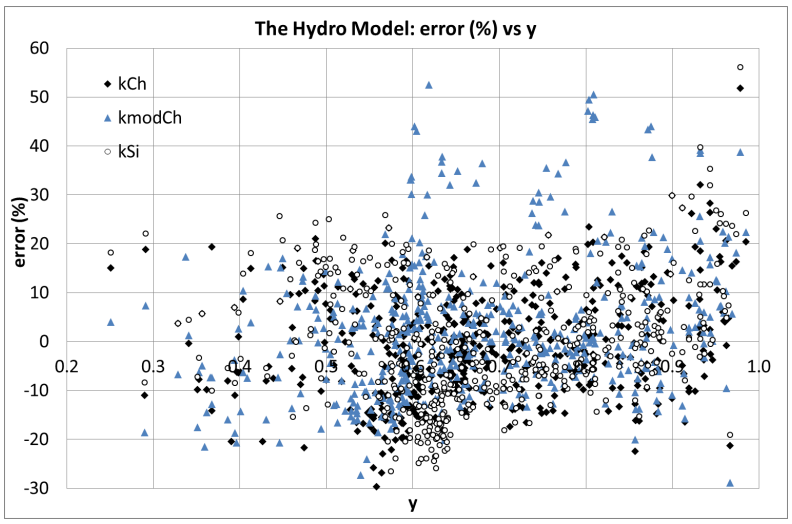

(c) Error vs $y = P_2/P_1$

Figure A.10: Error distribution for the Hydro Model with ρ_{TP} and different slip models, Porsgrunn data set

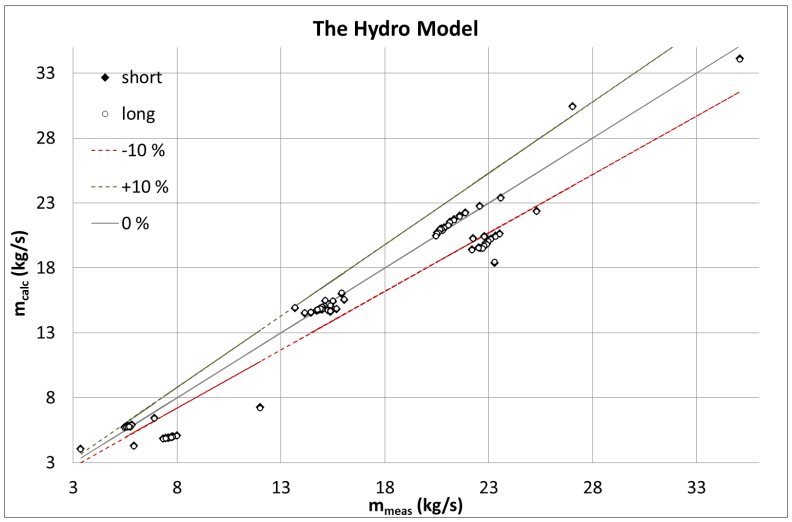

(a) Calculated vs. measured mass flow rate

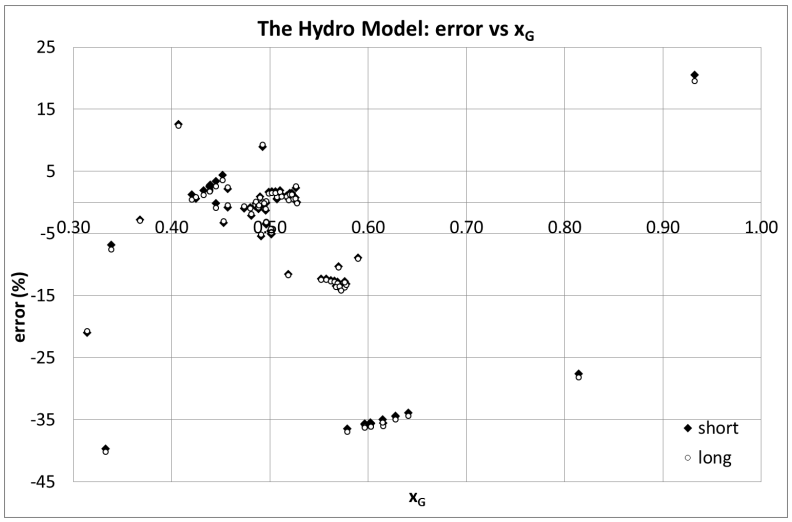

(b) Error vs. x_G

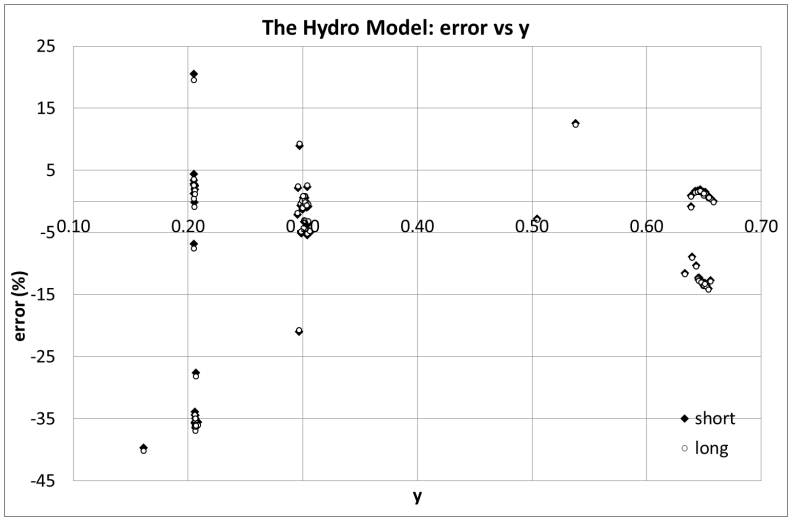

(c) Error vs $y = P_2/P_1$

Figure A.9: Error distribution for the Hydro model without pressure recovery, field data

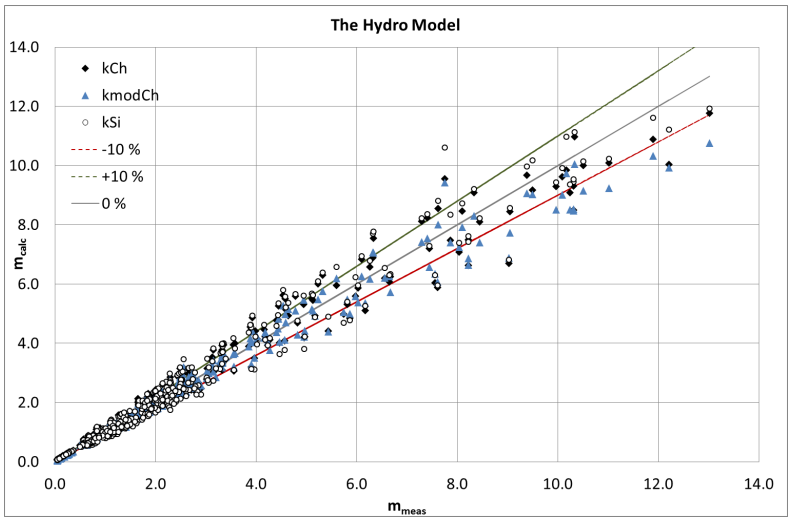

(a) Calculated vs measured flow rate

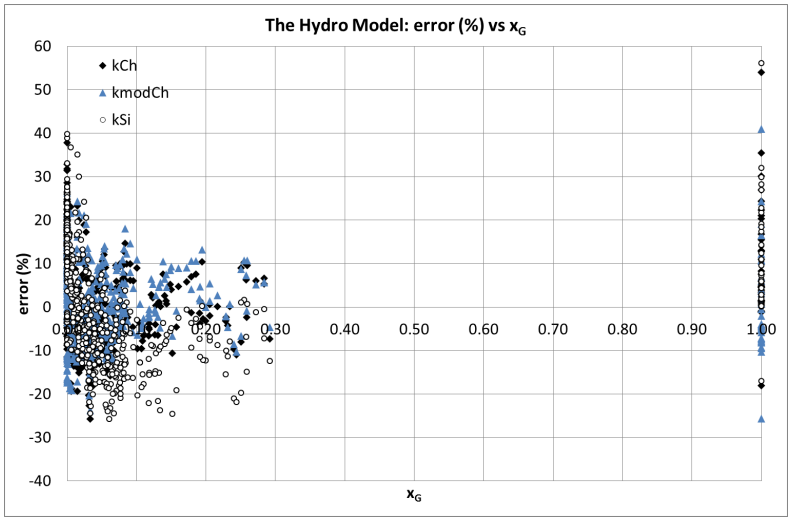

(b) Error vs x_G

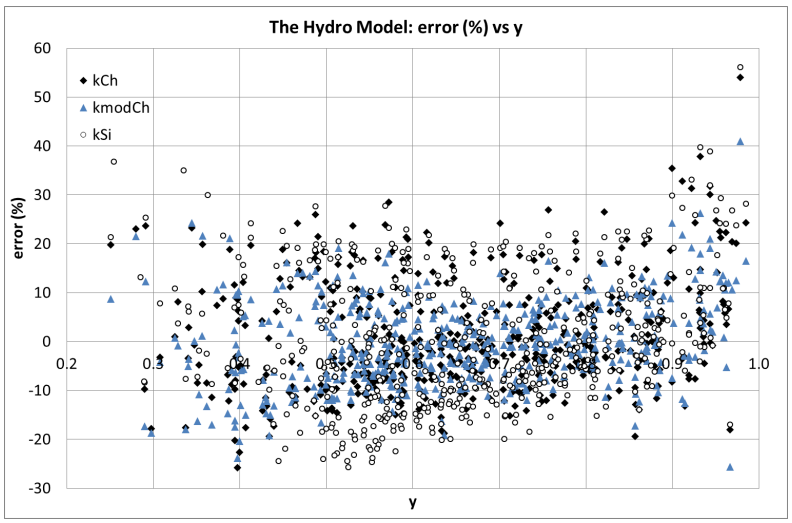

(c) Error vs $y = P_2/P_1$

Figure A.11: Error distribution for the Hydro Model with ρ_e and different slip models, Porsgrunn data set

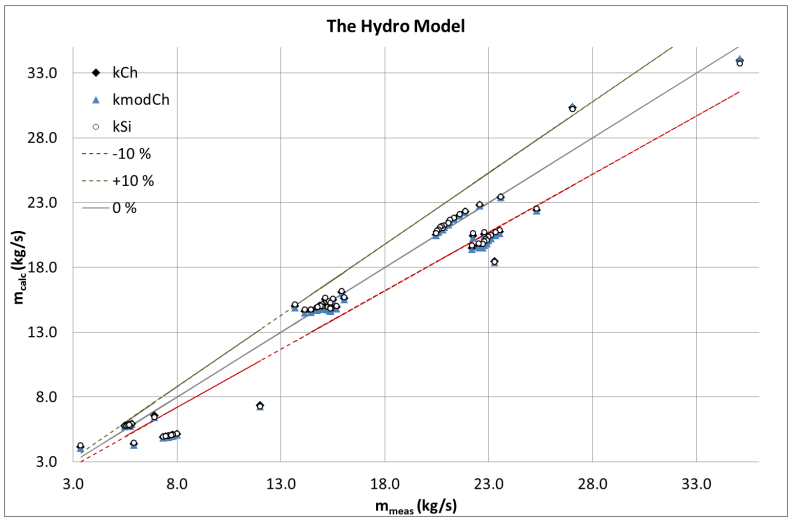

(a) Calculated vs measured flow rate

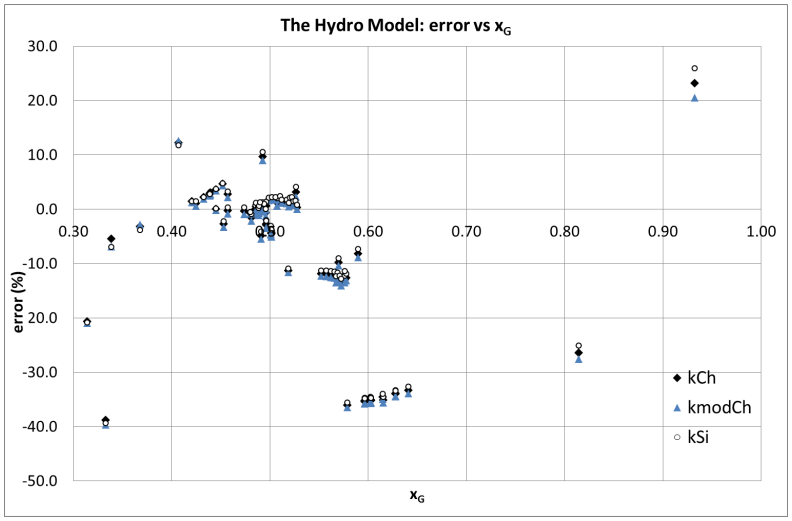

(b) Error vs x_G

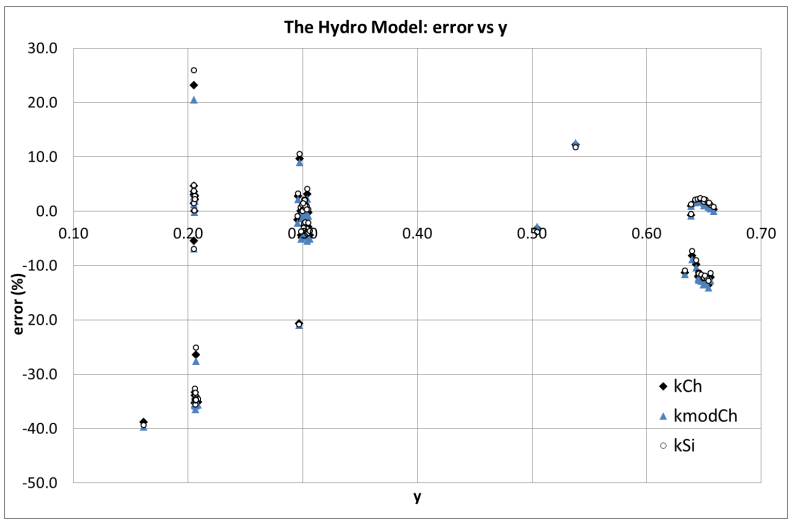

(c) Error vs $y = P_2/P_1$

Figure A.12: Error distribution for the Hydro Model with ρ_e and different slip models, field data

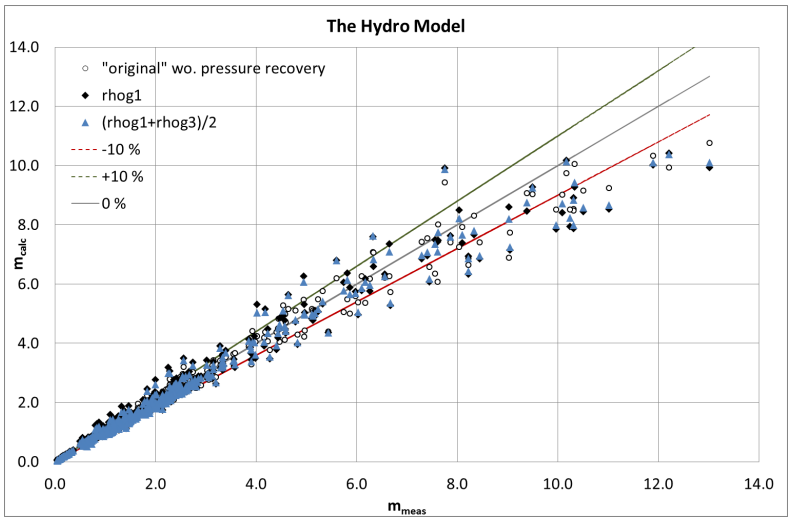

(a) Calculated vs. measured mass flow rate

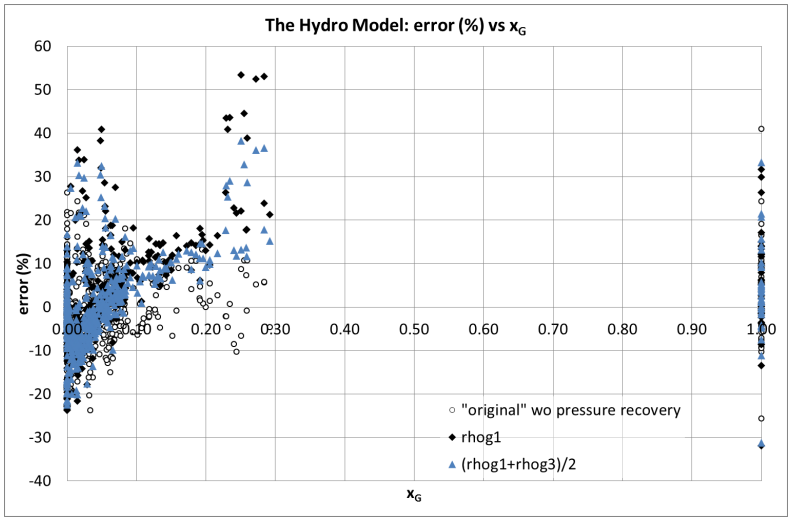

(b) Error vs. x_G

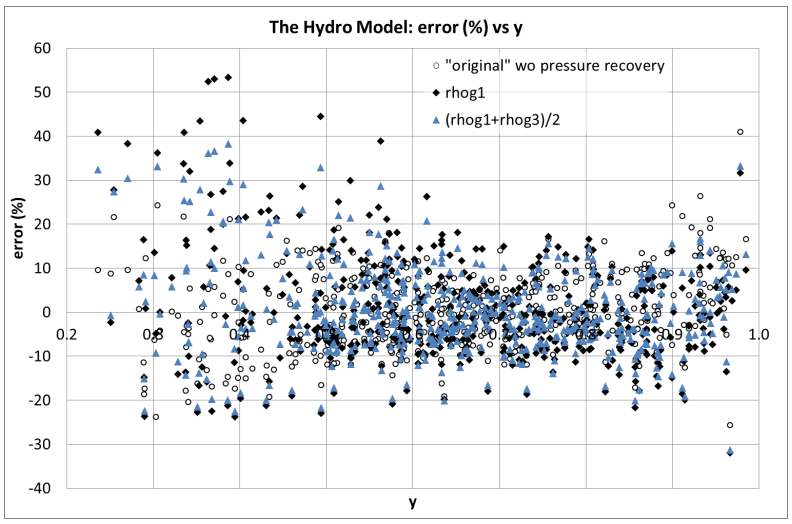

(c) Error vs. $y = P_2/P_1$

Figure A.13: Error distribution for the Hydro Model with constant gas density, Porsgrunn data set

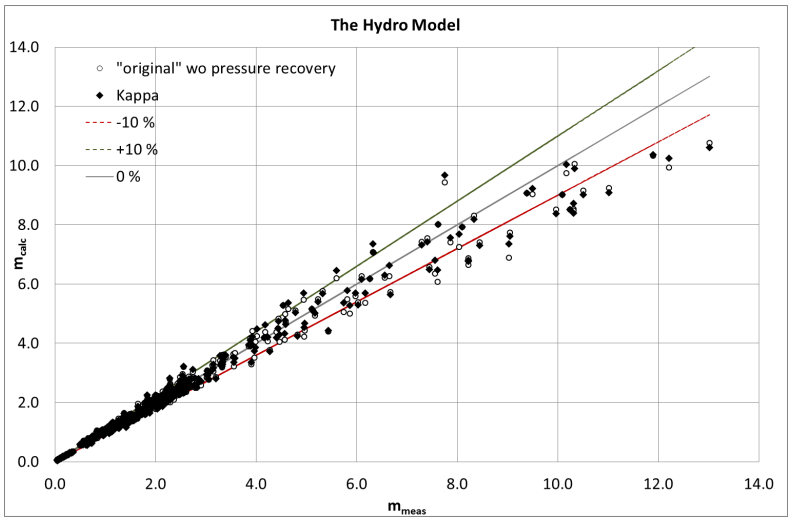

(a) Calculated vs. measured mass flow rate

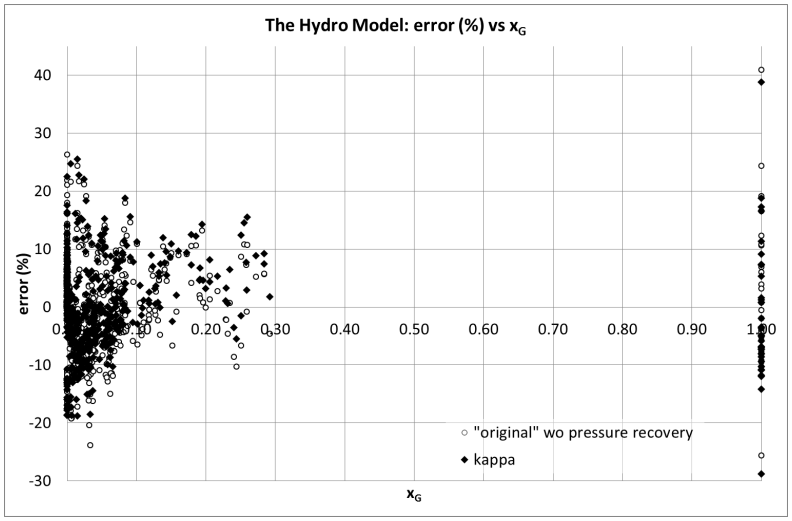

(b) Error vs. x_G

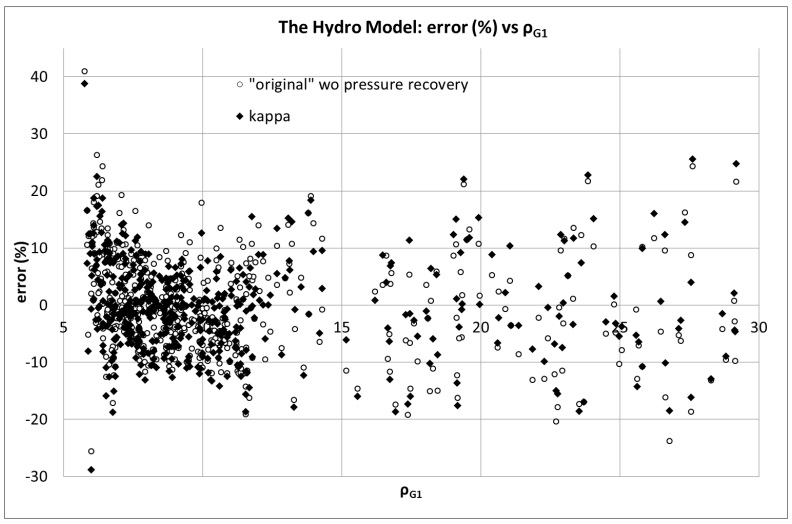

(c) Error vs. ρ_{G1}

Figure A.14: Error distribution for the Hydro Model with κ, Porsgrunn data set

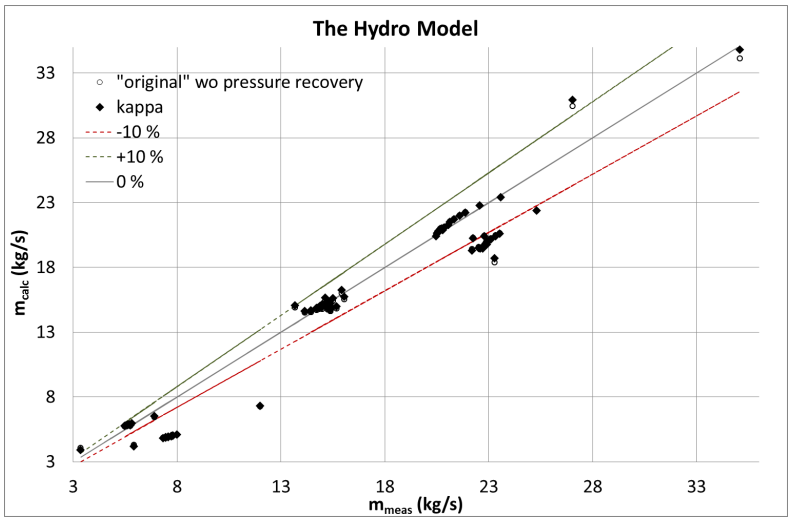

(a) Calculated vs. measured mass flow rate

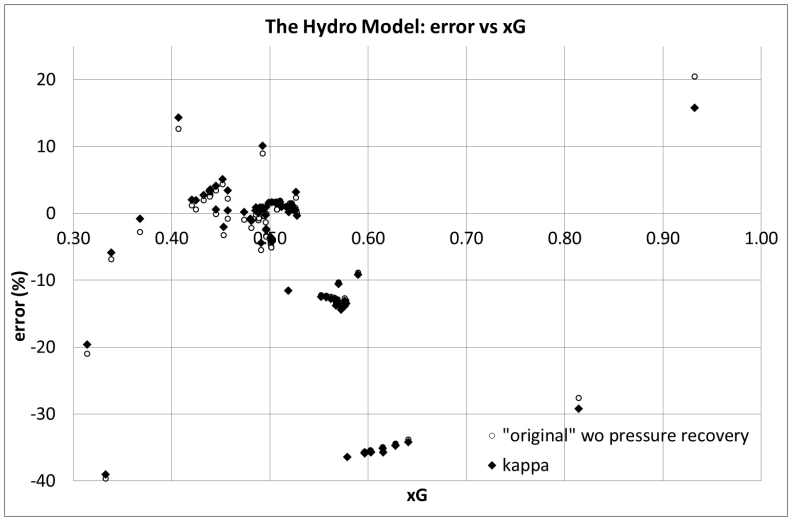

(b) Error vs. x_G

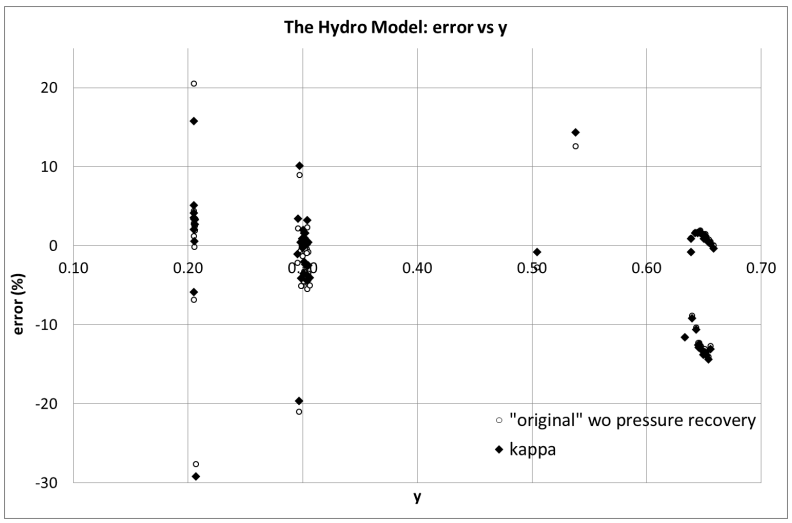

(c) Error vs. $y = P_2/P_1$

Figure A.15: Error distribution for the Hydro Model with κ, field data

B Additional Tables

Table B.1: Discharge coefficients for different combinations for the Bernoulli Equation, Porsgrunn data set

(a) Choke geometry: Cage

Choke opening:	11 mm	14 mm	18 mm
Bernoulli w/ρ_{TP} and k_{Ch}	0.61	0.61	0.54
Bernoulli w/ρ_{TP} and k_{Si}	0.48	0.61	0.52
Bernoulli w/ρ_e and k_{Ch}	0.63	0.65	0.59
Bernoulli w/$\Phi_{2P,Si}$ and k_{Ch}	0.61	0.66	0.58

(b) Choke geometry: Orifice

Choke opening:	11 mm	14 mm	18 mm
Bernoulli w/ρ_{TP} and k_{Ch}	0.58	0.59	0.59
Bernoulli w/ρ_{TP} and k_{Si}	0.51	0.58	0.54
Bernoulli w/ρ_e and k_{Ch}	0.62	0.62	0.63
Bernoulli w/$\Phi_{2P,Si}$ and k_{Ch}	0.58	0.62	0.61

Table B.2: Discharge coefficients for different combinations for the Bernoulli Equation, field data

Choke opening:	12 mm	22 mm	38 mm
Bernoulli w/ρ_{mix} and k_{Ch}	0.44	0.50	0.61
Bernoulli w/ρ_{mix} and k_{Si}	0.45	0.52	0.65
Bernoulli w/ρ_e and k_{Ch}	0.46	0.53	0.66
Bernoulli w/ρ_e and k_{Si}	0.47	0.54	0.67
Bernoulli w/$\Phi_{2P,Ch}$ and k_{Si}	0.47	0.54	0.67
Bernoulli w/$\Phi_{2P,Si}$ and k_{Ch}	0.59	0.74	1.12

Table B.3: The importance of u_1 for the largest choke opening, field data

i	$1/(A_1^2\rho_{e1}^2)$	$1/(C_D^2A_2^2\rho_{e2}^2)$	$(1)/(2)\,\%$
58	0.3814	39.7241	0.9601
59	0.9914	85.4631	1.1600
60	1.2764	117.2906	1.0882
61	1.2356	109.8116	1.1252
62	1.1914	102.9782	1.1569
63	1.2204	106.1319	1.1499
64	1.2527	109.2608	1.1465
65	1.2750	111.6489	1.1420
66	1.2978	113.4279	1.1442
67	1.3066	113.4294	1.1519
68	1.3223	115.0672	1.1491
69	1.3529	117.7446	1.1490
70	1.3473	116.2834	1.1587
71	1.3518	118.4128	1.1416
72	1.3690	118.1051	1.1592
73	0.4986	49.1776	1.0139
74	0.8693	70.9831	1.2246
75	0.9282	76.2498	1.2173
76	0.9787	80.3343	1.2182
77	1.0034	82.1781	1.2210
78	1.0309	84.1288	1.2254
79	1.0532	86.3835	1.2193
80	1.0732	87.3062	1.2292
81	1.1032	90.3405	1.2212
82	1.1178	90.4964	1.2352
83	1.1109	91.0666	1.2198
84	1.1213	92.3645	1.2140
85	1.1430	93.3871	1.2239
86	1.1513	94.1193	1.2233
87	1.1738	95.1685	1.2334

Table B.4: Al-Safran and Kelkar's model without pressure recovery

(a) Statistics (%)

	E_1	E_2	σ
Porsgrunn data set	-0.134	11.205	13.809
Field data	-7.170	9.627	13.824

Number of critical points	
Porsgrunn data set	64 (+17 in-between)
Field data	57 (+1 in-between)

(b) Discharge Coefficients, Porsgrunn data set

	$11\,mm$	$14\,mm$	$18\,mm$
Cage	1.04	1.11	0.94
Orifice	1.00	1.05	1.04

(c) Discharge coefficients, field data

$12\,mm$	$22\,mm$	$38\,mm$
1.11	1.23	1.23

C MATLAB Code

C.1 Bernoulli, Asheim, Sachdeva et al. and Al-Safran and Kelkar

```
clear all
% Declaring constants and global variables:
% ----------------------------------------------------------------------------

global A A2 xg xl rhog1 rhol P1 P3 n nug1 kappa Z T M eksc1
   eksc2 ekss
data = 87 ;  % number of data points
eksc1 = 1/2 ; % Exponent for kCh LM > 1
eksc2 = 1/4 ; % Exponent for kCh LM < 1
ekss = 1/6 ;  % Exponent for kSi
% % Recommended Values:
% CdB = 1 ;      % Bernoulli discharge coefficient
% CdBC = 1 ;     % Bernoulli, Chisholm; discharge coefficient
% CdBS = 1 ;     % Bernoulli, Simpson; discharge coefficient
% CdAs = 1 ;     % Asheim; discharge coefficient
% CdS = 0.85 ;   % Sachdeva; discharge coefficient
% CdA = 0.75 ;   % Al-Safran; discharge coefficient

% Initializing variables
% ----------------------------------------------------------------------------

mcalcBer = zeros(data,1) ;
mcalcBerSimp = zeros(data,1) ;
mcalcBerChis = zeros(data,1) ;
mcalcAsh = zeros(data,1) ;
mcalcSac = zeros(data,1) ;
mcalcAlS = zeros(data,1) ;

vxl    = zeros(data,1) ;
vrhol  = zeros(data,1) ;
Cl     = zeros(data,1) ;
vnug1  = zeros(data,1) ;
vnul   = zeros(data,1) ;
vkappa = zeros(data,1) ;
vn     = zeros(data,1) ;

vyact   = zeros(data,1) ;
vract   = zeros(data,1) ;
yccalcAsh = zeros(data,1) ;
yccalcSac = zeros(data,1) ;
rccalcAlS = zeros(data,1) ;
critflowAsh = zeros(data,1) ;
```

```
critflowSac = zeros(data,1) ;
critflowAlS = zeros(data,1) ;

vrhoBB = zeros(data,1) ;
vslipChi = zeros(data,1) ;
vslipSim = zeros(data,1) ;
vtwopC = zeros(data,1) ;
vtwopS = zeros(data,1) ;

vP2   = zeros(data,1) ;
betwr = zeros(30,8) ;
temp3 = zeros(10001,1) ;
ind = 0 ;

% Reading Input 1984 file
%
-------------------------------------------------------------------------------

D1     = xlsread('Input 1984.xlsx', 'Input', 'B2') ;
vA2    = xlsread('Input 1984.xlsx', 'Input', 'C2:C88') ;
vP1    = xlsread('Input 1984.xlsx', 'Input', 'E2:E88') ;
vP3    = xlsread('Input 1984.xlsx', 'Input', 'F2:F88') ;
vxg    = xlsread('Input 1984.xlsx', 'Input', 'G2:G88') ;
vxo    = xlsread('Input 1984.xlsx', 'Input', 'H2:H88') ;
vxw    = xlsread('Input 1984.xlsx', 'Input', 'I2:I88') ;
vrhog1 = xlsread('Input 1984.xlsx', 'Input', 'J2:J88') ;
vrhoo  = xlsread('Input 1984.xlsx', 'Input', 'K2:K88') ;
vrhow  = xlsread('Input 1984.xlsx', 'Input', 'L2:L88') ;
Cpg    = xlsread('Input 1984.xlsx', 'Input', 'M2') ;
Cvg    = xlsread('Input 1984.xlsx', 'Input', 'N2:N88') ;
Cpo    = xlsread('Input 1984.xlsx', 'Input', 'O2') ;
Cvo    = xlsread('Input 1984.xlsx', 'Input', 'P2') ;
Cpw    = xlsread('Input 1984.xlsx', 'Input', 'Q2') ;
Cvw    = xlsread('Input 1984.xlsx', 'Input', 'R2') ;
mmeas  = xlsread('Input 1984.xlsx', 'Input', 'T2:T88') ;
vT     = xlsread('Input 1984.xlsx', 'Input', 'U2:U88') ;
vZ     = xlsread('Input 1984.xlsx', 'Input', 'V2:V88') ;
vM     = xlsread('Input 1984.xlsx', 'Input', 'W2:W88') ;
vinch  = xlsread('Input 1984.xlsx', 'Input', 'X2:X88') ;
disp('Ferdig med å lese fra fil') ;
A = (pi/4)*D1^2 ;

% Pre-Calculations
%
-------------------------------------------------------------------------------

for i = 1:data
    sumx = vxg(i) + vxo(i) + vxw(i) ;
```

```
    vxg(i) = vxg(i) / sumx ;
    vxo(i) = vxo(i) / sumx ;
    vxw(i) = vxw(i) / sumx ;
    vxl(i) = vxo(i) + vxw(i) ;

    if ( vxw(i) == 0 )
        WC = 0 ;
    else
        WC = vxw(i)*vrhoo(i) / (vxw(i)*vrhoo(i)+vxo(i)*vrhow(i))
            ;
    end
    vrhol(i) = vrhoo(i)*(1-WC) + vrhow(i)*WC ;

    Cl(i) = vxo(i)*Cpo + vxw(i)*Cpw ;
    vnug1(i) = 1/vrhog1(i) ;
    vnul(i) = 1/vrhol(i) ;

    vkappa(i) = Cpg/Cvg(i) ;
    vn(i) = 1 + ( vxg(i)*(Cpg-Cvg(i)) )/( vxg(i)*Cvg(i) + vxl(i)
        *Cl(i) ) ;
%     vP2(i) = vP1(i) - (vP1(i)-vP3(i))/(1-(vA2(i)/A)^0.925) ;
    vP2(i) = vP3(i) ;
    vyact(i) = vP3(i)/vP1(i);
    vract(i) = vP2(i)/vP1(i) ;
end

% error1min1 = 1000 ;
% error1min2 = 1000 ;
% error1min3 = 1000 ;
% diff1 = zeros(27,1) ;
% diff2 = zeros(30,1) ;
% diff3 = zeros(30,1) ;
% minerror = 1000 ;
% for Cd = 0.92 : 0.01 : 1.25
%     CdA = Cd ;

for i = 1 : data
    A2 = vA2(i) ;
    xg = vxg(i) ;
    xl = vxl(i) ;
    rhol = vrhol(i) ;
    rhog1 = vrhog1(i) ;
    P1 = vP1(i) ;
    P3 = vP3(i) ;
    n = vn(i) ;
    nug1 = vnug1(i) ;
    kappa = vkappa(i) ;
    T = vT(i) ;
```

```
    Z = vZ(i) ;
    M = vM(i) ;
    if ( vinch(i) == 32 )
        CdB = 0.46 ;
        CdBC = 0.45 ;
        CdBS = 0.59 ;
        CdAs = 0.92 ;
        CdS = 0.82 ;
        CdA = 1.11 ;
    elseif ( vinch(i) == 56 )
        CdB = 0.53 ;
        CdBC = 0.52 ;
        CdBS = 0.74 ;
        CdAs = 1.04 ;
        CdS = 0.93 ;
        CdA = 1.23 ;
    elseif ( vinch(i) == 96 )
        CdB = 0.66 ;
        CdBC = 0.65 ;
        CdBS = 1.12 ;
        CdAs = 0.99 ;
        CdS = 0.91 ;
        CdA = 1.23 ;
    end
%%
%%
%% Bernoulli
%%
    ------------------------------------------------------------------------------

%       [mfl rhoB] = mflowBernoulli(CdB,1,2) ;
%       vrhoBB(i) = rhoB ;
%       mcalcBer(i) = mfl ;
%       [mfl rhoB sl tp] = mflowBernoulli(CdBC,2,2) ;
%       mcalcBerChis(i) = mfl ;
%       vslipChi(i) = sl ;
%       vtwopC(i) = tp ;
%       [mfl rhoB sl tp] = mflowBernoulli(CdBS,3,3) ;
%       mcalcBerSimp(i) = mfl ;
%       vslipSim(i) = sl ;
%       vtwopS(i) = tp ;
%%
%%
%% Asheim
%%
    ------------------------------------------------------------------------------

%       if ( xg <= 1e-3 )
```

```
%           yc = 0 ;
%       else
%           yc = findtop(CdAs) ;
%       end
%       yccalcAsh(i) = yc ;
%       if (vyact(i) <= yc)
%           y = yc ;
%           critflowAsh(i) = 1 ;
%       else
%           y = vyact(i) ;
%       end
%       mcalcAsh(i) = mflowAsheim(CdAs,y) ;
% %
% %
% % Sachdeva et al
% %
```

```
%       if ( xg <= 1e-3 )
%           yc = 0 ;
%       else
%           kk = kappa/(kappa-1) ;
%           sachdexpr = @(y) y - ( ( kk + xl*vnul(i)*(1-y)/(xg*
    nug1) ) / ( kk + n/2 +n*xl*vnul(i)/(xg*nug1*y^(-1/kappa)) + (
    n/2)*(xl*vnul(i)/(xg*nug1*y^(-1/kappa))) ) )^kk ;
%           yc = fzero(sachdexpr, [0 1]) ;
%       end
%       yccalcSac(i) = yc ;
%       if (vyact(i) <= yc )
%           y = yc ;
%           critflowSac(i) = 1 ;
%       else
%           y = vyact(i) ;
%       end
%       rhomix = 1/ (xg*nug1*y^(-1/kappa) + xl*vnul(i)) ;
%       temp =  xl*(1-y)/rhol + (xg*kk)*(nug1-y*nug1*y^(-1/kappa))
    ;
%       mcalcSac(i) = A2*CdS*sqrt(2*P1*rhomix^2*temp) ;
%
%
% Al-Safran et al
%
```

```
    kc = sqrt( 1 + xg*(rhol/rhog1 - 1) )*( 1 + 0.6*exp(-0.5*xg)
        ) ;
    ksub = (rhol/rhog1)^ekss ;
    if ( xg <= 1e-3 )
```

```
        critrc = 0 ;
        subrc = 0 ;
    else
        critrc = findrc(kc) ;
        subrc = findrc(ksub) ;
    end
    if ( (vract(i) <= critrc) && (vract(i) <= subrc) )    % No
       doubt: Critical flow
        rccalcAlS(i) = critrc ;
        critflowAlS(i) = 1 ;
        mcalcAlS(i)= mflowAlSafran(CdA,kc,critrc) ;
    elseif ( (vract(i) > critrc) && (vract(i) > subrc) ) % No
       doubt: Subcritical flow
        rccalcAlS(i) = subrc ;
        r = vract(i) ;
        mcalcAlS(i)= mflowAlSafran(CdA,ksub,r) ;
    else
        ind = ind + 1 ;
        betwr(ind,1) = i ;
        betwr(ind,2) = vract(i) ;
        betwr(ind,3) = critrc ;
        betwr(ind,4) = subrc ;
        % Critical flow equations
        if ( vract(i) <= critrc )
            betwr(ind,5) = mflowAlSafran(CdA,kc,critrc) ;
            betwr(ind,6 ) = 1;
        else
            r = vract(i) ;
            betwr(ind,5) = mflowAlSafran(CdA,ksub,r) ;
        end
        % Subcritical flow equations
        if ( vract(i) <= subrc )
            betwr(ind,7) = mflowAlSafran(CdA,kc,subrc) ;
            betwr(ind,8) = 1 ;
        else
            r = vract(i) ;
            betwr(ind,7) = mflowAlSafran(CdA,ksub,r) ;
        end
        mcalcAlS(i)= ( betwr(ind,5) + betwr(ind,7) )/2;
    end

end         % End for i
%
%
% Statistics
%
```

```
diffBer = zeros(data,1) ;
diffBerChis = zeros(data,1) ;
diffBerSimp = zeros(data,1) ;
diffAsh = zeros(data,1) ;
diffSac = zeros(data,1) ;
diffAlS = zeros(data,1) ;
for i = 1 : data
    diffBer(i) = 100*( mcalcBer(i)-mmeas(i) )/mmeas(i) ;
    diffBerChis(i) = 100*( mcalcBerChis(i)-mmeas(i) )/mmeas(i) ;
    diffBerSimp(i) = 100*( mcalcBerSimp(i)-mmeas(i) )/mmeas(i) ;
    diffAsh(i) = 100*( mcalcAsh(i)-mmeas(i) )/mmeas(i) ;
    diffSac(i) = 100*( mcalcSac(i)-mmeas(i) )/mmeas(i) ;
    diffAlS(i) = 100*( mcalcAlS(i)-mmeas(i) )/mmeas(i) ;
end
errorBer = [ mean(diffBer); mean(abs(diffBer)); std(diffBer) ]
   ;
errorBerChis = [ mean(diffBerChis); mean(abs(diffBerChis)); std(
   diffBerChis) ]  ;
errorBerSimp = [ mean(diffBerSimp); mean(abs(diffBerSimp)); std(
   diffBerSimp) ]  ;
errorAsh = [ mean(diffAsh); mean(abs(diffAsh)); std(diffAsh) ] ;
errorSac = [ mean(diffSac); mean(abs(diffSac)); std(diffSac)  ]
   ;
errorAlS = [ mean(diffAlS); mean(abs(diffAlS)); std(diffAlS) ] ;
summasummarium = [errorBer errorBerChis errorBerSimp errorAsh
   errorSac errorAlS] ;

% mcalc = mcalcAlS ; % REMEMBER TO CHANGE THIS PR MODEL
% a1 = 0 ;
% a2 = 0 ;
% a3 = 0 ;
% for i = 1 : data
%     if ( vinch(i) == 32 )
%         a1 = a1 + 1 ;
%         diff1(a1) = 100*( mcalc(i)-mmeas(i) ) / mmeas(i) ;
%     elseif ( vinch(i) == 56 )
%         a2 = a2 + 1 ;
%         diff2(a2) = 100*( mcalc(i)-mmeas(i) ) / mmeas(i) ;
%     elseif ( vinch(i) == 96 )
%         a3 = a3 + 1 ;
%         diff3(a3) = 100*( mcalc(i)-mmeas(i) ) / mmeas(i) ;
%     end
% end
% error11 = mean(abs(diff1)) ;
% error12 = mean(abs(diff2)) ;
% error13 = mean(abs(diff3)) ;
% if ( error11 < error1min1 )
%     error1min1 = error11 ;
```

```
%      Cdopt1 = Cd ;
% end
% if ( error12 < error1min2 )
%      error1min2 = error12 ;
%      Cdopt2 = Cd ;
% end
% if ( error13 < error1min3 )
%      error1min3 = error13 ;
%      Cdopt3 = Cd ;
% end
%
% end          % End for Cd
%
% fprintf('32inch:\n')
% fprintf('Cd: %4.2f and absolute average error: %8.6f\n',
    Cdopt1, error1min1) ;
% fprintf('56inch:\n')
% fprintf('Cd: %4.2f and absolute average error: %8.6f\n',
    Cdopt2, error1min2) ;
% fprintf('96inch:\n')
% fprintf('Cd: %4.2f and absolute average error: %8.6f\n',
    Cdopt3, error1min3) ;

%
%
% Writing to Output file
%
```

```
disp('Begynner å skrive til fil...') ;
text1 = {'mmeas', 'Bernoulli', 'Bernoulli w/C', 'Bernoulli w/S',
    'Asheim', 'Sachdeva', 'AlSafran', 'xg'} ;
text2 = {'Rel.error'; 'Abs.rel error'; 'St.deviation'} ;
xlswrite('Output2 1984.xlsx', text1, 'mflow', 'B1:I1')
xlswrite('Output2 1984.xlsx', mmeas, 'mflow', 'B2:B88') ;
xlswrite('Output2 1984.xlsx', mcalcBer, 'mflow', 'C2:C88') ;
xlswrite('Output2 1984.xlsx', mcalcBerChis, 'mflow', 'D2:D88') ;
xlswrite('Output2 1984.xlsx', mcalcBerSimp, 'mflow', 'E2:E88') ;
xlswrite('Output2 1984.xlsx', mcalcAsh, 'mflow', 'F2:F88') ;
xlswrite('Output2 1984.xlsx', mcalcSac, 'mflow', 'G2:G88') ;
xlswrite('Output2 1984.xlsx', mcalcAlS, 'mflow', 'H2:H88') ;
xlswrite('Output2 1984.xlsx', text2, 'mflow', 'B90:B92') ;
xlswrite('Output2 1984.xlsx', summasummarium, 'mflow', 'C90:H92'
   ) ;
xlswrite('Output2 1984.xlsx', vxg, 'mflow', 'I2:I88') ;

text1 = {'yact', 'yAsheim', 'crit?', 'ySachdeva', 'crit?'} ;
text2 = {'ract', 'rAlSafran', 'crit?', 'P2calc', 'P3'} ;
```

```
xlswrite('Output2 1984.xlsx', text1, 'y and r', 'B1:F1')
xlswrite('Output2 1984.xlsx', vyact, 'y and r', 'B2:B88') ;
xlswrite('Output2 1984.xlsx', yccalcAsh, 'y and r', 'C2:C88') ;
xlswrite('Output2 1984.xlsx', critflowAsh, 'y and r', 'D2:D88')
   ;
xlswrite('Output2 1984.xlsx', yccalcSac, 'y and r', 'E2:E88') ;
xlswrite('Output2 1984.xlsx', critflowSac, 'y and r', 'F2:F88')
   ;
xlswrite('Output2 1984.xlsx', text2, 'y and r', 'G1:K1')
xlswrite('Output2 1984.xlsx', vract, 'y and r', 'G2:G88') ;
xlswrite('Output2 1984.xlsx', rccalcAlS, 'y and r', 'H2:H88') ;
xlswrite('Output2 1984.xlsx', critflowAlS, 'y and r', 'I2:I88')
   ;
xlswrite('Output2 1984.xlsx', vP2, 'y and r', 'J2:J88') ;
xlswrite('Output2 1984.xlsx', vP3, 'y and r', 'K2:K88') ;

text1 = {'n', 'kappa', 'Bern rhom', 'kCh', 'Chi tp', 'kSi', 'Sim
   tp'} ;
xlswrite('Output2 1984.xlsx', text1, 'Data', 'B1:H1')
xlswrite('Output2 1984.xlsx', vn, 'Data', 'B2:B88') ;
xlswrite('Output2 1984.xlsx', vkappa, 'Data', 'C2:C88') ;
xlswrite('Output2 1984.xlsx', vrhoBB, 'Data', 'D2:D88') ;
xlswrite('Output2 1984.xlsx', vslipChi, 'Data', 'E2:E88') ;
xlswrite('Output2 1984.xlsx', vtwopC, 'Data', 'F2:F88') ;
xlswrite('Output2 1984.xlsx', vslipSim, 'Data', 'G2:G88') ;
xlswrite('Output2 1984.xlsx', vtwopS, 'Data', 'H2:H88') ;

text1 = {'datapunkt', 'ract', 'crit rc', 'sub rc', 'critrc->
   mcalc', 'critical?', 'subrc->mcalc','critical?'} ;
xlswrite('Output2 1984.xlsx', text1, 'AlSafran', 'A1:H1')
xlswrite('Output2 1984.xlsx', betwr, 'AlSafran', 'A2:H31') ;

disp('Ferdig!') ;

% vector = transpose(linspace(1,P1,1000)) ;
% masserate = zeros(1000,1) ;
% for o = 1 : 1000
%     trykk = vector(o) ;
%     masserate(o) = mflowAsheim(CdAs, (trykk/P1)) ;
% end
% xlswrite('Graf.xlsx', vector, 'Ark1', 'A2:A1001') ;
% xlswrite('Graf.xlsx', masserate, 'Ark1', 'B2:B1001') ;
```

C.2 The Hydro Model

```
clear all
% Declaring global and constant variables
%
-------------------------------------------------------------------------

global xg xl P1 P3 rhog1 rhol kappa A A2 rhoe1 Cc konst1 konst2
   z w y
data = 508 ;

a = 1 ; % Slip model: 1: modChisholm, 2: Chisholm 3: Simpson, 4:
    no slip, 5: linearized slip in integration only
c = 1 ; % Density: 1: momentum, 2: mix, 3: constant rhog = const
    rho e/m, 4: gas exp. for (1) and (3)
d = 1 ; % Integr.meth.: 1: original, 2: MATLAB, 3: trapezoidal

konst1 = 0.6 ;  % Original value, mod.Chisholm slip model: 0.6
konst2 = -5 ;   % Original value, mod.Chisholm slip model: -5
% --- Chisholm: z = 1, w = 1, y = 1/2 or 1/4
% --- mod.Chisholm: w = 1, y = 1/2, z has to be within for i = 1
    : data so that xg is defined
% --- Simpson: z = 1, w = 1, y = 1/6

% Reading the Input File
%
-------------------------------------------------------------------------

D1      = xlsread('Input.xlsx', 'Input', 'B2') ;
Cto     = xlsread('Input.xlsx', 'Input', 'C2:C509') ;
vP1     = xlsread('Input.xlsx', 'Input', 'E2:E509') ;
vP3     = xlsread('Input.xlsx', 'Input', 'F2:F509') ;
vxg     = xlsread('Input.xlsx', 'Input', 'G2:G509') ;
vxo     = xlsread('Input.xlsx', 'Input', 'H2:H509') ;
vxw     = xlsread('Input.xlsx', 'Input', 'I2:I509') ;
vrhog1  = xlsread('Input.xlsx', 'Input', 'J2:J509') ;
vrhoo   = xlsread('Input.xlsx', 'Input', 'K2:K509') ;
vrhow   = xlsread('Input.xlsx', 'Input', 'L2:L509') ;
Cpg     = xlsread('Input.xlsx', 'Input', 'M2') ;
Cvg     = xlsread('Input.xlsx', 'Input', 'N2:N509') ;
Cpo     = xlsread('Input.xlsx', 'Input', 'O2') ;
Cvo     = xlsread('Input.xlsx', 'Input', 'P2') ;
Cpw     = xlsread('Input.xlsx', 'Input', 'Q2') ;
Cvw     = xlsread('Input.xlsx', 'Input', 'R2') ;
[dummy, vtype] = xlsread('Input.xlsx', 'Input', 'S2:S509') ;
mmeas   = xlsread('Input.xlsx', 'Input', 'T2:T509') ;
A = (pi/4)*D1^2 ;
vA2 = A*Cto ;
```

```
% Initiating varables
%
-------------------------------------------------------------------------

vrhog2 = zeros(data,1) ;
vslip  = zeros(data,1) ;
vkappa = zeros(data,1) ;
vrhoe1 = zeros(data,1) ;
vrhoe2 = zeros(data,1) ;
vrhoe3 = zeros(data,1) ;
vrhol  = zeros(data,1) ;
vxl    = zeros(data,1) ;
mc     = zeros(data,1) ;
ms     = zeros(data,1) ;
mcalc  = zeros(data,1) ;
vP2    = zeros(data,1) ;
vP2c   = zeros(data,1) ;
vP2s   = zeros(data,1) ;
vcrit  = zeros(data,1) ;
diff = zeros(data,1) ;

% Pre-Calculations
%
-------------------------------------------------------------------------

for i = 1:data
    sumx = vxg(i) + vxo(i) + vxw(i) ;
    vxg(i) = vxg(i) / sumx ;
    vxo(i) = vxo(i) / sumx ;
    vxw(i) = vxw(i) / sumx ;
    vxl(i) = vxo(i) + vxw(i) ;
    WC = vxw(i)*vrhoo(i) / max( (vxw(i)*vrhoo(i)+vxo(i)*vrhow(i)
        ),1e-30 ) ;
    vrhol(i) = vrhoo(i)*(1-WC) + vrhow(i)*WC ;
    Cpmix = vxg(i)*Cpg+vxo(i)*Cpo+vxw(i)*Cpw ;
    Cvmix = vxg(i)*Cvg(i)+vxo(i)*Cvo+vxw(i)*Cvw ;
%       vkappa(i) = Cpmix / Cvmix ;
    vkappa(i) = Cpg / Cvg(i) ;
end

% tic
% for abc = 1 : 100

% The Hydro Choke Model
%
-------------------------------------------------------------------------
```

```
% error1min1 = 1000 ;
% error1min2 = 1000 ;
% error1min3 = 1000 ;
% error1min4 = 1000 ;
% error1min5 = 1000 ;
% error1min6 = 1000 ;
% for Cc = 0.50 : 0.01 : 0.65
% diff1 = zeros(86,1) ;
% diff2 = zeros(60,1) ;
% diff3 = zeros(123,1) ;
% diff4 = zeros(96,1) ;
% diff5 = zeros(59,1) ;
% diff6 = zeros(84,1) ;
for i = 1 : data
    if ( strcmp(vtype(i),'ORIF') )
        if ( Cto(i) == 0.02 )
            Cc = 0.57 ;
        elseif ( Cto(i) == 0.032 )
            Cc = 0.52 ;
        elseif ( Cto(i) == 0.052 )
            Cc = 0.57 ;
        end
    else
        if ( Cto(i) == 0.02 )
            Cc = 0.61 ;
        elseif ( Cto(i) == 0.032 )
            Cc = 0.55 ;
        elseif ( Cto(i) == 0.052 )
            Cc = 0.51 ;
        end
    end
    xg = vxg(i) ;
    xl = 1 - xg ;
    P1 = vP1(i) ;
    P3 = vP3(i) ;
    if ( c == 3 )
%       rhog1 = vrhog1(i) ;
        temp = vkappa(i) ;
        rhog1 = vrhog1(i).*(1 + (P3./P1).^(1./temp)) / 2 ;
        vrhog1(i) = rhog1 ;
%       For constant rhog: set kappa = 1e30 ;
        kappa = 1e30 ;
    else
        rhog1 = vrhog1(i) ;
        kappa = vkappa(i) ;
    end
    rhol = vrhol(i) ;
    w = 1 ;
```

```
    if ( a == 1 )
        z = 1 + konst1.*exp(konst2.*xg) ;
        y = 1/2 ;
    elseif ( a == 2 )
        z = 1 ;
    elseif ( a == 3 )
        z = 1 ;
        y = 1/6 ;
    end
    A2 = vA2(i) ;
    rhoe1 = momdens(P1,1,4,4) ;    %% Special case: no slip at
       position 1
    rhoe3 = momdens(P3,1,4,4) ;    %% Special case: no slip at
       position 3

% Maximum as critical point
   ------------------------------------------
    if ( xg == 0 )
        P2c = 0.1 ;
    else
        derivmflow12 = @(P) mflow12deriv(P,a,c,d) ;
        P2c = fzero(derivmflow12, [1 P1-1]) ;
        if ( isnan(P2c) )
            P2c = findtop(P1) ;
        end
    end
% % Critical pressure
   ------------------------------------------
%         if ( xg == 0 )
%             P2c = 0.1 ;
%         else
%             mflow = @(P) sqmflow12(P,a,c,d) - sqmflowc(P,a,c)
   ;
%             P2c = fzero(mflow, [2 P1-1]) ;
%         end
% No pressure recovery
   ------------------------------------------
        P2s = P3 ;
%
   ------------------------------------------------------------------------


        vP2c(i) = P2c ;
        mc(i) = sqrt(sqmflowc(P2c,a,c)) ;
        ms(i) = sqrt(sqmflow12(P2s,a,c,d)) ;
        vP2s(i) = P2s ;
        if ( P2s < vP2c(i) )
            mcalc(i) = mc(i) ;
            vcrit(i) = 1 ;
```

```
            tmpP = P2c ;
        else
            mcalc(i) = ms(i) ;
            vP2s(i) = P2s ;
            tmpP = P2s ;
        end
        vP2(i) = tmpP ;
        if ( c == 3 )
            vrhog2(i) = rhog1 ;
        else
            vrhog2(i) = gasdensity(tmpP) ;
        end
        if ( a == 2 )
            LM = (xl/xg)*sqrt(vrhog2(i)/rhol) ;
            if ( LM > 1 )
                y = 1/2 ;
                vslip(i) = slipfunction(vrhog2(i),1) ;
                vrhoe2(i) = momdens(tmpP,1,1,c) ;
            else
                y = 1/4 ;
                vslip(i) = slipfunction(vrhog2(i),3) ;
                vrhoe2(i) = momdens(tmpP,1,3,c) ;
                disp(i) ;
            end
        else
            vslip(i) = slipfunction(vrhog2(i),a) ;
            vrhoe2(i) = momdens(tmpP,1,a,c) ;
        end
        vrhoe1(i) = rhoe1 ;
        vrhoe3(i) = rhoe3 ;
end                     % End for-i 1:data
% end
% time = toc

% Statistics
% ------------------------------------------------------------------
for i = 1:data
    diff(i) = 100*( mcalc(i)-mmeas(i) ) / mmeas(i) ;
end
error1 = mean(abs(diff)) ;
stdev = std(diff) ;
error2 = mean(diff) ;
% a1 = 0 ;
% a2 = 0 ;
% a3 = 0 ;
% a4 = 0 ;
% a5 = 0 ;
% a6 = 0 ;
```

```
% for i = 1 : data
% if ( strcmp(vtype(i),'ORIF') )
%     if ( Cto(i) == 0.02 )
%         a1 = a1 + 1 ;
%         diff1(a1) = 100*( mcalc(i)-mmeas(i) ) / mmeas(i) ;
%     elseif ( Cto(i) == 0.032 )
%         a2 = a2 + 1 ;
%         diff2(a2) = 100*( mcalc(i)-mmeas(i) ) / mmeas(i) ;
%     elseif ( Cto(i) == 0.052 )
%         a3 = a3 + 1 ;
%         diff3(a3) = 100*( mcalc(i)-mmeas(i) ) / mmeas(i) ;
%     end
% else
%     if ( Cto(i) == 0.02 )
%         a4 = a4 + 1 ;
%         diff4(a4) = 100*( mcalc(i)-mmeas(i) ) / mmeas(i) ;
%     elseif ( Cto(i) == 0.032 )
%         a5 = a5 + 1 ;
%         diff5(a5) = 100*( mcalc(i)-mmeas(i) ) / mmeas(i) ;
%     elseif ( Cto(i) == 0.052 )
%         a6 = a6 + 1 ;
%         diff6(a6) = 100*( mcalc(i)-mmeas(i) ) / mmeas(i) ;
%     end
% end
% end
% error11 = mean(abs(diff1)) ;
% error12 = mean(abs(diff2)) ;
% error13 = mean(abs(diff3)) ;
% error14 = mean(abs(diff4)) ;
% error15 = mean(abs(diff5)) ;
% error16 = mean(abs(diff6)) ;
% if ( error11 < error1min1 )
%     error1min1 = error11 ;
%     Cdopt1 = Cc ;
% end
% if ( error12 < error1min2 )
%     error1min2 = error12 ;
%     Cdopt2 = Cc ;
% end
% if ( error13 < error1min3 )
%     error1min3 = error13 ;
%     Cdopt3 = Cc ;
% end
% if ( error14 < error1min4 )
%     error1min4 = error14 ;
%     Cdopt4 = Cc ;
% end
% if ( error15 < error1min5 )
```

```
%      error1min5 = error15 ;
%      Cdopt5 = Cc ;
% end
% if ( error16 < error1min6 )
%      error1min6 = error16 ;
%      Cdopt6 = Cc ;
% end
% end                    % End for-CC
% fprintf('ORIFICE:\n')
% fprintf('Cto=0.020:\n')
% fprintf('Cd: %4.2f and absolute average error: %8.6f\n',
    Cdopt1, error1min1) ;
% fprintf('Cto=0.032:\n')
% fprintf('Cd: %4.2f and absolute average error: %8.6f\n',
    Cdopt2, error1min2) ;
% fprintf('Cto=0.052:\n')
% fprintf('Cd: %4.2f and absolute average error: %8.6f\n',
    Cdopt3, error1min3) ;
% fprintf('CAGE:\n')
% fprintf('Cto=0.020:\n')
% fprintf('Cd: %4.2f and absolute average error: %8.6f\n',
    Cdopt4, error1min4) ;
% fprintf('Cto=0.032:\n')
% fprintf('Cd: %4.2f and absolute average error: %8.6f\n',
    Cdopt5, error1min5) ;
% fprintf('Cto=0.052:\n')
% fprintf('Cd: %4.2f and absolute average error: %8.6f\n',
    Cdopt6, error1min6) ;

disp('Begynner å skrive til fil') ;
% Writing to Output file
%
    ------------------------------------------------------------------------


text1 = {'xg', 'xo', 'xw', 'P2', 'mcalc', 'P2c', 'mc', 'P2s', '
    ms', 'rhog1', 'rhog2', 'kappa', 'rhol', 'slip', 'critical?',
    'rhoe1', 'rhoe2', 'rhoe3'} ;
text2 = {'Standard deviation:'; 'Abs. Average Rel. error:'; '
    Average Rel. error:'; 'Critical points:'} ;
xlswrite('Output.xlsx', text1, 'Output1', 'B1:S1') ;
xlswrite('Output.xlsx', vxg, 'Output1', 'B2:B509') ;
xlswrite('Output.xlsx', vxo, 'Output1', 'C2:C509') ;
xlswrite('Output.xlsx', vxw, 'Output1', 'D2:D509') ;
xlswrite('Output.xlsx', vP2, 'Output1', 'E2:E509') ;
xlswrite('Output.xlsx', mcalc, 'Output1', 'F2:F509') ;
xlswrite('Output.xlsx', vP2c, 'Output1', 'G2:G509') ;
xlswrite('Output.xlsx', mc, 'Output1', 'H2:H509') ;
xlswrite('Output.xlsx', vP2s, 'Output1', 'I2:I509') ;
```

```
xlswrite('Output.xlsx', ms, 'Output1', 'J2:J509') ;
xlswrite('Output.xlsx', vrhog1, 'Output1', 'K2:K509') ;
xlswrite('Output.xlsx', vrhog2, 'Output1', 'L2:L509') ;
xlswrite('Output.xlsx', vkappa, 'Output1', 'M2:M509') ;
xlswrite('Output.xlsx', vrhol, 'Output1', 'N2:N509') ;
xlswrite('Output.xlsx', vslip, 'Output1', 'O2:O509') ;
xlswrite('Output.xlsx', vcrit, 'Output1', 'P2:P509') ;
xlswrite('Output.xlsx', vrhoe1, 'Output1', 'Q2:Q509') ;
xlswrite('Output.xlsx', vrhoe2, 'Output1', 'R2:R509') ;
xlswrite('Output.xlsx', vrhoe3, 'Output1', 'S2:S509') ;
xlswrite('Output.xlsx', text2, 'Output1', 'A511:A514') ;
xlswrite('Output.xlsx', stdev, 'Output1', 'C511') ;
xlswrite('Output.xlsx', error1, 'Output1', 'C512') ;
xlswrite('Output.xlsx', error2, 'Output1', 'C513') ;
xlswrite('Output.xlsx', sum(vcrit), 'Output1', 'C514') ;
```

D Input Data

Applies to both data sets:

$C_{P,G}$	1020 J/kg
$C_{P,o}$	2160 J/kg
$C_{V,o}$	2010 J/kg
$C_{P,w}$	4170 J/kg
$C_{V,w}$	4170 J/kg

D.1 Porsgrunn data

$d_1 = 0.0779\,m$

An extract of the Porsgrunn data set follows:

	Cto = A2/A1	P1	P3	xg	xo	xw	rhog1
1	0.02	8.47E+05	7.62E+05	1.0000	0.0000	0.0000	6.4059
2	0.02	1.00E+06	7.57E+05	1.0000	0.0000	0.0000	7.5864
3	0.02	1.22E+06	7.52E+05	1.0000	0.0000	0.0000	9.2270
4	0.02	1.39E+06	7.34E+05	1.0000	0.0000	0.0000	10.5451
5	0.02	8.37E+05	7.63E+05	0.0000	1.0000	0.0000	6.3891
6	0.02	9.18E+05	7.54E+05	0.0000	1.0000	0.0000	7.0074
7	0.02	1.06E+06	7.43E+05	0.0000	1.0000	0.0000	8.0664
8	0.02	1.25E+06	7.43E+05	0.0000	1.0000	0.0000	9.5417
9	0.02	1.49E+06	7.31E+05	0.0000	1.0000	0.0000	11.3386
10	0.02	8.36E+05	7.51E+05	0.0000	0.0000	1.0000	6.3815
11	0.02	9.74E+05	7.47E+05	0.0000	0.0000	1.0000	7.4119
12	0.02	1.24E+06	7.52E+05	0.0000	0.0000	1.0000	9.4361
13	0.02	1.58E+06	7.38E+05	0.0000	0.0000	1.0000	12.0235
14	0.02	8.41E+05	7.43E+05	0.0076	0.8626	0.1300	6.3998
15	0.02	9.50E+05	7.49E+05	0.0083	0.8802	0.1110	7.2517
16	0.02	1.14E+06	7.57E+05	0.0038	0.8677	0.1280	8.7020
17	0.02	1.31E+06	7.50E+05	0.0000	0.8829	0.1170	9.9688
18	0.02	1.40E+06	7.43E+05	0.0000	0.8648	0.1350	10.6537
19	0.02	8.74E+05	7.69E+05	0.0121	0.4336	0.5540	6.6715
20	0.02	1.01E+06	7.50E+05	0.0095	0.4506	0.5400	7.7097
21	0.02	1.15E+06	7.45E+05	0.0015	0.4565	0.5420	8.7513
22	0.02	1.38E+06	7.49E+05	0.0009	0.4529	0.5460	10.5015
23	0.02	8.87E+05	7.84E+05	0.0095	0.0917	0.8990	6.7499
24	0.02	9.84E+05	7.40E+05	0.0075	0.0711	0.9210	7.4421
25	0.02	1.17E+06	7.39E+05	0.0035	0.0901	0.9060	8.8488
26	0.02	1.38E+06	7.36E+05	0.0035	0.0793	0.9170	10.5340
27	0.02	1.08E+06	7.53E+05	0.0843	0.7846	0.1310	8.2186
28	0.02	1.20E+06	7.59E+05	0.0401	0.8524	0.1080	9.1600
29	0.02	1.40E+06	7.72E+05	0.0282	0.8819	0.1260	10.6537
30	0.02	1.48E+06	7.53E+05	0.0189	0.8655	0.1160	11.2278
31	0.02	1.06E+06	7.49E+05	0.0786	0.3786	0.5420	8.0664
32	0.02	1.21E+06	7.53E+05	0.0413	0.4207	0.5380	9.2078
33	0.02	1.44E+06	7.61E+05	0.0293	0.4381	0.5330	10.9920

	Cto = A2/A1	P1	P3	xg	xo	xw	rhog1
34	0.02	1.55E+06	7.53E+05	0.0169	0.4478	0.5360	11.7952
35	0.02	1.16E+06	7.73E+05	0.0822	0.0578	0.8600	8.8274
36	0.02	1.44E+06	7.66E+05	0.0576	0.0977	0.8450	10.9581
37	0.02	1.48E+06	7.59E+05	0.0343	0.0411	0.9250	11.2625
38	0.02	1.25E+06	7.34E+05	0.1329	0.7341	0.1340	9.5122
39	0.02	1.42E+06	7.36E+05	0.0771	0.8104	0.1130	10.8059
40	0.02	1.34E+06	7.32E+05	0.1309	0.3761	0.4930	10.1971
41	0.02	1.43E+06	7.42E+05	0.0677	0.4199	0.5130	10.8820
42	0.02	1.41E+06	7.62E+05	0.1181	0.0966	0.7850	10.7298
43	0.02	1.47E+06	7.34E+05	0.0610	0.1101	0.8290	11.1864
44	0.02	1.42E+06	7.39E+05	0.1574	0.7216	0.1210	10.8059
45	0.02	1.40E+06	7.16E+05	0.1518	0.3552	0.4940	10.8207
46	0.02	1.45E+06	7.31E+05	0.1340	0.1020	0.7630	11.2424
47	0.02	9.50E+05	7.55E+05	0.0456	0.8211	0.1330	7.2517
48	0.02	1.18E+06	7.63E+05	0.0283	0.0708	0.9010	9.0074
49	0.02	1.32E+06	8.04E+05	0.0153	0.8558	0.1290	10.0140
50	0.02	1.50E+06	7.77E+05	0.0102	0.8829	0.1070	11.3796
51	0.02	1.15E+06	7.60E+05	0.0326	0.0710	0.8960	8.7513
52	0.02	1.17E+06	7.54E+05	0.0222	0.4889	0.4880	8.9310
53	0.02	1.40E+06	8.23E+05	0.0202	0.4429	0.5370	10.6209
54	0.02	1.50E+06	7.68E+05	0.0099	0.4465	0.5430	11.4147
55	0.02	9.73E+05	7.58E+05	0.0406	0.0875	0.8720	7.4272
56	0.02	1.13E+06	7.36E+05	0.0270	0.0727	0.9000	8.5991
57	0.02	1.47E+06	8.01E+05	0.0214	0.0863	0.8920	11.1864
58	0.02	1.53E+06	7.75E+05	0.0099	0.0937	0.8960	11.6072
417	0.02	2.39E+06	1.34E+06	0.2841	0.6519	0.0637	16.7884
418	0.02	2.85E+06	1.24E+06	0.2289	0.6651	0.1060	19.1468
419	0.02	1.99E+06	1.14E+06	0.2591	0.0585	0.6820	14.3046
420	0.02	2.43E+06	1.14E+06	0.2511	0.0498	0.6990	17.4675
421	0.02	3.06E+06	1.30E+06	0.2406	0.0640	0.6950	21.3729
422	0.02	3.71E+06	1.51E+06	0.2444	0.0619	0.6940	24.9925
423	0.02	1.55E+06	1.05E+06	0.0635	0.8238	0.1130	11.6870
424	0.02	2.54E+06	1.39E+06	0.0570	0.8300	0.1130	18.4193
425	0.02	3.21E+06	1.63E+06	0.0514	0.8376	0.1110	23.0072
426	0.02	3.78E+06	1.87E+06	0.0513	0.8325	0.1170	25.8168
427	0.02	1.56E+06	9.72E+05	0.0768	0.0822	0.8410	11.8713
428	0.02	2.30E+06	1.29E+06	0.0613	0.0849	0.8540	17.6112
429	0.02	3.11E+06	1.29E+06	0.0584	0.0763	0.8650	22.2905
430	0.02	1.88E+06	1.14E+06	0.0267	0.8449	0.1280	14.3064
431	0.02	2.63E+06	1.35E+06	0.0234	0.8550	0.1220	19.5905
432	0.02	3.20E+06	1.54E+06	0.0147	0.8611	0.1240	23.3427
433	0.02	3.85E+06	1.75E+06	0.0149	0.8576	0.1270	27.3558
434	0.02	1.72E+06	1.13E+06	0.0382	0.0820	0.8800	12.8509
435	0.02	2.76E+06	1.32E+06	0.0328	0.0784	0.8890	20.6211
436	0.02	3.47E+06	1.60E+06	0.0301	0.0836	0.8860	25.6923
437	0.02	3.94E+06	1.83E+06	0.0318	0.0791	0.8890	28.8260

	Cto = A2/A1	P1	P3	xg	xo	xw	rhog1
438	0.02	2.21E+06	1.04E+06	0.0060	0.0777	0.9160	16.7145
487	0.02	1.59E+06	9.91E+05	0.0000	0.0000	1.0000	12.3668
488	0.02	2.35E+06	1.05E+06	0.0000	0.0000	1.0000	18.0501
489	0.02	2.74E+06	1.08E+06	0.0000	0.0000	1.0000	20.6595
490	0.02	3.14E+06	1.12E+06	0.0000	0.0000	1.0000	23.3190
491	0.02	3.53E+06	1.16E+06	0.0000	0.0000	1.0000	25.5984

	rhoo	rhow	cvg	Choke type	Meas m
1	810	1000	724	ORIF	0.051
2	810	1000	724	ORIF	0.091
3	810	1000	724	ORIF	0.129
4	810	1000	724	ORIF	0.158
5	810	1000	724	ORIF	0.574
6	810	1000	724	ORIF	0.897
7	810	1000	724	ORIF	1.270
8	810	1000	724	ORIF	1.650
9	810	1000	724	ORIF	2.010
10	810	1000	724	ORIF	0.765
11	810	1000	724	ORIF	1.290
12	810	1000	724	ORIF	1.910
13	810	1000	724	ORIF	2.300
14	810	1000	724	ORIF	0.661
15	810	1000	724	ORIF	0.949
16	810	1000	724	ORIF	1.360
17	810	1000	724	ORIF	1.650
18	810	1000	724	ORIF	1.860
19	810	1000	724	ORIF	0.656
20	810	1000	724	ORIF	1.080
21	810	1000	724	ORIF	1.490
22	810	1000	724	ORIF	1.870
23	810	1000	724	ORIF	0.707
24	810	1000	724	ORIF	1.120
25	810	1000	724	ORIF	1.590
26	810	1000	724	ORIF	1.990
27	810	1000	724	ORIF	0.642
28	810	1000	724	ORIF	1.030
29	810	1000	724	ORIF	1.373
30	810	1000	724	ORIF	1.620
31	810	1000	724	ORIF	0.669
32	810	1000	724	ORIF	1.090
33	810	1000	724	ORIF	1.510
34	810	1000	724	ORIF	1.810
35	810	1000	724	ORIF	0.746
36	810	1000	724	ORIF	1.210
37	810	1000	724	ORIF	1.550

	rhoo	rhow	cvg	Choke type	Meas m
38	810	1000	724	ORIF	0.633
39	810	1000	724	ORIF	1.010
40	810	1000	724	ORIF	0.736
41	810	1000	724	ORIF	1.130
42	810	1000	724	ORIF	0.820
43	810	1000	724	ORIF	1.240
44	810	1000	724	ORIF	0.685
45	810	1000	724	ORIF	0.740
46	810	1000	724	ORIF	0.809
47	810	1000	724	ORIF	0.611
48	810	1000	724	ORIF	1.130
49	810	1000	724	ORIF	1.360
50	810	1000	724	ORIF	1.730
51	810	1000	724	ORIF	1.030
52	810	1000	724	ORIF	1.200
53	810	1000	724	ORIF	1.500
54	810	1000	724	ORIF	1.890
55	810	1000	724	ORIF	0.731
56	810	1000	724	ORIF	1.140
57	810	1000	724	ORIF	1.620
58	810	1000	724	ORIF	2.050
417	771	990	740	ORIF	0.668
418	771	990	740	ORIF	0.956
419	771	990	740	ORIF	0.647
420	771	990	740	ORIF	0.843
421	771	990	740	ORIF	1.075
422	771	990	740	ORIF	1.268
423	771	990	740	ORIF	0.946
424	771	990	740	ORIF	1.521
425	771	990	740	ORIF	1.785
426	771	990	740	ORIF	2.022
427	771	990	740	ORIF	1.047
428	771	990	740	ORIF	1.592
429	771	990	740	ORIF	2.293
430	771	990	740	ORIF	1.364
431	771	990	740	ORIF	1.838
432	771	990	740	ORIF	2.288
433	771	990	740	ORIF	2.536
434	771	990	740	ORIF	1.435
435	771	990	740	ORIF	2.325
436	771	990	740	ORIF	2.775
437	771	990	740	ORIF	3.063
438	771	990	740	ORIF	2.650
487	771	990	740	ORIF	2.100
488	771	990	740	ORIF	3.130
489	771	990	740	ORIF	3.578

	rhoo	rhow	cvg	Choke type	Meas m
490	771	990	740	ORIF	3.995
491	771	990	740	ORIF	4.412

D.2 Field data

$d_1 = 0.10\,m$

	A2	P1	Psep	xg	xo	xw	rhog1
1	1.267E-04	1.895E+07	3.889E+06	0.9323	0.0677	0.0000	179.57
2	1.267E-04	1.894E+07	3.889E+06	0.3385	0.6615	0.0000	179.51
3	1.267E-04	1.895E+07	3.889E+06	0.4204	0.5796	0.0000	179.63
4	1.267E-04	1.893E+07	3.889E+06	0.4394	0.5606	0.0000	179.45
5	1.267E-04	1.897E+07	3.889E+06	0.4518	0.5482	0.0000	179.75
6	1.267E-04	1.891E+07	3.889E+06	0.4395	0.5605	0.0000	179.22
7	1.267E-04	1.890E+07	3.889E+06	0.4388	0.5612	0.0000	179.16
8	1.267E-04	1.891E+07	3.889E+06	0.4387	0.5613	0.0000	179.28
9	1.267E-04	1.895E+07	3.889E+06	0.4451	0.5549	0.0000	179.57
10	1.267E-04	1.888E+07	3.889E+06	0.4388	0.5612	0.0000	179.04
11	1.267E-04	1.893E+07	3.889E+06	0.4452	0.5548	0.0000	179.39
12	1.267E-04	1.888E+07	3.889E+06	0.4324	0.5676	0.0000	179.04
13	1.267E-04	2.205E+07	3.558E+06	0.3330	0.6670	0.0000	204.14
14	1.267E-04	1.864E+07	3.889E+06	0.6157	0.3843	0.0000	176.95
15	1.267E-04	1.878E+07	3.889E+06	0.8144	0.1856	0.0000	178.15
16	1.267E-04	1.885E+07	3.889E+06	0.6278	0.3722	0.0000	178.74
17	1.267E-04	1.883E+07	3.889E+06	0.6150	0.3850	0.0000	178.56
18	1.267E-04	1.886E+07	3.889E+06	0.6411	0.3589	0.0000	178.80
19	1.267E-04	1.884E+07	3.889E+06	0.6026	0.3974	0.0000	178.62
20	1.267E-04	1.884E+07	3.889E+06	0.5789	0.4211	0.0000	178.62
21	1.267E-04	1.882E+07	3.889E+06	0.6279	0.3721	0.0000	178.50
22	1.267E-04	1.885E+07	3.889E+06	0.5965	0.4035	0.0000	178.74
23	1.267E-04	1.886E+07	3.889E+06	0.5964	0.4036	0.0000	178.80
24	1.267E-04	1.880E+07	3.889E+06	0.6027	0.3973	0.0000	178.27
25	1.267E-04	1.881E+07	3.889E+06	0.6027	0.3973	0.0000	178.39
26	1.267E-04	1.882E+07	3.889E+06	0.5966	0.4034	0.0000	178.45
27	1.267E-04	1.877E+07	3.889E+06	0.6028	0.3972	0.0000	178.09
28	3.879E-04	1.471E+07	4.475E+06	0.5267	0.4733	0.0000	139.93
29	3.879E-04	1.463E+07	4.413E+06	0.4532	0.5468	0.0000	139.10
30	3.879E-04	1.460E+07	4.385E+06	0.4929	0.5071	0.0000	138.82
31	3.879E-04	1.462E+07	4.364E+06	0.4855	0.5145	0.0000	139.03
32	3.879E-04	1.455E+07	4.385E+06	0.4882	0.5118	0.0000	138.26
33	3.879E-04	1.453E+07	4.357E+06	0.4883	0.5117	0.0000	138.05
34	3.879E-04	1.458E+07	4.364E+06	0.4861	0.5139	0.0000	138.54
35	3.879E-04	1.448E+07	4.399E+06	0.4915	0.5085	0.0000	137.57
36	3.879E-04	1.455E+07	4.364E+06	0.4958	0.5042	0.0000	138.26
37	3.879E-04	1.447E+07	4.371E+06	0.4966	0.5034	0.0000	137.50
38	3.879E-04	1.447E+07	4.371E+06	0.4891	0.5109	0.0000	137.43

	A2	P1	Psep	xg	xo	xw	rhog1
39	3.879E-04	1.445E+07	4.371E+06	0.4942	0.5058	0.0000	137.29
40	3.879E-04	1.445E+07	4.371E+06	0.5071	0.4929	0.0000	137.29
41	3.879E-04	1.445E+07	4.357E+06	0.5071	0.4929	0.0000	137.29
42	3.879E-04	1.444E+07	4.357E+06	0.5071	0.4929	0.0000	137.22
43	3.879E-04	1.467E+07	4.357E+06	0.3139	0.6861	0.0000	139.51
44	3.879E-04	1.464E+07	4.357E+06	0.4928	0.5072	0.0000	139.24
45	3.879E-04	1.463E+07	4.399E+06	0.4248	0.5752	0.0000	139.10
46	3.879E-04	1.462E+07	4.330E+06	0.4569	0.5431	0.0000	139.03
47	3.879E-04	1.456E+07	4.440E+06	0.4572	0.5428	0.0000	138.40
48	3.879E-04	1.460E+07	4.433E+06	0.4737	0.5263	0.0000	138.82
49	3.879E-04	1.460E+07	4.316E+06	0.4811	0.5189	0.0000	138.75
50	3.879E-04	1.452E+07	4.413E+06	0.4913	0.5087	0.0000	137.98
51	3.879E-04	1.451E+07	4.385E+06	0.4962	0.5038	0.0000	137.84
52	3.879E-04	1.449E+07	4.420E+06	0.4963	0.5037	0.0000	137.64
53	3.879E-04	1.451E+07	4.413E+06	0.5011	0.4989	0.0000	137.84
54	3.879E-04	1.453E+07	4.371E+06	0.5009	0.4991	0.0000	138.12
55	3.879E-04	1.445E+07	4.426E+06	0.5013	0.4987	0.0000	137.29
56	3.879E-04	1.444E+07	4.323E+06	0.5014	0.4986	0.0000	137.22
57	3.879E-04	1.444E+07	4.316E+06	0.5014	0.4986	0.0000	137.22
58	1.140E-03	1.014E+07	5.116E+06	0.3677	0.6323	0.0000	92.50
59	1.140E-03	8.170E+06	5.178E+06	0.5187	0.4813	0.0000	72.37
60	1.140E-03	8.025E+06	5.137E+06	0.5899	0.4101	0.0000	70.92
61	1.140E-03	7.929E+06	5.102E+06	0.5700	0.4300	0.0000	69.95
62	1.140E-03	7.867E+06	5.081E+06	0.5524	0.4476	0.0000	69.33
63	1.140E-03	7.832E+06	5.054E+06	0.5572	0.4428	0.0000	68.98
64	1.140E-03	7.791E+06	5.033E+06	0.5622	0.4378	0.0000	68.57
65	1.140E-03	7.763E+06	5.012E+06	0.5656	0.4344	0.0000	68.30
66	1.140E-03	7.736E+06	5.012E+06	0.5690	0.4310	0.0000	68.02
67	1.140E-03	7.695E+06	4.999E+06	0.5675	0.4325	0.0000	67.61
68	1.140E-03	7.688E+06	4.999E+06	0.5709	0.4291	0.0000	67.54
69	1.140E-03	7.660E+06	4.999E+06	0.5760	0.4240	0.0000	67.27
70	1.140E-03	7.639E+06	4.999E+06	0.5727	0.4273	0.0000	67.06
71	1.140E-03	7.681E+06	4.999E+06	0.5777	0.4223	0.0000	67.47
72	1.140E-03	7.619E+06	4.999E+06	0.5762	0.4238	0.0000	66.86
73	1.140E-03	9.508E+06	5.116E+06	0.4068	0.5932	0.0000	86.00
74	1.140E-03	8.191E+06	5.233E+06	0.4803	0.5197	0.0000	72.58
75	1.140E-03	8.060E+06	5.150E+06	0.4900	0.5100	0.0000	71.26
76	1.140E-03	7.970E+06	5.123E+06	0.4990	0.5010	0.0000	70.36
77	1.140E-03	7.915E+06	5.102E+06	0.5022	0.4978	0.0000	69.81
78	1.140E-03	7.853E+06	5.081E+06	0.5055	0.4945	0.0000	69.19
79	1.140E-03	7.832E+06	5.068E+06	0.5104	0.4896	0.0000	68.98
80	1.140E-03	7.784E+06	5.068E+06	0.5122	0.4878	0.0000	68.50
81	1.140E-03	7.743E+06	5.033E+06	0.5173	0.4827	0.0000	68.09
82	1.140E-03	7.715E+06	5.061E+06	0.5191	0.4809	0.0000	67.82
83	1.140E-03	7.757E+06	5.054E+06	0.5206	0.4794	0.0000	68.23
84	1.140E-03	7.743E+06	5.033E+06	0.5224	0.4776	0.0000	68.09

	A2	P1	Psep	xg	xo	xw	rhog1
85	1.140E-03	7.695E+06	5.033E+06	0.5243	0.4757	0.0000	67.61
86	1.140E-03	7.688E+06	5.033E+06	0.5260	0.4740	0.0000	67.54
87	1.140E-03	7.639E+06	5.033E+06	0.5279	0.4721	0.0000	67.06

	rhoo	rhow	cvg	Meas m.flow	T	Z	M	Opening
1	657.62	1000	740	3.362	350.928	0.7985	0.0221	32
2	657.67	1000	740	6.921	350.928	0.7985	0.0221	32
3	657.57	1000	740	5.831	350.928	0.7985	0.0221	32
4	657.72	1000	740	5.628	350.928	0.7984	0.0221	32
5	657.48	1000	740	5.484	350.928	0.7986	0.0221	32
6	657.92	1000	740	5.627	350.928	0.7983	0.0221	32
7	657.97	1000	740	5.635	350.928	0.7983	0.0221	32
8	657.87	1000	740	5.635	350.928	0.7984	0.0221	32
9	657.62	1000	740	5.568	350.928	0.7985	0.0221	32
10	658.07	1000	740	5.635	350.928	0.7982	0.0221	32
11	657.77	1000	740	5.760	350.928	0.7984	0.0221	32
12	658.07	1000	740	5.703	350.928	0.7982	0.0221	32
13	635.67	1000	740	12.007	350.928	0.8174	0.0221	32
14	659.82	1000	740	7.591	350.928	0.7973	0.0221	32
15	658.82	1000	740	5.924	350.928	0.7978	0.0221	32
16	658.32	1000	740	7.457	350.928	0.7981	0.0221	32
17	658.47	1000	740	7.591	350.928	0.7980	0.0221	32
18	658.27	1000	740	7.323	350.928	0.7981	0.0221	32
19	658.42	1000	740	7.725	350.928	0.7981	0.0221	32
20	658.42	1000	740	7.996	350.928	0.7981	0.0221	32
21	658.52	1000	740	7.457	350.928	0.7980	0.0221	32
22	658.32	1000	740	7.794	350.928	0.7981	0.0221	32
23	658.27	1000	740	7.794	350.928	0.7981	0.0221	32
24	658.72	1000	740	7.725	350.928	0.7979	0.0221	32
25	658.62	1000	740	7.725	350.928	0.7979	0.0221	32
26	658.57	1000	740	7.794	350.928	0.7980	0.0221	32
27	658.87	1000	740	7.725	350.928	0.7978	0.0221	32
28	688.76	1000	740	14.152	350.928	0.7958	0.0221	56
29	689.38	1000	740	16.054	350.928	0.7960	0.0221	56
30	689.59	1000	740	14.899	350.928	0.7961	0.0221	56
31	689.43	1000	740	15.104	350.928	0.7960	0.0221	56
32	690.00	1000	740	15.035	350.928	0.7963	0.0221	56
33	690.15	1000	740	15.035	350.928	0.7964	0.0221	56
34	689.79	1000	740	14.980	350.928	0.7962	0.0221	56
35	690.51	1000	740	14.845	350.928	0.7965	0.0221	56
36	690.00	1000	740	14.980	350.928	0.7963	0.0221	56
37	690.56	1000	740	14.709	350.928	0.7966	0.0221	56
38	690.62	1000	740	14.913	350.928	0.7966	0.0221	56
39	690.72	1000	740	14.777	350.928	0.7966	0.0221	56
40	690.72	1000	740	14.441	350.928	0.7966	0.0221	56

	rhoo	rhow	cvg	Meas m.flow	T	Z	M	Opening
41	690.72	1000	740	14.441	350.928	0.7966	0.0221	56
42	690.77	1000	740	14.441	350.928	0.7967	0.0221	56
43	689.07	1000	740	23.280	350.928	0.7959	0.0221	56
44	689.28	1000	740	13.685	350.928	0.7960	0.0221	56
45	689.38	1000	740	15.926	350.928	0.7960	0.0221	56
46	689.43	1000	740	15.133	350.928	0.7960	0.0221	56
47	689.89	1000	740	15.520	350.928	0.7962	0.0221	56
48	689.59	1000	740	15.315	350.928	0.7961	0.0221	56
49	689.64	1000	740	15.383	350.928	0.7961	0.0221	56
50	690.20	1000	740	15.679	350.928	0.7964	0.0221	56
51	690.31	1000	740	15.251	350.928	0.7964	0.0221	56
52	690.46	1000	740	15.251	350.928	0.7965	0.0221	56
53	690.31	1000	740	15.386	350.928	0.7964	0.0221	56
54	690.10	1000	740	15.386	350.928	0.7963	0.0221	56
55	690.72	1000	740	15.386	350.928	0.7966	0.0221	56
56	690.77	1000	740	15.386	350.928	0.7967	0.0221	56
57	690.77	1000	740	15.386	350.928	0.7967	0.0221	56
58	722.93	1000	740	35.086	350.928	0.8292	0.0221	96
59	737.26	1000	740	25.302	350.928	0.8544	0.0221	96
60	738.29	1000	740	22.261	350.928	0.8565	0.0221	96
61	738.98	1000	740	22.791	350.928	0.8578	0.0221	96
62	739.43	1000	740	23.534	350.928	0.8587	0.0221	96
63	739.67	1000	740	23.332	350.928	0.8592	0.0221	96
64	739.97	1000	740	23.126	350.928	0.8599	0.0221	96
65	740.16	1000	740	22.994	350.928	0.8603	0.0221	96
66	740.36	1000	740	22.857	350.928	0.8607	0.0221	96
67	740.65	1000	740	22.925	350.928	0.8613	0.0221	96
68	740.70	1000	740	22.791	350.928	0.8614	0.0221	96
69	740.90	1000	740	22.586	350.928	0.8618	0.0221	96
70	741.05	1000	740	22.723	350.928	0.8621	0.0221	96
71	740.75	1000	740	22.522	350.928	0.8615	0.0221	96
72	741.19	1000	740	22.206	350.928	0.8624	0.0221	96
73	727.55	1000	740	27.043	350.928	0.8367	0.0221	96
74	737.11	1000	740	23.580	350.928	0.8541	0.0221	96
75	738.05	1000	740	22.564	350.928	0.8560	0.0221	96
76	738.69	1000	740	21.885	350.928	0.8572	0.0221	96
77	739.08	1000	740	21.618	350.928	0.8580	0.0221	96
78	739.53	1000	740	21.347	350.928	0.8589	0.0221	96
79	739.67	1000	740	21.142	350.928	0.8592	0.0221	96
80	740.02	1000	740	21.074	350.928	0.8600	0.0221	96
81	740.31	1000	740	20.869	350.928	0.8606	0.0221	96
82	740.51	1000	740	20.801	350.928	0.8610	0.0221	96
83	740.21	1000	740	20.733	350.928	0.8604	0.0221	96
84	740.31	1000	740	20.668	350.928	0.8606	0.0221	96
85	740.65	1000	740	20.602	350.928	0.8613	0.0221	96
86	740.70	1000	740	20.532	350.928	0.8614	0.0221	96

	rhoo	rhow	cvg	Meas m.flow	T	Z	M	Opening
87	741.05	1000	740	20.465	350.928	0.8621	0.0221	96